

# Oriented Object Detection in Optical Remote Sensing Images using Deep Learning: A Survey

Kun Wang<sup>1,2†</sup>, Zi Wang<sup>1,2†</sup>, Zhang Li<sup>1,2\*</sup>, Ang Su<sup>1,2</sup>,  
Xichao Teng<sup>1,2</sup>, Erting Pan<sup>1,2</sup>, Minhao Liu<sup>3</sup>, Qifeng Yu<sup>1,2</sup>

<sup>1</sup>\*College of Aerospace Science and Engineering, National University of Defense Technology, Deya Road, Changsha, 410000, Hunan Province, China.

<sup>2</sup>Hunan Provincial Key Laboratory of Image Measurement and Vision Navigation, National University of Defense Technology, Deya Road, Changsha, 410000, Hunan Province, China.

<sup>3</sup>Videogrammetry Innovation Center, Hunan Institute of Advanced Technology, Qingshan Road, Changsha, 410000, Hunan Province, China.

\*Corresponding author(s). E-mail(s): [zhangli\\_nudt@163.com](mailto:zhangli_nudt@163.com);  
Contributing authors: [wangkun21@nudt.edu.cn](mailto:wangkun21@nudt.edu.cn); [wangzi16@nudt.edu.cn](mailto:wangzi16@nudt.edu.cn);  
[suang@nudt.edu.cn](mailto:suang@nudt.edu.cn); [tengari@buaa.edu.cn](mailto:tengari@buaa.edu.cn); [panerting@whu.edu.cn](mailto:panerting@whu.edu.cn);  
[lmh313@nudt.edu.cn](mailto:lmh313@nudt.edu.cn); [yuqifeng@nudt.edu.cn](mailto:yuqifeng@nudt.edu.cn);

†Equal contribution.

## Abstract

Oriented object detection is one of the most fundamental and challenging tasks in remote sensing, aiming to locate and classify objects with arbitrary orientations. Recent advancements in deep learning have significantly enhanced the capabilities of oriented object detection. Given the rapid development of this field, this paper presents a comprehensive survey of recent advances in oriented object detection. To be specific, we begin by tracing the technical evolution from horizontal object detection to oriented object detection and highlighting the specific challenges, including feature misalignment, spatial misalignment, and oriented bounding box (OBB) regression problems. Subsequently, we further categorize existing methods into detection framework, OBB regression, and feature representations, and providing an in-depth discussion on how these approaches address the above challenges. In addition, we cover several publicly available datasets and evaluation protocols. Furthermore, we provide a comprehensive comparison and analysis of

state-of-the-art methods. Toward the end of this paper, we identify several future directions for oriented object detection.

**Keywords:** Oriented object detection, Remote sensing, Deep learning

# 1 Introduction

With the rapid advancement of remote sensing (RS) technologies, an increasing number of images with various resolutions and distinct spectra can be easily obtained by optical satellites or unmanned aerial vehicles (UAVs). Naturally, there is an imperative need within the research community to investigate a variety of advanced technologies for automatically and efficiently processing and analyzing massive RS images. As a pivotal foundation of automatic analysis for RS images, object detection aims to identify objects of predefined categories from given images and to regress a precise localization of each object instance (Liu et al., 2020; Zou et al., 2023). Currently, object detection constitutes a vital component in a broad range of RS applications, encompassing intelligent monitoring (Zhao et al., 2018), precision agriculture (Osco et al., 2021), urban planning (Burochin et al., 2014), port management (Zhang et al., 2021), and military reconnaissance (Liu et al., 2022).

Objects in RS images typically exhibit arbitrary orientations due to the bird-eye view (BEV), making the general (horizontal) object detection methods inadequate. In contrast to general object detection that represents object localization via a horizontal bounding box (HBB), oriented object detection (also called rotated object detection) employs an oriented bounding box (OBB) to tightly pack the oriented object, as shown in Fig. 2. The OBB can not only provide orientation information but also locate the object precisely. Consequently, oriented object detection has attracted considerable attention, especially within the past five years. Although enormous methods exist, a comprehensive survey specifically focused on oriented object detection is still lacking. Given the continued maturity and increasing concerns about this field, this paper seeks to present a thorough analysis of recent efforts and systematically summarize their achievements.

## 1.1 Comparisons with Related Surveys

In object detection, quite a number of prominent surveys have been published in recent years, as summarized in Tab. 1. Numerous notable surveys concentrate on generic (horizontal) object detection that aims to detect horizontal objects in natural scenarios (Liu et al., 2020; Wu et al., 2020; Zhao et al., 2019; Zou et al., 2023). These surveys cover various aspects, including deep learning based detection frameworks, training strategies, feature representation, evaluation metrics, and typical applications.

Furthermore, several efforts are devoted to a specific category, such as text detection (Ye and Doermann, 2015), and pedestrian detection (Cao et al., 2022). Additionally, there are also surveys paying their attention to object detection under specific conditions, including small object detection (Cheng et al., 2023), few-shot

**Table 1** Summary of related object detection surveys in recent years. **Top:** generic object detection. **Middle:** object detection focusing on specific tasks. **Bottom:** RS object detection.

Survey Title	Publication	Descriptions
Deep Learning for Generic Object Detection: A Survey (Liu et al., 2020)	IJCV 2020	A comprehensive survey of the recent progress in generic object detection brought about by deep learning
Recent Advances in Deep Learning for Object Detection (Wu et al., 2020)	Neucom 2020	A survey focuses on deep learning in generic object detection from detection components, learning strategies, and applications
Object Detection With Deep Learning: A Review (Zhao et al., 2019)	TNNLS 2020	A review on deep learning for generic object detection and other specific subtasks
Object Detection in 20 Years: A Survey (Zou et al., 2023)	PROC 2023	A survey focuses on object detection spanning over 20 years of history
Text Detection and Recognition in Imagery: A Survey (Ye and Doermann, 2015)	TPAMI 2015	A survey about methods, sub-problems, and special issues of text detection and recognition
From Handcrafted to Deep Features for Pedestrian Detection: A Survey (Cao et al., 2022)	TPAMI 2022	A survey on recent deep features based methods in pedestrian detection
Towards Large-Scale Small Object Detection: Survey and Benchmarks (Cheng et al., 2023)	TPAMI 2023	A survey of small object detection and two large-scale small object detection benchmarks under driving scenario and aerial scene
Few-Shot Object Detection: A Survey (Pannone, 2022)	ACM 2022	A survey on few-shot object detection through data augmentation, transfer learning, distance metric learning, and meta-learning
A Survey of Self-Supervised and Few-Shot Object Detection (Huang et al., 2023)	TPAMI 2023	Categorization, review, and comparison for few-shot and self-supervised object detection methods
A Survey on Object Detection in Optical Remote Sensing Images (Cheng and Han, 2016)	ISPRS 2016	A review on traditional object detection methods in RS images
Object Detection in Optical Remote Sensing Images: A Survey and A New Benchmark (Li et al., 2020)	ISPRS 2020	A review on deep learning based horizontal object detection in RS, and a large-scale, publicly available benchmark for RS object detection
Remote Sensing Object Detection Meets Deep Learning: A Meta-review of Challenges and Advances (Zhang et al., 2023)	GRSM 2023	A survey on challenges and advances in RS object detection, including multi-scale object detection, rotated object detection, weak object detection, tiny object detection, and object detection with limited supervision
Ship Detection and Classification from Optical Remote Sensing Images: A Survey (Li et al., 2021)	CJA 2021	A survey of RS ship detection schemes from 1978 to 2020
Methods for Small, Weak Object Detection in Optical High-Resolution Remote Sensing Images: A Survey of Advances and Challenges (Han et al., 2021)	GRSM 2021	A survey of challenges and recent advances for RS small, weak object detection
Deep Learning for Unmanned Aerial Vehicle-Based Object Detection and Tracking: A survey (Wu et al., 2022)	GRSM 2022	A survey on deep learning approaches in UAV object detection and tracking from static object detection, video object detection, and multiple object detection
A Comprehensive Survey of Oriented Object Detection in Remote Sensing Images (Wen et al., 2023)	ESWA 2023	A survey on oriented object detection, including rotation invariance, anchor-free mechanism, and loss function.

object detection (Pannone, 2022), and weakly-supervised object detection (Zhang et al., 2022).

Although a few surveys analyze and summarize RS object detection, they frequently lack in-depth analysis for oriented object detection (Cheng and Han, 2016; Li et al., 2020, 2021; Han et al., 2021; Wu et al., 2022). Zhang et al. (2023) classify the sub-categories belonging to RS object detection as oriented object detection, merely providing a brief introduction to OBB representation and rotation-insensitive feature

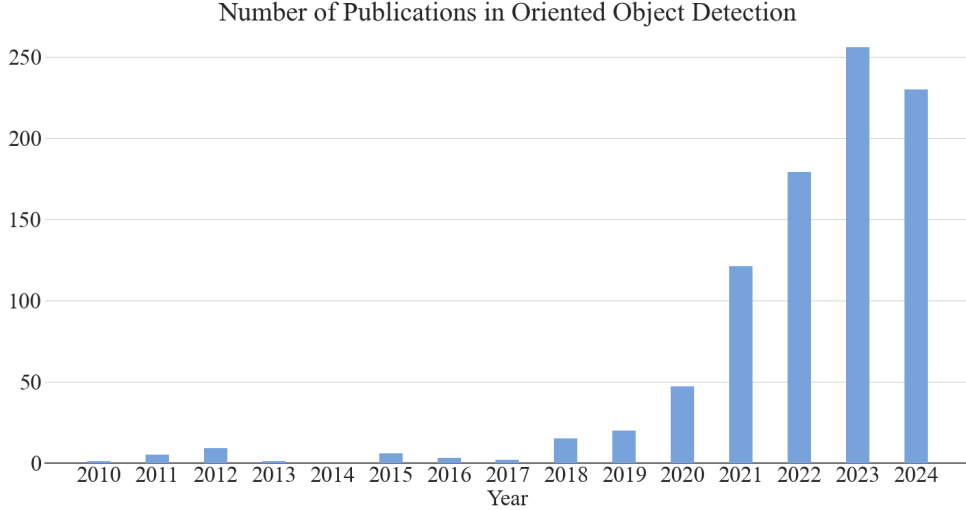


**Fig. 1** Increasing number of publications in oriented object detection from 2010 to 2024.

learning. [Wen et al. \(2023\)](#) only focuses on describing the details of previous oriented object detection methods.

Different from previous object detection surveys, which focus on general object detection methods ([Liu et al., 2020](#); [Wu et al., 2020](#); [Zhao et al., 2019](#); [Zou et al., 2023](#)), other related fields ([Ye and Doermann, 2015](#); [Cao et al., 2022](#); [Cheng et al., 2023](#); [Pannone, 2022](#); [Zhang et al., 2022](#)), RS horizontal object detection ([Cheng and Han, 2016](#); [Li et al., 2020, 2021](#); [Han et al., 2021](#); [Wu et al., 2022](#)), or a limited number of oriented object detection models ([Zhang et al., 2023](#); [Wen et al., 2023](#)), this work systematically and comprehensively reviews recent advances in the field. Especially, in comparison to existing surveys related to oriented object detection ([Zhang et al., 2023](#); [Wen et al., 2023](#)), our survey provide a deeper, more comprehensive dive into this field, a better taxonomy of the literature, and present discussions regarding challenges, comparison, and future directions. It involves in-depth analyses on various aspects, many of which, to the best of our knowledge, have never been discussed in oriented object detection. In particular, we review the technical evolution from horizontal to oriented object detection and summarize the main challenges. We systematically summarize and discuss recent advancements under proposed taxonomies (including detection frameworks, OBB regression, feature representation, and common issues). We provide a comprehensive comparison of state-of-the-art methods on typical datasets, along with an in-depth analysis of the pros and cons of these methods.

## 1.2 Scope

[Fig. 1](#) shows the increasing number of publications related to "oriented object detection" or "rotated object detection" over the past decade or so. Particularly in the last

five years, there has been an explosive growth in the number of papers on deep learning based oriented object detection, rendering it impractical to review all of them. Consequently, it is necessary to establish selection criteria to limit our focus to influential papers published in top journals and conferences. Owing to these constraints, we extend our sincere apologies to authors whose works are not included in this paper. It is worth highlighting that we restrict our attention to oriented object detection in single images. Nevertheless, for completeness and better readability, some well-known works on horizontal object detection are also included.

### 1.3 Contributions

Our contribution is manifested in four aspects:

(1) **A comprehensive review of the technical evolution from horizontal object detection to oriented object detection.** Based on the characteristics of RS images and current object detection models, we categorize the main challenges in oriented object detection into four main parts, including feature misalignment, spatial misalignment, OBB regression problems, and common issues.

(2) **A thorough taxonomy of oriented object detection methods.** Aiming to help researchers gain a deeper understanding of the key features of oriented object detection methods, we categorize and summarize existing oriented object detection methods according to detection frameworks, OBB regression, feature representation, and common issues.

(3) **A comprehensive comparison of state-of-the-art methods.** We provide a comprehensive comparison of state-of-the-art methods on typical datasets, along with an in-depth analysis of the pros and cons of these methods. This analysis aims to offer valuable insights into the efficacy and applicability of these methods in addressing the main challenges of oriented object detection.

(4) **Overview of open issues and future directions.** We thoroughly look over several essential issues, shedding light on potential directions for future research, i.e., lightweight methods, scenario-specific datasets, multi-modal datasets, and large-scale datasets, as well as multi-modal large models.

The structure of this paper is organized as follows. We first introduce the development from horizontal object detection to oriented object detection and highlight the major challenges in Sec. 2. Then, we review deep neural networks (DNN) based detection frameworks in Sec. 3. Furthermore, we discuss the OBB regression and feature representation in Sec. 4 and Sec. 5, respectively. In addition, we summarize other common issues encountered in RS scenarios in Sec. 6. After an overview of commonly used datasets is provided in Sec. 7, we analyze and compare the state-of-the-art methods in Sec. 8. Finally, we conclude our work and discuss the future directions of oriented object detection in Sec. 9.

## 2 From Horizontal Object Detection to Oriented Object Detection

The early object detection methods rely on handcrafted descriptors (Lowe, 2004; Dalal and Triggs, 2005; Fei-Fei and Perona, 2005; Wright et al., 2009) and machine learning

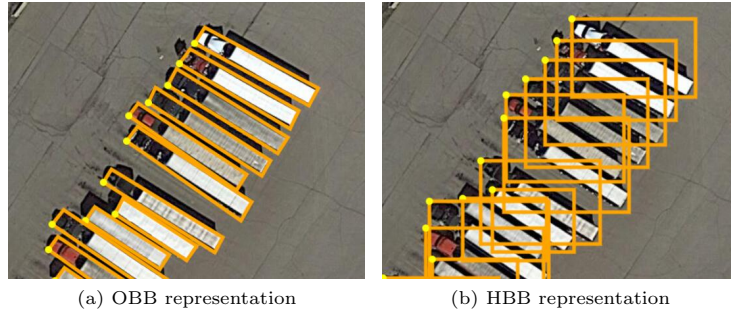


**Fig. 2** Comparison between OBB and HBB (Xia et al., 2018; Ding et al., 2022). (a) OBB representation of objects. (b) is a failure case of the HBB representation, which brings high overlap compared to (a).

algorithms (Cortes and Vapnik, 1995; Blaschke, 2010; Leitloff et al., 2010; Blaschke et al., 2014). These methods often show limited performance due to the weak feature representations. Although lag far behind in accuracy, their instructive insights still have a profound impact on modern detectors, *e.g.*, sliding windows (Viola and Jones, 2001, 2004), hard negative mining, and bounding box regression (Felzenszwalb et al., 2008, 2010). Readers interested in early object detection methods are referred to the recent survey (Cheng and Han, 2016) that provides an in-depth analysis of classical object detection methods in RS.

The world has witnessed impressive progress in computer vision with the advance of deep neural networks (DNN) since 2012 (Hinton and Salakhutdinov, 2006; LeCun et al., 2015; Chen et al., 2018; He et al., 2016; Krizhevsky et al., 2012, 2017). Owing to the persistent enhancement of computing resources, DNN can learn high-level patterns from large-scale datasets in an end-to-end manner. The pioneering studies bring a little glimmer to the object detection field, especially in light of the fact that the performance of handcrafted features-based detectors reached a plateau after 2010. Since then, a growing number of DNN-based detectors have emerged and have dominated the state-of-the-art, thanks to their powerful feature representation.

Early research in the deep learning era is primarily concerned with designing horizontal object detectors (Girshick et al., 2014; Girshick, 2015; Ren et al., 2015, 2017; Liu et al., 2016; Lin et al., 2017, 2020; Redmon et al., 2016; Redmon and Farhadi, 2017; Hei and Jia, 2020; Duan et al., 2019; Zhou et al., 2019; Yang et al., 2019) for natural scene images taken from a horizontal perspective. Naturally, as horizontal object detectors evolve rapidly, numerous studies are harnessing their immense potential in RS scenarios, *e.g.*, RCNN series (Girshick et al., 2014; Girshick, 2015; Ren et al., 2015, 2017), YOLO series (Redmon et al., 2016; Redmon and Farhadi, 2017), and RetinaNet (Lin et al., 2017, 2020). Subsequently, a growing number of efforts pivoted towards refining network structures and crafting innovative data augmentation techniques, all aimed at tackling the core challenges in RS object detection, including scale variation (Liang et al., 2020; Ye et al., 2022; Liu et al., 2022; Khan et al., 2022), complex background (Lu et al., 2021; Huang et al., 2022; Ma et al., 2022), and weak feature responses (Tian et al., 2022; Wu et al., 2022).

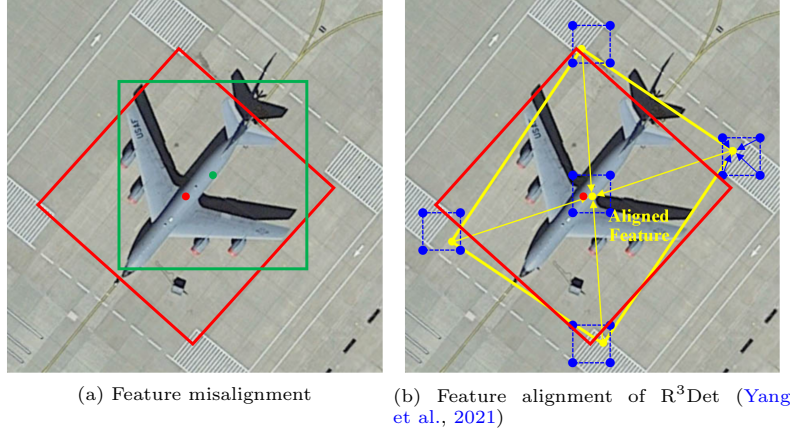


**Fig. 3** Illustration of feature misalignment and feature alignment. (a) The misalignment between oriented objects and the axis-aligned feature representation of anchor. (b) A example of feature alignment proposed by R<sup>3</sup>Det (Yang et al., 2021), which align the feature representation by integrating the features according to the five refined points of the predicted obb. The red, green, and blue boxes represent the ground truth (GT), anchor, and predicted obb, respectively. The blue and yellow points denote anchor points and refined feature points, respectively. The blue and yellow arrows denote feature interpolation and feature alignment operation, respectively.

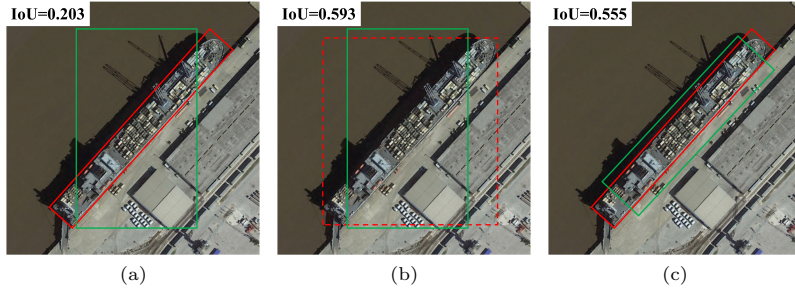


**Fig. 4** Illustration of spatial misalignment. (a) The IoU between horizontal anchor and oriented object is very small, causing spatial misalignment. (b)~(c) Calculating the IoU between either horizontal anchor and horizontal bounding rectangle of object, or rotated anchor and oriented object, can alleviate the spatial misalignment. The red and green boxes represent the GT and anchor, respectively.

Nevertheless, RS images are typically captured from the BEV, leading to objects appearing in arbitrary orientations. Hence, directly applying horizontal object detectors in RS images may encounter the following problems: (1) The intersection-over-union (IoU) between an HBB and the adjacent HBBs can be very large in dense arrangement scenarios, especially for objects with extremely large aspect ratios, as illustrated in Fig. 2b. Thus, the non-maximum suppression (NMS) technique tends to cause missed detection. (2) HBBs are inclined to contain background, whereas OBBs can tightly enclose the objects, achieving more precise localization, as shown in Fig. 2a.

Given the above predicament of HBB, OBB is considered more appropriate for RS object detection.

With the remarkable development of detection frameworks (Ren et al., 2015, 2017; Lin et al., 2017, 2020; Redmon et al., 2016; Carion et al., 2020), backbone networks (He et al., 2016; Liu et al., 2021), and robust feature representation (Liu et al., 2022; Dosovitskiy et al., 2021), the field of object detection has achieved dramatic breakthroughs. Naturally, an intuitive strategy for designing oriented object detectors is to modify representative horizontal object detectors by predicting additional parameters to represent OBB (Zhou et al., 2022). However, such a straightforward strategy is plagued by several additional challenges, mainly including feature misalignment, spatial misalignment, and OBB regression problems.

(1) **Feature Misalignment.** The prevailing generic object detectors typically contain a feature extraction network followed by a detection head, where the latter leverages the feature representations generated from the former to make decisions. However, the feature representations are generally extracted via axis-aligned convolutions, thereby exposing non-negligible misalignment with oriented objects, as shown in Fig. 3a. Such a misaligned feature representation degrades the performance of oriented object detectors, due to the lack of rotational information, making the detector struggle to identify objects and regress precise OBBs.

(2) **Spatial Misalignment.** In addition to feature misalignment, the widely used anchor-based detection methods also struggle with spatial misalignment. Generic anchor-based detectors typically use horizontal anchors as priors thereby having limited overlaps to oriented objects, especially for objects with extremely large aspect ratios, as shown in Fig. 4a. This poses a significant challenge to generic label assignment strategies (Ren et al., 2015, 2017), which assign positive or negative samples depending on the overlaps. Thus, the naïve anchor generation mechanism is likely unable to provide sufficient positive samples during the training process.

(3) **OBB Regression Problems.** Current detectors commonly utilize the regression paradigm to represent the locations of objects, which has been proven to be effective and yields dramatic achievement. The most commonly used representation methods for OBB include  $\theta$ -based and quadrilateral representation. However, the former suffers from the periodicity of angle (PoA), causing the angular boundary discontinuity (Yang et al., 2021; Yang et al., 2022; Qian et al., 2021, 2022). Concretely, a small angle difference may cause a large loss change when the angular value approaches the angular boundary range. On the other hand, the later faces challenges related to vertex ordering, because the inappropriate vertex sorting may cause inconsistencies between the vertex sequences of the predicted OBB and the ground truth (GT). Overall, both PoA and vertex ordering problem can seriously confuse the network, leading to training instability. For more details please refer to Sec. A and Sec. B of the Appendix.

To cope with the above dilemmas, various works have been made and achieved notable advancements. Several methods construct well-designed **detection frameworks** by devising rotated proposal generation networks (Sec. 3.1) or refined heads (Sec. 3.2) to remedy feature misalignment. To deal with spatial misalignment,

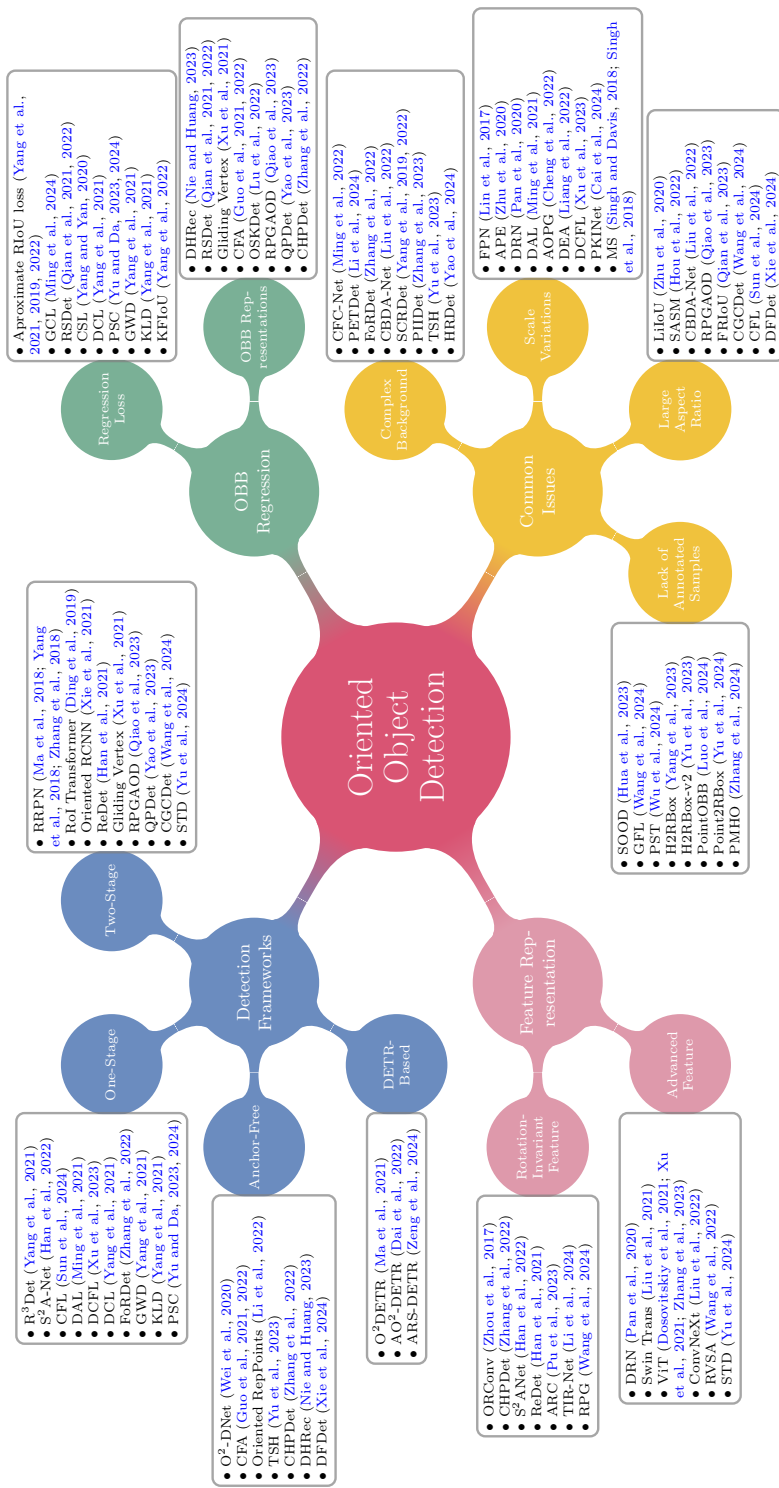
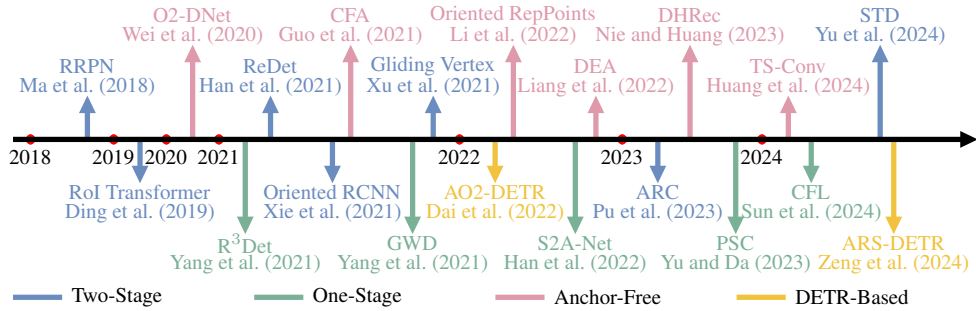


Fig. 5 Structured taxonomy of the deep learning based oriented object detection methods in this survey.



**Fig. 6** Chronological overview of the representative oriented object detection frameworks.

researchers focus on improving the assignment schemes (Sec. 3.1) or adopting anchor-free mechanisms (Sec. 3.3). As for OBB regression problems, several efforts intend to design effective **OBB regression** through developing new loss functions (Sec. 4.1) or OBB representation (Sec. 4.2). In addition, high-quality **feature representations** are crucial for object detection, hence a great deal of effort is concentrated on network designs for better feature representations, including rotation-invariant feature representations (Sec. 5.1) and advanced feature representations (Sec. 5.2). We also cover the solutions for several **common issues** (Sec. 6) in RS scenarios. Fig. 5 shows the taxonomy of oriented object detection methods in this survey.

### 3 Detection Frameworks

It is widely accepted that object detection methods can be categorized into two primary groups: two-stage and one-stage detection (Liu et al., 2020; Zou et al., 2023). The former works in a coarse-to-fine paradigm, whereas the latter accomplishes classification and regression in one step, thereby exhibiting high efficiency but performing poorly on accuracy. In contrast to the aforementioned two categories that rely on anchor mechanisms, anchor-free methods directly detect objects without the need for predefined anchors. In addition, a series of DETR-based methods have merged recently, regarding the detection process as a set prediction task, thereby effectively eliminating several hand-craft components, *e.g.*, NMS and anchor mechanism. Considering that each category has pros and cons, we divide the representative oriented object detectors into four categories: two-stage, one-stage, anchor-free, and DETR-based. Several milestone methods are presented in Fig. 6. Next, we will concisely review how each category addresses feature misalignment and spatial misalignment via deliberate framework design.

#### 3.1 Two-Stage

Among numerous prominent two-stage detectors (Ren et al., 2015, 2017; Lin et al., 2017; Cai and Vasconcelos, 2018; He et al., 2020; Qiao et al., 2021), Faster RCNN (Ren et al., 2015, 2017) armed with FPN (Lin et al., 2017) commonly serves as a benchmark

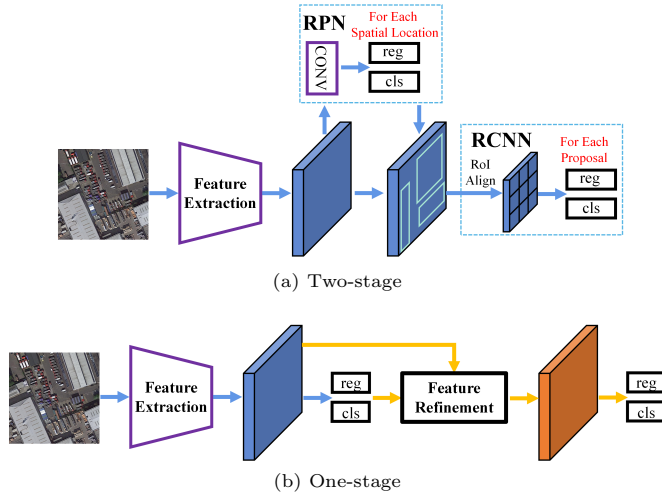


**Fig. 7** The basic architecture of two-stage and one-stage detectors. (a) Two-stage detectors first utilize RPN to predict a set of proposals, then extract corresponding region features for classification and refined regression. (b) One-stage detectors predict the class probabilities and locations for each spatial location. Most of them add a refined stage to alleviate the feature misalignment. The **blue** arrows denote the workflow of RetinaNet (Lin et al., 2017, 2020), while the **orange** arrows denote the workflow of refined stage.

due to its exceptional accuracy and efficient design. As depicted in Fig. 7a, its workflow consists of the following pipeline: Feature Extraction, Region proposal networks (RPN), and Regions with CNN features (RCNN). In the first stage, a sparse set of high-quality region proposals, that can potentially contain objects, are generated via RPN (Chavali et al., 2016; Hosang et al., 2016). During the second stage, the region features are extracted for each proposal and then used for classification and refined regression via RCNN. Finally, several post-processing operations, such as NMS, are leveraged to finalize the detection results (omitted in Fig. 7a). Its oriented version, termed as Rotated Faster RCNN or Faster RCNN OBB, predicts the orientation of each object by adding an extra channel in the regression branch.

However, the naïve RPN only generates horizontal region proposals as regions of interest (RoIs), as shown in Fig. 9a. Apart from the feature misalignment caused by axis-aligned convolutions, another factor that may impair the final performance is the feature misalignment between horizontal RoI (HRoI) and OBB, as shown in Fig. 8a. The feature misalignment significantly harms feature representation, making the detectors struggle to identify objects and regress precise OBBs yet inspiring successive innovations.

To cope with the feature misalignment, various efforts are dedicated to generating rotated proposals and then adopting rotated RoI (RRoI) operators to extract spatial-aligned features, as shown in Fig. 8b. RPPN (Ma et al., 2018; Yang et al., 2018; Zhang et al., 2018) incorporates rotated anchors to accommodate objects of various orientations. In addition to scales and aspect ratios, different orientation parameters are added to further generate additional rotated anchors, as shown in Fig. 9b. Such a scheme can alleviate the spatial misalignment (shown in Fig. 4c) thereby achieving

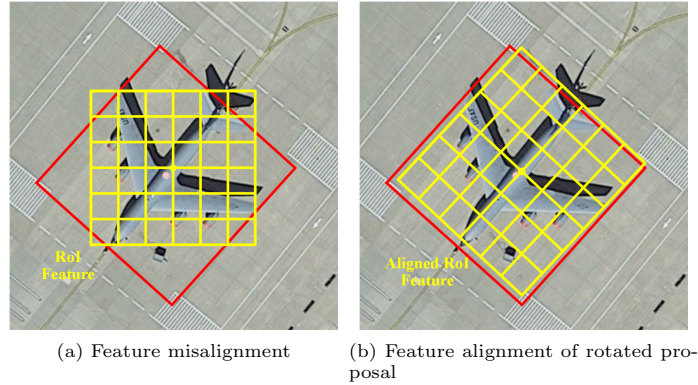


**Fig. 8** Illustration of feature misalignment in two-stage detectors. (a) The feature misalignment between oriented object and horizontal region proposal. (b) Detectors can extract aligned features from rotated region proposal.

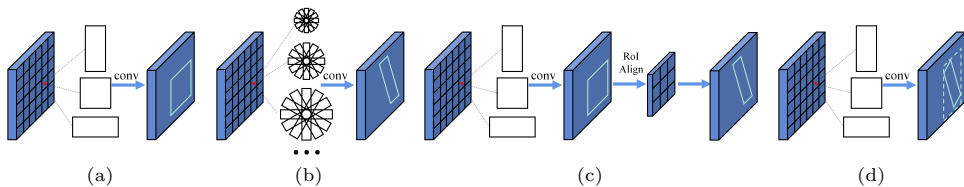


**Fig. 9** The comparisons of different strategies for proposal generation. (a) RPN only generates horizontal proposals (Ren et al., 2015, 2017). (b) RRPN densely places rotated anchors with different scales, ratios, and angles (Ma et al., 2018; Yang et al., 2018; Zhang et al., 2018). (c) RoI Transformer generates rotated proposal from horizontal RoI via RPN, RoI Alignment, and OBB regression (Ding et al., 2019). (d) Oriented RCNN can generate high-quality rotated proposals using a lightweight module (Xie et al., 2021).

better performance in terms of recall. However, the redundant rotated anchors bring about expensive computation and memory consumption.

To reduce the number of rotated anchors, RoI Transformer (Ding et al., 2019) retains the naïve RPN structure to alleviate spatial misalignment (shown in Fig. 4b), and then introduces a lightweight RoI Learner module. As shown in Fig. 9c, RRoI Learner converts HRoIs directly into RRoIs, generating precise RRoIs without enormous rotated anchors, thus enhancing efficiency and accuracy. Yet, the added complexity of the RoI Learner, including an extra RoI operator and regression stage, makes the network less efficient.

Consequently, Xie et al. (2021) design a simpler structure, Oriented RCNN, to generate high-quality RRoIs from horizontal anchors directly, as shown in Fig. 9d. This lightweight module benefits from the proposed Midpoint Offset representation, which includes the corresponding external HBB and the offsets of vertexes w.r.t the midpoints of the external HBB. This representation maintains horizontal regression mechanisms, ensuring stable training compared to regressing OBBs from horizontal anchors. Benefiting from the design of oriented RPN and Midpoint Offset representation, Oriented

RCNN can achieve competitive accuracy to advanced two-stage detectors and reach approximate efficiency to one-stage detectors.

The excellent design of RoI Transformer and Oriented RCNN tackles the spatial misalignment and feature misalignment in two-stage detectors, laying the foundation for subsequent research in this field. Numerous subsequent two-stage detectors adopt RoI Transformer or Oriented RCNN as their baseline framework, harnessing exceptional feature representation (*e.g.*, ReDet (Han et al., 2021), RVSA (Wang et al., 2022), ARC (Pu et al., 2023), STD (Yu et al., 2024)) or crafting superior OBB representation (*e.g.*, Gliding Vertex (Xu et al., 2021), RPGAOD (Qiao et al., 2023), QPDet (Yao et al., 2023)) and loss functions (*e.g.*, FRIOU (Qian et al., 2023), CGCDet (Wang et al., 2024), GCL (Ming et al., 2024)) to enhance their performance. These methods will be discussed in detail in the subsequent section.

### 3.2 One-Stage

As illustrated in Fig. 7b, one-stage detectors first extract multi-level feature maps and then predict the class probabilities and locations for each anchor per spatial location. Due to the absence of RPN and RoI operators, one-stage detectors encounter more severe feature misalignment than two-stage ones. Thus, a series of one-stage algorithms are developed to alleviate the dilemma, such as R<sup>3</sup>Det (Yang et al., 2021) and S<sup>2</sup>A-Net (Han et al., 2022).

R<sup>3</sup>Det (Yang et al., 2021) adopts a feature refinement module (FRM) to align features. First, R<sup>3</sup>Det transforms the horizontal anchors into rotated anchors, which can provide more accurate positional and oriented information. Then, FRM employs pixel-wise feature interpolation to integrate features from five locations (*i.e.*, one center and four corners) of the corresponding refined rotated anchors, as shown in Fig. 3b. Similarly, S<sup>2</sup>A-Net (Han et al., 2022) aligns features using Alignment Convolution (AlignConv), a variant of deformable convolution (Dai et al., 2017). The offset field of AlignConv is inferred from the guidance of rotated anchors. Both FRM and AlignConv operate in a coarse-to-fine manner but differ significantly from the RRoi operator. Notably, they follow a full convolution structure with fewer sampling points, resulting in increased efficiency.

Based on S<sup>2</sup>A-Net, CFL (Sun et al., 2024) introduces a Spatial Transform Selection (STS) strategy and a Critical Feature Sampling (CFS) module. STS dynamically assigns labels by calculating IoU thresholds based on aspect ratios, angle differences, and the initial IoU threshold determined by ATSS (Zhang et al., 2020). The adaptable IoU threshold controls the number of samples assigned to the easy object while ensuring enough positive samples for hard one with large aspect ratio and angle difference. CFS incorporates a deformable convolution in which the sampling positions are derived from initial detection results (center point, vertices, and midpoints) combined with a learnable offset field.

Both R<sup>3</sup>Det and S<sup>2</sup>A-Net utilize the extra refined head of for feature alignment, making them popular baseline choices for one-stage detectors. These methods further solve spatial misalignment and OBB regression problem via innovative sample assignment strategies (*e.g.*, DAL (Ming et al., 2021), DCFL (Xu et al., 2023)) or regression loss (*e.g.*, DCL (Yang et al., 2021), FoRDet (Zhang et al., 2022), GWD (Yang et al.,

2021), KLD (Yang et al., 2021), PSC (Yu and Da, 2023, 2024)). In the following section, we will provide a detailed introduction to these methods.

### 3.3 Anchor-Free

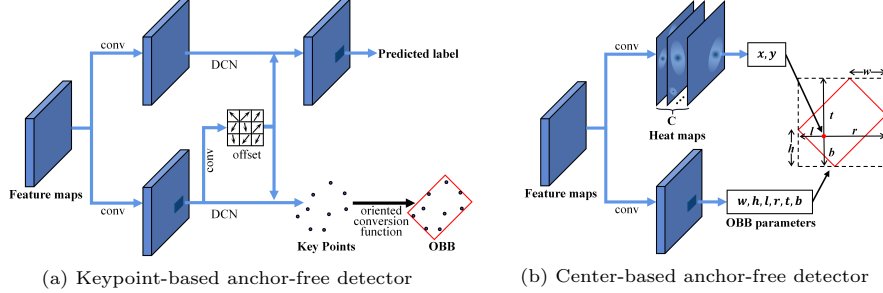


**Fig. 10** The basic architecture of keypoint-based and center-based anchor-free detectors.

The above two categories follow the anchor paradigm which suffers from spatial misalignment between horizontal anchor and OBB. To tackle the above issues, a constellation of anchor-free methods are developed to detect objects without relying on preset anchors. These methods eliminate anchor-related hyper-parameters, showing potential in the generalization to wide applications (Zhang et al., 2020). According to the representation of OBB, anchor-free methods can be divided into keypoint-based and center-based methods.

Keypoint-based methods first locate a set of adaptive or self-constrained key points and then circumscribe object’s spatial extent, as shown in Fig. 10a. For instance, O<sup>2</sup>-DNet (Wei et al., 2020) first locates the midpoints of four sides of the OBB by regressing the offsets from the center point. Then, two sets of opposite midpoints are connected to form two mutually perpendicular midlines, which are decoded to represent the OBB. In addition, a self-supervision loss constrains the perpendicular relationship between two middle lines and a collinear relationship between the center point and two opposite midpoints. Following the RepPoints (Yang et al., 2019), CFA (Guo et al., 2021, 2022) utilizes the deformable convolution (Dai et al., 2017) to generate a convex hull for each oriented object. The convex hull, represented by irregular sample points, is refined using a Convex Intersection over Union (CIoU) loss. To alleviate feature aliasing between densely packed objects, convex-hull set splitting and feature anti-aliasing strategies are designed to refine the convex-hulls and adaptively optimal feature assignment.

Furthermore, to predict the high-quality oriented reppoints, Oriented RepPoints (Li et al., 2022) designs an Adaptive Points Assessment and Assignment (APAA) scheme to measure the quality of reppoints. APAA assesses reppoints across four dimensions (classification, localization, orientation alignment, and point-wise correlation) to select high-quality ones, without adding computational burden during inference. Subsequently, Yu et al. (2023) propose a dynamic information aggregation

(DIA) module based on multi-head self-attention mechanism (Vaswani et al., 2017). By mining the relationships between reppoints, DIA not only helps to obtain more accurate positions of reppoints but also enriches the feature representations, thereby further boosting localization accuracy.

Center-based methods generally generate multiple probabilistic heatmaps and a series of feature maps. As shown in Fig. 10b, the heatmaps provide a set of candidates (peak points) as coarse center points, while the feature maps regress transformation parameters to represent the OBB. Nowadays, most center-based methods are dedicated to designing a variety of OBB representations to address the PoA problems, including CHPDet (Zhang et al., 2022), GGHL (Huang et al., 2022), DHRec (Nie and Huang, 2023). However, these methods typically follow the one-stage paradigms and tend to predict coarse locations due to feature misalignment, while state-of-the-art methods generally contain one or multiple refined stages to improve performance.

Hence, an effective scheme for boost performance is leveraging anchor-free methods to generate coarse detection results that are then refined via subsequent feature alignment stage, *e.g.*, AOPG (Cheng et al., 2022), DEA (Liang et al., 2022), DRDet (Zhang et al., 2023), TS-Conv (Huang et al., 2024). AOPG (Cheng et al., 2022) initially produces coarse oriented boxes via the rotated FCOS manner (Tian et al., 2019), subsequently refining them into high-quality oriented proposals. DEA (Liang et al., 2022) leverages two parallel branches, which generate proposals using anchor-free and anchor-based approaches respectively, followed by an interactive sample screening procedure to select high-quality training samples.

In contrast to the above two methods that capitalize on the merits of anchor-free techniques to mitigate spatial misalignment and facilitate appropriate sample assignment, DRDet (Zhang et al., 2023) and TS-Conv (Huang et al., 2024) concentrate on feature refinement. DRDet (Zhang et al., 2023) adopts two perpendicular rotated lines to represent OBB. Then, an orientation-guided feature encoder (OFD) is designed to encode the orientation-aware information into refined features along each rotated line. Compared to rectangular feature, the line features extracted from OFD can introduce less noise and alleviate the feature aliasing caused by overlapping objects. TS-Conv (Huang et al., 2024) designs different sampling offsets for localization and classification to alleviate the task misalignment problem (*i.e.*, localization and classification tasks may focus on different feature regions (Song et al., 2020)). The sampling offsets are restricted by initial OBBs predicted via an anchor-free manner, allowing for dynamic adaptation to objects with various shapes.

### 3.4 DETR-Based

In addition to the above convolution-based methods, DETR-based detectors show great potential and achieve state-of-the-art performance in the detection community, including DETR (Carion et al., 2020) and its variants (Zhu et al., 2021; Sun et al., 2021; Gao et al., 2021). Based on DETR (Carion et al., 2020), O<sup>2</sup>DETR (Ma et al., 2021) is proposed to utilize the Transformer for the oriented object detection task. In addition, the depthwise separable convolutions (Sifre and Mallat, 2013; Chollet, 2017; Haase and Amthor, 2020) is introduced to replace the computationally complex self-attention mechanism, making networks more lightweight and speeding up the training.

To tackle feature misalignment, Dai et al. (2022) propose AO2-DETR by improving Deformable DETR (Zhu et al., 2021), which design an oriented proposal generation mechanism and an adaptive oriented proposal refinement (OPR) module for aligning the features. Recently, several improved DETR-based detectors have been proposed for generic object detection, *e.g.*, DN-DETR (Li et al., 2022), DAB-DETR (Liu et al., 2022), and DINO (Zhang et al., 2022), bringing about dramatic breakthroughs in accuracy and convergence speed. ARS-DETR (Zeng et al., 2024) attempts to exploit DINO (Zhang et al., 2022) for oriented object detection tasks. Compared to other advanced oriented object detectors, it achieves greater detection accuracy in the more rigorous metric (*i.e.*, AP<sub>75</sub>), but lags in the standard metric (*i.e.*, AP<sub>50</sub>). Worse still, the long training convergence time and heavy computation cost are still open problems.

### 3.5 Discussion

Feature misalignment and spatial misalignment will seriously impair the performance of oriented object detection. To tackle these issues, substantial research has contributed to modifying the detection frameworks. Existing two-stage detectors typically design efficient and precisely oriented proposal generation modules, leveraging RRoI operators to extract rotated aligned features. Similarly, one-stage detectors are inclined to incorporate an extra refined stage for feature alignment. Thus, the above two schemes can empower the detectors to mine the rotation-related information, thereby enhancing the semantic representation of oriented objects.

Nevertheless, spatial misalignment remains a persistent issue. Anchor-free detectors address this by eliminating the anchor mechanism and, in advanced methods, incorporating extra feature refinement stages to further mitigate feature misalignment. In addition, DETR-based methods provide a new detection paradigm and receive widespread concerns. However, the exploration of DETR-based methods in oriented object detection is not comprehensive enough, requiring further research to accelerate training convergence and reduce computation overheads.

Well-designed detection frameworks are conducive to alleviating feature and spatial misalignment but fail to address the PoA problems. Besides, the extracted features are not equipped with rotation-invariance as the convolution operators are axis-aligned. To overcome these dilemmas, the suitable OBB regression and the powerful feature representation of oriented objects are also widely studied, since they can be seamlessly integrated into various detection frameworks. Next, we will discuss the OBB regression and feature representation.

## 4 OBB Regression

Oriented object detectors typically locate objects in a regression fashion. Specifically, the customized regression head predicts the orientation parameters when using the most frequently used  $\theta$ -based representation. Unfortunately, such a regression paradigm suffers from several limitations, including inconsistency between metric and loss, and angular boundary discontinuity. For more details about the above issues please refer to Sec. A of the Appendix or corresponding papers (Qian et al., 2021,

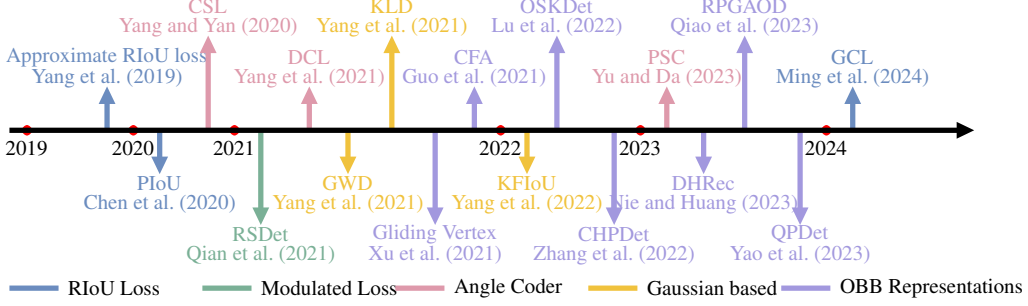


**Fig. 11** Chronological overview of oriented object detection methods for addressing OBB regression problems.

2022; Yang et al., 2021, 2022; Xu et al., 2021). To tackle these issues, existing oriented object detection methods usually develop novel loss functions or or alternative representations for OBB. Several representative methods are shown in Fig. 11. Next, we will briefly introduce them and discuss their pros and cons.

## 4.1 Regression Loss

(1) **Inconsistency between Metric and Loss.** The inconsistency between metric and loss generally implies that an optimum choice for the regression task may not guarantee a high localization accuracy in terms of IoU. To bridge this gap, existing generic object detectors generally introduce IoU-induced loss functions, such as GIoU (Rezatofighi et al., 2019) and DIoU (Zheng et al., 2020). However, these IoU-induced losses cannot be incorporated directly into oriented object detection due to the in-differentiable nature of RIoU (Yang et al., 2021). Thus, several differentiable functions are designed to approximate RIoU loss (Yang et al., 2019, 2021, 2022). PIoU (Chen et al., 2020) introduces a differentiable kernel function that accumulates the contribution of interior overlapping pixels to approximate the intersection area. Several solutions (Yang et al., 2019, 2022, 2021) integrate RIoU as a loss weight of the regression loss:

$$L_{RIoU} = \frac{L_{reg}}{|L_{reg}|} \cdot |g(RIoU)| \quad (1)$$

$L_{reg}$  denotes the commonly used smooth L1 loss (Ren et al., 2015, 2017).  $g(\cdot)$  is a loss function related to RIoU, *e.g.*,  $-\log(\cdot)$ . Such a loss is composed of a normalized regression loss  $\frac{L_{reg}}{|L_{reg}|}$  controlling the direction of gradient propagation, and a scalar  $g(RIoU)$  adjusting gradient magnitude. When the RIoU is close to 1,  $g(RIoU) \approx 0$ , and  $L_{reg}$  is approximately equal to 0, effectively mitigating the inconsistency between the metric and regression loss.

Apart from designing regression loss to approach RIoU, Ming et al. (2024) analyze the gradient of RIoU loss and propose the Gradient Calibration Loss (GCL). GCL constructs a corrected gradient w.r.t RIoU, angular error, and scale, and then calculates the optimized regression loss through integration. Despite these efforts, angle regression still faces challenges, particularly the problem of PoA.

(2) **Angular Boundary Discontinuity.** Owing to PoA, the regression loss will sharply increase when the angle approaches its boundary or the aspect ratio closes to 1, seriously confusing the networks and causing training instability. Thus, several methods have been proposed to address these issues, which can be divided into three types:

*Modulated rotated loss* (Qian et al., 2021, 2022). The modulated Rotated loss adds an extra loss item based on the naïve regression loss to eliminate the angular boundary discontinuity. Specifically, it first transforms the original predicted OBB  $b_p = (x_p, y_p, w_p, h_p, \theta_p)$  to another form  $b'_p = (x_p, y_p, h_p, w_p, \theta_p - \frac{\pi}{2})$ <sup>1</sup>, and then take the minimum of their regression loss, *i.e.*,  $\min \{L_{reg}(b_p, b_g), L_{reg}(b'_p, b_g)\}$ , where  $b_g$  denotes the corresponding GT. Such a scheme can adaptively choose the appropriate representation of the predicted OBB making the smallest loss value, thereby mitigating the sudden increase in loss near angular boundaries. However, this approach does not fully resolve the metric-loss inconsistency.

*Angle coder* (Yang and Yan, 2020; Yang et al., 2021; Yu and Da, 2023, 2024). The circular smooth label (CSL) approach discretizes angles into intervals and predicts a discrete angle via classification (Yang and Yan, 2020). Besides, to increase the error tolerance to adjacent angles and handle the PoA, CSL uses a window function for angle label smoothing. Although CSL eliminates the boundary discontinuity, its heavy prediction layer harms the efficiency. To tackle these issues, Yang et al. (2021) further adopt Densely Coded Labels (DCL) to reduce the code length. Furthermore, Wang et al. (2022) analyze the limitations of CSL when directly applying continuous Focal Loss functions (Lin et al., 2017, 2020) to the soft labels of angle classification. Specifically, when the label  $y \neq 1$ , the extreme point of the derivative of Focal Loss functions  $FL(x)$  is not at  $x = y$ , causing inaccurate angle prediction. Thus, Gaussian focal-CSL (GF-CSL) is designed to obtain more accurate angle predictions with higher responses at peaks via adaptive Gaussian attenuation on the negative angle categories. However, the hyper-parameters have a significant impact on the performance of these methods. Even worse, the optimal settings on different datasets are also different thereby requiring laborious tuning.

To solve this problem, Yu and Da (Yu and Da, 2023, 2024) design a differentiable angle coder, named Phase-Shifting Coder (PSC). PSC encodes the angle into a periodic phase to solve the boundary discontinuity problem. Moreover, an advanced version, PSCD, maps angles into phases of different frequencies to further solve the square-like problem.

*Gaussian distribution based methods* (Yang et al., 2021; Yang et al., 2022; Yang et al., 2021, 2022). The Gaussian distribution based methods provide a unified and elegant solution to the problems of boundary discontinuity and the square-like problem. First, the OBB  $b = (x, y, w, h, \theta)$  is converted to a 2-D Gaussian distribution  $\mathcal{N}(m, \Sigma)$ , where  $m = (x, y)$  and  $\Sigma$  is a matrix associated with  $w, h, \theta$ :

$$\Sigma^{\frac{1}{2}} = \begin{bmatrix} \frac{w}{2} \cos^2 \theta + \frac{h}{2} \sin^2 \theta & \frac{w-h}{2} \cos \theta \sin \theta \\ \frac{w-h}{2} \cos \theta \sin \theta & \frac{h}{2} \cos^2 \theta + \frac{w}{2} \sin^2 \theta \end{bmatrix} \quad (2)$$

---

<sup>1</sup>It is noteworthy that the modulated rotated loss is customized for OBB representation under the OpenCV definition, which is intractable to the exchangeability of edges and PoA.

Then a distance function is used to measure two Gaussian distributions, such as Gaussian Wasserstein Distance (GWD) (Yang et al., 2021) or Kullback-Leibler Divergence (KLD) (Yang et al., 2021). Furthermore, the measure is converted into an approximate IoU loss using a nonlinear transformation to obtain metric-loss consistency. The merit of Gaussian distribution is that the angle is encoded by trigonometric function thereby not constrained by PoA. Moreover, the OBB parameters are joint-optimized dynamically so that they can influence each other during training.

Despite their advantages, both GWD and KLD only maintain value-level consistency instead of trend-level consistency between RIoU and regression loss. To achieve better trend-level alignment, the KFIOU loss is proposed, which is differentiable and does not require additional hyperparameters. KFIOU can calculate the overlapping area between two Gaussian distributions, resulting in improved performance compared to GWD and KLD.

## 4.2 OBB Representations

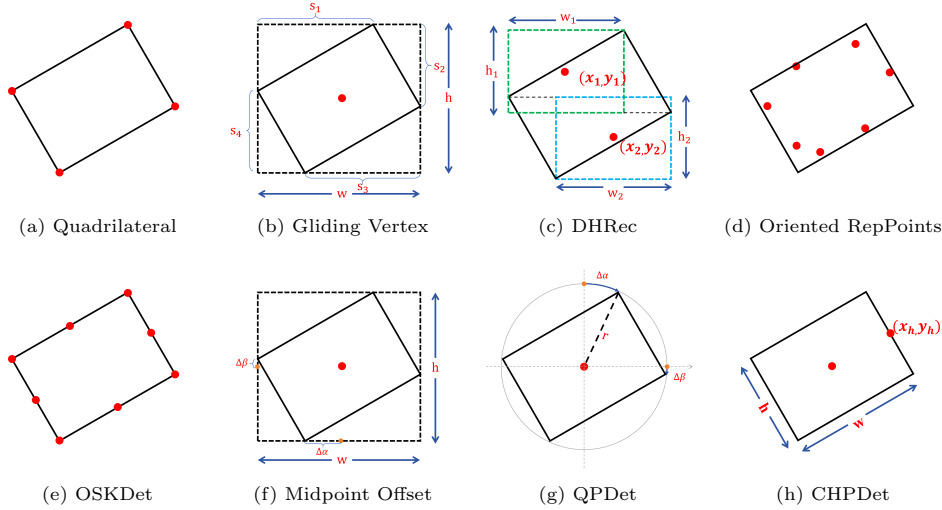


**Fig. 12** Comparison of different OBB representation methods. The red dots and parameters denote corresponding OBB parameters.

To handle the angular boundary discontinuity, the most straightforward approach is to design a novel OBB representation. One common scheme exploits new parameters to redefine the OBB, *e.g.*, quadrilateral representation (Xu et al., 2021), DHRec (Nie and Huang, 2023). The quadrilateral representation adopts coordinates of four vertices to represent OBB but suffers from the inconsistency of vertex sorting<sup>2</sup> between predictions and GT, as shown in Fig. 12a. RSDet (Qian et al., 2021, 2022) mitigates this by introducing a modulated loss that considers different vertex orderings, minimizing the

<sup>2</sup>For more detail please refer to Sec. B of the Appendix.

**Table 2** Comparison of different OBB representation methods.

Methods	Advantages	Disadvantages
Quadrilateral representation (Xia et al., 2018; Qian et al., 2021, 2022)	A direct method that can compactly enclose oriented objects with large deformation and has been widely adopted to annotate objects in large-scale RS datasets.	It suffers from the inconsistency of vertex sorting, and can only represent irregular quadrilaterals, but not rectangles.
Gliding Vertex (Xu et al., 2021)	A concise but effective method that can eliminate vertex sorting.	It can only represent irregular quadrilaterals, but not rectangles. It cannot accurately represent nearly horizontal objects.
DHRec (Nie and Huang, 2023)	It can directly use horizontal object detectors to regress OBBs, thus freeing it from the trouble of PoA and vertex sorting.	It requires too many parameters to ensure the uniqueness of OBB representation.
CFA and Oriented RepPoints (Guo et al., 2021, 2022; Li et al., 2022)	The adaptive points learning method can capture the geometric information of oriented objects and avoid vertex sorting and PoA.	It requires complicated post-processing operations to convert reppoints into an OBB.
OSKDet (Lu et al., 2022)	The keypoints can capture the critical features of vertex and edge area, which could better match the object shape. The unordered keypoints representation scheme can avoid the confusion of vertex sorting.	It requires complicated post-processing operations to convert irregular keypoints into an OBB.
Midpoint Offset (Xie et al., 2021)	A concise yet effective OBB representation method that can eliminate PoA.	It generally generates a parallelogram and requires a post-processing procedure for regularization.
QPDet (Yao et al., 2023)	A simple OBB representation method, needing just five parameters, which can avoid the generation of irregular bounding boxes.	It will suffer from new PoA of $\Delta\alpha$ and $\Delta\beta$ when representing nearly horizontal objects.
CHPDet (Zhang et al., 2022)	Employ a head point to indicate the direction, effectively eliminating PoA.	The accuracy of the orientation depends on the precision of the center point and the head point. When the positions of either are inaccurate, it will affect the overall precision of the target’s location.

regression loss across these variations. Furthermore, Xu et al. (2021) propose an effective way by gliding the vertex of the horizontal anchor on each corresponding side, as shown in Fig. 12b. Specifically, it regresses four length ratios representing the gliding offset on each corresponding side, eliminating the confusion caused by vertex sorting. To remedy the confusion for nearly horizontal objects, it directly selects horizontal detection guided by the predicted obliquity factor, albeit with slight imprecise regression. DHRec (Nie and Huang, 2023) encodes the OBB using double HBBs derived from the sorted horizontal and vertical coordinates, as shown in Fig. 12c. Hence, such a method allows harnessing any horizontal object detector to predict OBB.

In addition, several anchor-free methods utilize keypoints to denote an OBB, which can provide rich semantic features for oriented objects. Following the RepPoints (Yang et al., 2019), CFA (Guo et al., 2021, 2022) and Oriented RepPoints (Li et al., 2022) utilize the deformable convolution (Dai et al., 2017) to generate a group of reppoints, as shown in Fig. 12d. A minimum bounding rectangle is then computed for each set

of predicted reppoints to yield detection results. OSKDet (Lu et al., 2022) encodes 8 ordered points (4 vertices and 4 midpoints) to represent an OBB based on the consideration that the object has more obvious features at the vertex and edge areas, as shown in Fig. 12e. Furthermore, an orientation-sensitive heatmap is designed to better fit the shape, allowing the model to learn the orientation and shape implicitly.

Despite the angular discontinuity has been eliminated, the redesigned OBB representations still have their limitations. Quadrilateral representation is irregular and DHRec adds extra position and oblique factors to ensure the uniqueness of the representations. Meanwhile, the keypoints rely on a complicated post-processing operator to generate a rectangular box.

Therefore, there is another scheme for OBB representation that only uses extra parameters to determine the orientation of objects. The classical Midpoint Offset representation (Xie et al., 2021) infers orientation via midpoint offset, as shown in Fig. 12f, but typically produces parallelograms requiring regularization. Based on Midpoint Offset representation, Qiao et al. (2023) analyze the geometric relationship between the OBB and its external HBB to derive the height directly from the width and two offsets, only using five parameters to generate the high-quality OBB directly from the horizontal anchors. QPDet (Yao et al., 2023) adopt two symmetrical offsets w.r.t the quadrant points to account for rotation and aspect ratio, and a single parameter (radius  $r$ ) controls the scale, as shown in Fig. 12g. CHPDet (Zhang et al., 2022) define a head point to indicate the orientation but require proper annotations that specify the direction of the object head in the range of  $2\pi$ , as shown in Fig. 12h. These strategies of orientation representation can discard angle regression, thus naturally eliminating the angular boundary discontinuity. Additionally, the pros and cons of above OBB representation methods are summarized in Tab. 2.

### 4.3 Discussion

As stated above, an enormous amount of research effort is committed to resolving the challenges encountered by OBB regression. Redesigning novel regression loss for mainstream  $\theta$ -based representation empowers the detectors to solve the inconsistency problem and eliminate the confusion caused by PoA, thereby enhancing the stability of network back-propagation. Especially, Gaussian distribution based methods draw upon the trigonometric encoder and joint optimization to achieve strong performance. On the other hand, novel OBB representation schemes can avoid orientation regression, in which the completely redefined OBB representations commonly rely on complex post-processing or extra constraints, while the orientation representations provide a simple yet efficient way to determine the orientation. Nevertheless, only a handful of novel OBB representation schemes take into account the inconsistency problem.

## 5 Feature Representation

Robust and discriminative feature representations play a pivotal role in improving both localization and classification. As a result, the most recent improvements in detection accuracy have been via research into enhancing feature representation through innovative network architectures. In this section, we review the effort devoted to improving

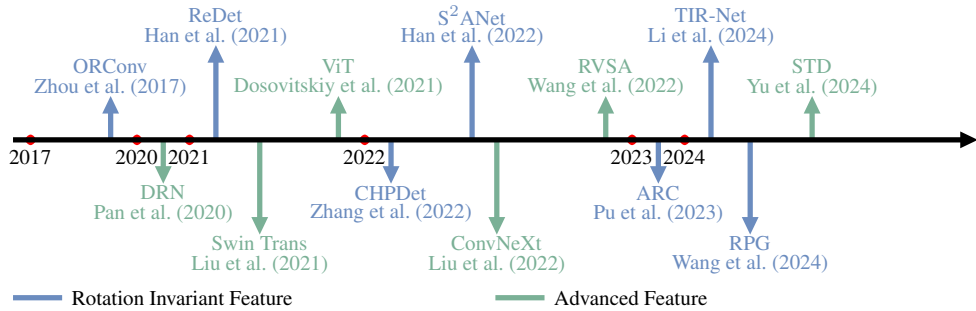


**Fig. 13** Chronological overview of feature representation methods.

feature representations of oriented objects, *i.e.*, rotation-invariant feature representation, and advanced feature representation. Several milestone methods are shown in Fig. 13.

## 5.1 Rotation-Invariant Feature Representations

Rotation-invariance is an essential problem when learning visual feature representations for oriented objects (Lowe, 2004; Han et al., 2021; Yu et al., 2024). The commonly used approaches, including RRoI operators (Ma et al., 2018; Yang et al., 2018; Ding et al., 2019) and random rotation data augmentation (Han et al., 2021), are sub-optimal, as they can only extract approximately rotation-invariant features (Lenc and Vedaldi, 2015; Worrall et al., 2017).

Recently, the exploration of rotation-sensitive feature extraction networks bring new insight to the community, which utilize different channels to represent feature information from different orientations, *e.g.*, oriented response convolution (ORConv) (Zhou et al., 2017), group equivariant convolutional neural networks(G-CNN) (Cohen and Welling, 2016; Worrall et al., 2017; Marcos et al., 2017; Weiler and Cesa, 2019; Weiler et al., 2018). Building on this, several works, *e.g.*, RRD (Liao et al., 2018), CHPDet (Zhang et al., 2022), S<sup>2</sup>ANet (Han et al., 2022), replace ordinary convolution modules with ORConv to obtain orientation-dependent responses which are then transformed to rotation-invariant features using ORAlign and ORPooling. Additionally, ReDet (Han et al., 2021) incorporates G-CNN into the detector for rotation-equivariant feature generation, whereafter, a rotation-invariant roI align operator is designed to adaptively extract rotation-invariant features from equivariant ones according to the predicted orientations. Furthermore, Li et al. (2024) introduce selective rotation of the kernel (SKR) to enhance classification features. SKR module rotates the convolution kernel at different angles to extract rotation-invariant features, in which the output channel dimension of corresponding rotated convolution kernel is obtained by network learning adaptively.

In contrast to ORConv and G-CNN extracting features via static kernels oriented in a group of fixed orientations, ARC (Pu et al., 2023) rotates the convolution kernels dynamically according to the orientation of the objects, where the orientation is predicted in a data-dependent manner. As a result, ARC can capture the rotation

information of objects with different orientations and boost the feature representation under the oriented object detection scenario.

However, Wang et al. (2024) point out that cyclic shift phenomena exhibited by features after rotation-equivariant network are unstable due to the dilation and pooling operations. To maintain rotation-equivariant for features, a rotation-robust prototype generation (RPG) is designed, including a stabilization module and an enhancement module. The former aggregates features of different orientations to generate rotation-robust prototype, while the latter employ the prototype to enhance original features in each group.

## 5.2 Advanced Feature Representations

In addition to rotation-invariant networks, advanced feature extraction networks, particularly Vision Transformer (Vaswani et al., 2017; Dosovitskiy et al., 2021; Liu et al., 2021), have played a crucial role in high-precision detection. ConvNeXt (Liu et al., 2022) is another notable architecture that has also contributed to the field, though its discussion will be brief in this context.

Recently, Vision Transformer has achieved significant success in computer vision (Dosovitskiy et al., 2021; Liu et al., 2021; Han et al., 2023), primarily due to its self-attention mechanism that captures global feature representations. This exceptional capacity for feature representation lead to its increasing adoption in object detection, yielding remarkable results. Representative architectures like the ViT series (Dosovitskiy et al., 2021; Xu et al., 2021; Zhang et al., 2023) and Swin Transformer (Liu et al., 2021) can serve directly as the backbone networks, showing more excellent feature representation capability than CNN. Furthermore, the unsupervised pertaining scheme, MAE (He et al., 2022), makes notable progress in developing ViT for object detection. Consequently, the powerful Vision Transformer architectures contribute to establishing a solid foundation for delivering outstanding achievements in oriented object detection.

Nevertheless, their utilization in oriented object detection is fairly unexplored, *e.g.*, an essential problem is how to extract rotation-related features. Wang et al. (2022) addressed this by designing rotated varied-size window attention (RVSA) based on ViT, which adaptively generates locally oriented windows at different sizes, locations, and angles. Although RVSA outperforms all previous methods, it relies on the self-attention mechanism to create oriented windows, without explicitly leveraging guiding information.

STD (Yu et al., 2024), on the other hand, adopts a controlled scheme for manipulating the feature extraction process according to the decoupled OBB parameters, *i.e.*, center position, sizes, and angles. It follows a divide-and-conquer fashion that estimates the position, size, and angle via separate network branches at different stages. Further, the cascaded activation masks created by the decoupled OBB parameters are integrated to gradually enhance features extracted by stacked Transformer blocks. The progressive refinement of feature representation enables STD to reach state-of-the-art performance, achieving 82.24% and 98.55% mAP on DOTA-V1.0 (Xia et al., 2018) and HRSC2016 (Liu et al., 2016) datasets, respectively.

More recently, ConvNeXt (Liu et al., 2022) gradually modified the standard ResNet according to a series of design decisions of Swin Transformer (Liu et al., 2021) and demonstrated pure CNNs outperform the vision transformers in terms of accuracy and robustness. Meanwhile, ConvNeXt can maintain the efficiency of standard CNNs, thus becoming the dominant architecture in many applications.

### 5.3 Discussion

Investigation of feature representation can lead to the improvement of the whole object detection field. ORConv and G-CNN empower the model to mine rotation-invariant features by utilizing different channels to represent feature information from different orientations, while advanced feature extraction networks are dedicated to enhancing the semantic representation via powerful and well-designed architectures. Although the former is conducive to extracting rotation-invariant features in both spatial and channel dimensions, they are built on conventional CNN modules which fall behind the latter. Thus, it's crucial to validate the effectiveness of integrating the rotation-invariant feature extraction networks and advanced ones. We hope further research effort is conducted to explore more powerful rotation-invariant and high-level semantic feature representation for oriented object detection.

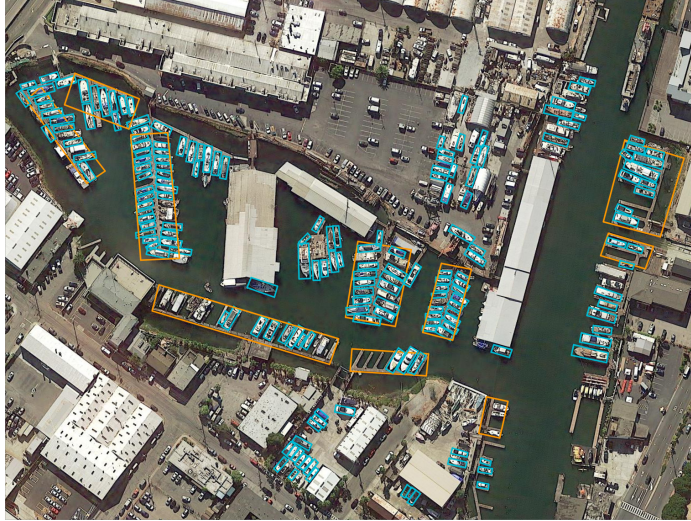
## 6 Common Issues in RS scenarios

In addition to the specific challenges associated with oriented object detection, several common issues still exist regarding RS scenarios, *e.g.*, complex background, scale variations, large aspect ratio, and lack of annotated samples, as shown in Fig. 14. Several representative methods for tracking these common issues are shown in Fig. 15.

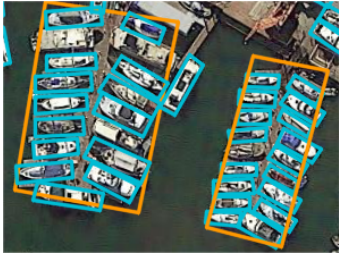
### 6.1 Complex Backgrounds

Due to the wide visual field and complex earth's surface, RS images typically contain a variety of complex backgrounds, causing significant interference in detection. Objects are frequently surrounded by different backgrounds, necessitating detectors with heightened discriminative capabilities. Besides, the presence of backgrounds with textures and shapes resembling the objects leads to a high incidence of false positives.

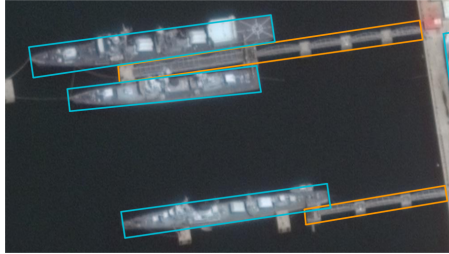
To this end, a series of efforts have been made to suppress background noise and emphasize the valuable areas of the objects. CFC-Net (Ming et al., 2022) and PETDet (Li et al., 2024) both combine channel attention and spatial attention modules to learn the semantic correlation between foreground and background. However, these methods rely on a self-attention mechanism and lack direct foreground guidance. To enhance the discrimination of foreground, Zhang et al. (2022) proposes a foreground relation module for foreground-contextual representations under the supervision of the designed foreground map. Similarly, CBDA-Net (Liu et al., 2022) builds two parallel spatial attention streams to capture center and boundary attention features, which could assist detectors in improving object localization accuracy. Besides, SCRDet (Yang et al., 2019) adopts the pixel attention network to generate a saliency map that can separate foreground from background, and use Squeeze-and-Excitation



(a) Complex backgrounds



(b) Scale variations



(c) Large aspect ratio

**Fig. 14** Illustration of common issues in RS scenarios (Xia et al., 2018; Ding et al., 2022). (a)~(c) Examples of complex backgrounds, scale variations, and large aspect ratio, respectively.

(SE) blocks (Hu et al., 2020) as the channel attention network to enhance the saliency map further.

Building on SCRDet, SCRDet++ (Yang et al., 2022) proposes an instance-level denoising (InLD) module that weakens the feature response of the background region while decouples the features of different categories into their corresponding channels. Similar to InLD, several methods (Zhang et al., 2023; Yu et al., 2023; Yao et al., 2024; Zheng et al., 2024) introduce semantic mask modules that is supervised by the class-wise mask transformed from the oriented GT. The semantic mask modules separate the features of different categories in channel dimension, which can facilitate the networks to reduce both the background and interclass interference.

## 6.2 Scale Variations

As the ground sampling distance (GSD) can range from a few centimeters to hundreds of meters, the RS images taken by different sensors usually have large-scale variations. Additionally, even within the same category, object instances exhibit wide-ranging

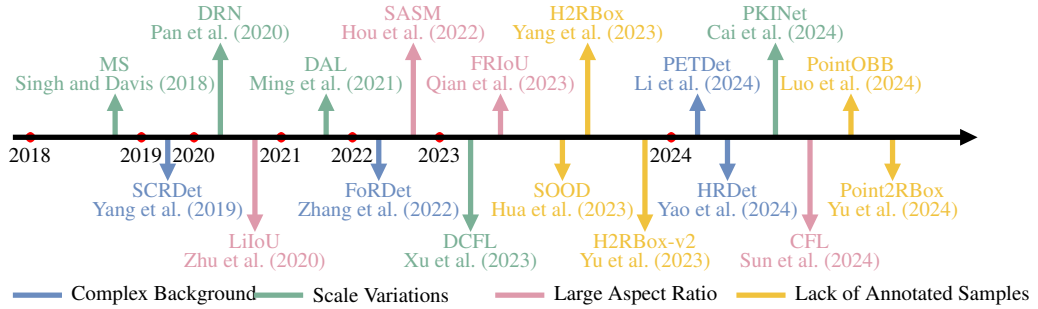


**Fig. 15** Chronological overview of oriented object detection methods for tracking common issues.

sizes. These inter-class and intra-class scale variations pose additional challenges. Especially, the most critical challenge mainly focuses on small objects due to their insufficient feature information, inaccurate localization, and inadequate positive samples (Cheng et al., 2023). Worse still, things get tougher when it comes to oriented objects due to the extra orientation regression and limited overlaps with anchor boxes.

In recent years, a large number of effective strategies have been made to enhance the robustness and adaptability of detectors for objects with various scales, which can be classified into two categories: network-level and data-level methods. Network-level methods are committed to developing novel network structures for multi-scale features extraction, *e.g.*, feature pyramid architectures (Lin et al., 2017) and its variants (Tian et al., 2024), and multi-branch architectures (Li et al., 2019; Pan et al., 2020; Cai et al., 2024). Pan et al. (2020) design a feature selection module to adjust receptive fields, which proposes a channel attention network to adaptively fuse the feature extracted by using kernels of various sizes, aspect ratios, and orientations. PKINet (Cai et al., 2024) employs parallel multi-scale convolution kernels without dilation to effectively capture features across varying receptive fields. Data-level methods, on the other hand, strive to design data augmentation strategies that are independent of the network architectures and can be generalized to any detectors. Multi-scale training and testing is a useful data augmentation approach that scaling input images at different resolutions (Singh and Davis, 2018; Singh et al., 2018), has been shown to reduce overfitting and improve generalization (Ren et al., 2015, 2017; Russakovsky et al., 2015). However, it will inevitably lead to poor time efficiency.

Beyond enhancing the semantic representation or amplifying object size, several optimal assignment strategies have emerged to enable adequate sample assignments for small-oriented objects. Since the anchor-free methods can generate more positive samples of small objects that are apt to be ignored in the anchor-based methods. Consequently, approaches like APE (Zhu et al., 2020) and AOPG (Cheng et al., 2022) generate samples in an anchor-free manner, refining them for high-quality detection results. Liang et al. (2022) propose a dynamic enhancement anchor network that combines the advantages of anchor-free and anchor-based methods and uses an interactive sample screening procedure to yield higher-quality training samples.

Rather than relying on IoU alone, several methods (Ming et al., 2021; Zhang et al., 2023; Fu et al., 2024; Huang et al., 2024) collaborate the prior (*e.g.*, IoU between anchor and GT) and posterior information (*e.g.*, classification and localization confidence) as the evaluation criteria to screen positive samples. Such a scheme can push the detectors to dynamically mine high quality anchors as positive. In contrast to using static priors (*e.g.*, anchor boxes or points) with fixed stride, Xu et al. (2023) design a dynamic prior with a coarse-to-fine assigner. Concretely, it first uses deformable convolution (Dai et al., 2017) to adaptively adjust the prior location and then leverages the coarse prior matching and finer posterior constraint to dynamically assign samples. Such a strategy can adaptively assign positive or negative samples according to the objects’ shape and posterior information, boosting the performance of mainstream detectors on small objects.

### 6.3 Large Aspect Ratio

RS images frequently encompass several categories with extremely large aspect ratios, such as bridges, ships, and harbors. The RIoU between these categories with anchors exhibit significant sensitivity to orientation errors, thereby causing two primary challenges, *i.e.*, spatial misalignment and inaccurate localization.

Accordingly, a series of well-designed assignment strategies and regression loss are proposed to remedy corresponding issues. Zhu et al. (2020) introduce length-independent IoU (LiIoU). LiIoU intercepts part of the object box along its long side based on the length of the anchor, and subsequently calculates the IoU between the intercepted object box and anchor. It facilitates the assignment of more positive samples to long objects compared to the conventional IoU, thereby enhancing the recall rate. Qian et al. (2023) emphasize that the sampling locations of positive samples should be close to the center distribution of the oriented GT. This is because that two horizontal anchors, despite having the same IoU with the external HBB of an oriented GT with large aspect ratio, can differ considerably in their coverage of the GT. Consequently, Qian et al. (2023) and Wang et al. (2024) both combine the horizontal IoU and sample feature alignment overlap to evaluate the quality of anchor, in which the sample feature alignment overlap is defined as the ratio of the intersection between the horizontal anchor and the oriented GT to the GT itself, reflecting the overlap proportion of oriented object features.

Furthermore, inspired by ATSS (Zhang et al., 2020), SASM (Hou et al., 2022) and CFL (Sun et al., 2024) use a monotonic decreasing function of aspect ratio as a weight for the IoU threshold that controls the sample assignment. This approach allows long objects to be assigned a lower IoU threshold. Additionally, several methods (Liu et al., 2022; Qiao et al., 2023; Gong et al., 2024; Xie et al., 2024) construct the weighted orientation loss that depend on aspect ratio, effectively mitigating the effect of aspect ratio on orientation regression.

## 6.4 Lack of Oriented-Annotated Samples

Relying on massive and laborious annotations, oriented object detection have shown significant advancement in recent years. However, OBB annotation is a time-consuming and expensive process, resulting in many detection datasets that use HBB annotations not providing OBB annotations, thereby restricting the potential scope of the application. To alleviate the annotation burden, researchers have explored two avenues: weakly supervised learning, in which OBB annotations are replaced by HBB-level or even point-level annotations, and semi-supervised learning, in which only a few images from the whole training dataset are annotated.

Mainstream semi-supervised oriented object detection methods commonly follow the pseudo-labeling framework, consisting of a teacher model and a student model. The teacher model, an Exponential Moving Average (EMA) (Tarvainen and Valpola, 2017) of the student model at historical training iterations, generates pseudo-labels on unannotated images. They are trained iteratively by the following steps: Teacher model provides pseudo-labels for unannotated images in a batch, while student model makes predictions for both annotated and unannotated ones. Then, computing loss for the student model’s predictions. However, the unsupervised nature of the teacher model introduces noise that can mislead the student model’s training, especially considering the arbitrary orientations of objects, which further impacts pseudo-label quality. Therefore, current semi-supervised oriented object detection methods (Hua et al., 2023; Wang et al., 2024; Wu et al., 2024) are committed to generating high-quality pseudo-labels.

SOOD (Hua et al., 2023) introduces two loss functions, termed rotation-aware adaptive weighting (RAW) loss and global consistency (GC) loss. RAW focus on the orientation consistency between each pseudo-label-prediction pair, dynamically weighting each them by their orientation gap. GC measures the global similarity between the pseudo-labels and the predictions, effectively mitigating the noise disturbance and implicitly regularizes object relations. Wang et al. (2024) provides an in-depth analysis of the limitation of conventional pseudo-labels and dense pseudo-labels (Zhou et al., 2022) methods. The former adopts a fixed threshold, while the latter uses a fixed quantity, both failing to adaptively select high-quality pseudo-labels. To address this, Global Focal Learning is proposed to judge important regions based on the difference between the prediction of teacher model and student model, guiding the networks to focus more on inconsistent regions during the training. Besides, Pseudo-Siamese Teacher (Wu et al., 2024) adopts two teacher models updated by different optimizations to improve reliability of pseudo-labels, using Jensen-Shannon divergence to eliminate inconsistent pseudo-labels.

Mainstream weakly-supervised oriented object detection methods commonly consist of multiple branches respectively fed with multiple augmented views of the input image. Then, various consistent losses are designed to align the features or predictions of different views. H2RBox (Yang et al., 2023), the first HBB annotation-based weakly-supervised method, follows a weakly- and self-supervised angle learning paradigm. The weakly-supervised part calculates regression loss between the external HBB of predicted OBB and horizontal GT, while the self-supervised part measures the consistency of the predicted angles in two views with different rotation augmentation. Based

on H2RBox, H2RBox-v2 (Yu et al., 2023) leverages reflection symmetry to learn the orientation of objects in a self-supervised manner. Furthermore, a CircumIoU loss is designed, empowering H2RBox-v2 compatible with random rotation augmentation.

Compared to OBB and HBB annotations, point annotations show lower costs and higher efficiency<sup>3</sup>. The main challenge of point annotation-based method lies in enabling the model to perceive the orientation and scale of the objects based on point annotations. PointOBB (Luo et al., 2024) design a resized view (by random scaling) and a rot/flip view (by random rotating or vertical flipping) based on original view. Upon these three views, a scale augmentation module and an angle acquisition module are constructed. The former aims to perceive object scale by improving the consistency of predicted scores between original and resized views, while the latter incorporates self-supervised angle learning to predict angles.

Furthermore, Yu et al. (2024) present Point2RBox, including Synthetic Pattern Knowledge Combination and Transform Self-Supervision. The former first generates synthetic patterns with known boxes by sampling around each labeled point, and then overlaid these patterns on the original image, providing the knowledge for network to estimate the size and angle. The latter is similarly to PointOBB, which uses original and transformed (randomly selected from rotate, flip, and scale) view to perceive the size and orientation between objects. In addition, Zhang et al. (2024) propose a progressive method, named Point-to-Mask-to-HBB-to-OBB (PMHO), to achieve oriented object detection. However, this framework is time-consuming, with each component being optimized independently, relying heavily on the capabilities of well-trained models such as SAM (Kirillov et al., 2023).

## 6.5 Discussion

Complex background, scale variations, large aspect ratio, and lack of oriented-annotated samples are crucial issues in RS object detection tasks, which evolve more severely when it comes to oriented object detection tasks. As stated above, a number of works have been proposed to tackle these issues from various perspectives, *e.g.*, data augmentation, assignment strategies, re-weighted orientation loss, attention mechanism, self-supervised loss, and pseudo-labeling framework. Unfortunately, exploration into solutions for these issues is far from mature and so further research may be beneficial. For instance, there is still a significant performance gap in detecting small/long and normal objects even for state-of-the-art detectors. On the other hand, the general split-and-detect scheme is inefficient during inference due to too many empty patches that only contain background. Several prior works have provided preliminary consideration on these points, *e.g.*, super-resolution-based object detection (Shermeyer and Van Etten, 2019; Liu et al., 2023; Zhang et al., 2023), focus-and-detect schemes (Duan et al., 2021; Koyun et al., 2022). Additionally, the accuracy of semi/weakly-supervised oriented object detection is still far from satisfactory, lagging significantly behind the fully supervised methods. Combining weakly-supervised and semi-supervised methods may bring new breakthroughs (Wu et al., 2024).

---

<sup>3</sup>According to <https://cloud.google.com/ai-platform/data-labeling/pricing>, the cost of point annotations is about 50.0% lower than HBB and 104.8% lower than OBB, and their time-consuming is just 1.2x more than image-level annotations

## 7 Evaluation Protocol and Datasets

### 7.1 Evaluation Protocol

Accuracy and efficiency are both the most crucial criteria in evaluating the performance of oriented object detectors. The evaluation protocol for OBB is slightly different from that for HBB as IoU is replaced with RIoU. Efficiency evaluation uses frame per second (FPS), defined as the number of image frames processed by a detector per second, while accuracy evaluation takes into account both precision and recall. The most universally agreed metric for accuracy evaluation is average precision (AP).

For the object detection task, the detector outputs  $M$  predicted results  $\{(b_j, c_j, s_j)\}_{j=1}^M$ , wherein each item contains an OBB  $b_j$ , and a category label  $c_j$  with corresponding confidence score  $s_j$ . Then, the predicted results are assigned to GT objects  $\{(b_k^*, c_k^*)\}_{k=1}^N$  based on RIoU and category, where  $b_k^*$ ,  $c_k^*$  and the superscript  $*$  denotes the OBB, category label, and GT respectively. A predicted result  $(b_j, c_j, s_j)$  which is assigned a GT object  $(b_k^*, c_k^*)$  is judged to be a true positive (TP) if the following criteria are met:

- (1) The predicted label  $c_j$  is in accordance with the label  $c_k^*$  of GT object.
- (2) The RIoU between the predicted OBB  $b_j$  and the GT OBB  $b_k^*$ , denoted by  $\text{RIoU}(b, b^*)$ , is not smaller than the predefined RIoU threshold  $T_{\text{RIoU}}$ . Otherwise, it is regarded as a false positive (FP).

Once the number of TP and FP has been obtained, precision and recall can be calculated. Precision is the proportion of correctly predicted instances among the total predicted results, while recall is the proportion of all positive instances predicted by the detector among the total GT objects. The formulas are defined as follows:

$$\text{Prec}(T_s) = \frac{N_{TP}}{N_{TP} + N_{FP}} \quad (3)$$

$$\text{Rec}(T_s) = \frac{N_{TP}}{N_{TP} + N_{FN}} = \frac{N_{TP}}{N} \quad (4)$$

where  $N_{TP}$ ,  $N_{FP}$ , and  $N_{FN}$  denote the number of TP, FP, and false negative (FN), respectively, which are determined by score threshold  $T_s$  and  $T_{\text{RIoU}}$ . Note that the precision and the recall are functions of the confidence threshold  $T_s$  with a fixed  $T_{\text{RIoU}}$ .

However, neither precision nor recall can evaluate the accuracy of a detector independently, while AP can combine both precision and recall. For each category, by varying  $T_s$  from 1.0 to 0.0 gradually, the recall increases as  $N_{TP}$  increases, and a list of pairs  $(\text{Prec}, \text{Rec})$  can be obtained. This allows precision to be considered as a discrete function of recall, *i.e.*, the precision-recall curve (PRC), denoted by  $P(R)$ . The AP value is obtained by computing the average value of precision  $P(R)$  over the interval from  $R = 0.0$  to  $R = 1.0$ :

$$\text{AP} = \frac{1}{N} \sum_{n=0}^{\text{Rec}(0)} \max_{R \geq \frac{n}{N}} P(R) \quad (5)$$

Ultimately, to evaluate the overall accuracy of all categories, the mean AP (mAP) averaged over all categories is adopted as the final metric of evaluation.

**Table 3** Comparison of public RS image datasets.

	Dataset	Publication	Category	Quantity	Instance	GSD	Resolution
Early	SZTAKI-INRIA (Benedek et al., 2012)	TPAMI 2012	1	9	665	-	$600 \times 500 \sim 1,400 \times 800$
	3K vehicle (Liu and Mattyus, 2015)	GRSL 2015	1	20	14,235	0.13m	$5,516 \times 3,744$
	UCAS-AOD (Zhu et al., 2015)	ICIP 2015	2	2,420	14,596	-	$1,280 \times 659$
	VEDAI (Razakarivony and Jurie, 2016)	JVCIR 2016	9	1,210	3,640	0.125m	$1,024 \times 1,024$
	HRSC2016 (Liu et al., 2016)	GRSL 2016	25	1,070	2,976	0.4~2m	$300 \times 300 \sim 1,500 \times 900$
	DOTA-V1.0 (Xia et al., 2018)	CVPR 2018	15	2,806	188,282	0.1~4.5m	$800 \times 800 \sim 20,000 \times 20,000$
Modern	DOTA-V1.5	—	16	2,806	403,318	0.1~4.5m	$800 \times 800 \sim 20,000 \times 20,000$
	DOTA-V2.0 (Ding et al., 2022)	TPAMI 2022	18	11,268	1,793,658	0.1~4.5m	$800 \times 800 \sim 29,200 \times 27,620$
	FGSD (Chen et al., 2020)	arxiv 2020	43	5,634	2,612	0.12~1.93m	$930 \times 930$
	ShipRSImageNet (Zhang et al., 2021)	JSTAR 2021	50	3,435	17,573	0.12~6m	$930 \times 930 \sim 1,400 \times 1,000$
	DIOR-R (Cheng et al., 2022)	TGRS 2022	20	23,463	192,518	0.5~30m	$800 \times 800$
	DroneVehicle (Sun et al., 2022)	TCSVT 2022	5	56,878	953,087	-	$640 \times 512$
	FAIR1M (Sun et al., 2022)	ISPRS 2022	37	42,796	>1,000,000	0.3~0.8m	$600 \times 600 \sim 10,000 \times 10,000$
	GLH-Bridge (Li et al., 2024)	TPAMI2024	1	6,000	59,737	0.3~1.0m	$2,048 \times 2,048 \sim 16,384 \times 16,384$

## 7.2 Datasets

Recently, several research groups have released dozens of high-quality RS image datasets, each of which dramatically boosts the development of RS object detection. Datasets annotated only with HBBs are not covered here, including DIOR (Li et al., 2020), LEVIR (Zou and Shi, 2018), NWPU VHR-10 (Cheng et al., 2014), RSOD (Xiao et al., 2015; Long et al., 2017), xView (Lam et al., 2018), and HRRSD (Zhang et al., 2019). In addition, several oriented object detection datasets with horizontal views, e.g., text detection datasets (Karatzas et al., 2015), and datasets from different modalities, like SAR datasets (Wei et al., 2020; Lei et al., 2021), exhibit significant differences in viewing angles, scenes, and imaging characteristics when compared to optical remote sensing datasets. Thus, this paper will not introduce these datasets. In this subsection, we only focus on introducing optical RS datasets annotated with OBBs, including SZTAKI-INRIA (Benedek et al., 2012), 3K vehicle (Liu and Mattyus, 2015), UCAS-AOD (Zhu et al., 2015), VEDAI (Razakarivony and Jurie, 2016), HRSC2016 (Liu et al., 2016), DOTA (Xia et al., 2018; Ding et al., 2022), ShipRSImageNet (Zhang et al., 2021), DIOR-R (Cheng et al., 2022), DroneVehicle (Sun et al., 2022), FAIR1M (Sun et al., 2022), and GLH-Bridge (Li et al., 2024). Tab. 3 statistics the parameters of the above RS oriented object detection datasets for intuitive comparison. Given that the emergence of DOTA greatly promotes the development of oriented object detection, we divide the dataset into two parts: early and modern datasets, based on the timeline of DOTA’s introduction. Only the most typical among the above datasets are described in detail due to the space restriction. For more details please refer to Sec. C of Appendix.

**DOTA** (Xia et al., 2018; Ding et al., 2022) contains large quantities of objects with a considerable variety of orientations, scales, and appearances. The images are selected from different sensors and platforms, including Google Earth, GF-2 Satellite, and UAVs. There are three versions of this dataset. The number of images and instances in three versions of DOTA are summarized in Tab. 4. DOTA-V1.0 (Xia et al., 2018) and DOTA-V1.5 share the same images, which are split into training, validation, and test subsets. As an extension of DOTA-V1.0, DOTA-V1.5 annotates extremely small instances whose sizes are equal to or less than 10 pixels. Compared with the previous versions, DOTA-V2.0 (Ding et al., 2022) contains more images collected from Google Earth, GF-2 Satellites, and aerial platforms. In addition, a large number of images are taken under an oblique view and a lower foreground ratio to approach

**Table 4** Comparison of the three versions of DOTA. The number of images and instances of each split subset is counted.

		V1.0	V1.5	V2.0
Images	Training	1,411		1,830
	Validation	458		593
	Test/Test-dev	937		2,792
	Test-challenge	-		6,053
	Total	2,806		11,268
Instances	Training	98,990	210,631	268,627
	Validation	28,853	69,565	81,048
	Test/Test-dev	60,439	121,893	353,346
	Test-challenge	-	-	1,090,637
	Total	188,282	403,318	1,793,658

the real-world application scenes. The number of instances has increased to about 1.8 million. Moreover, it contains two test subsets, namely test-dev and test-challenge. The latter comprises a greater number of object instances (around 1.1 million) and more complicated scenes, making the task more challenging.

**DIOR-R** (Cheng et al., 2022) is a large-scale dataset that contains 192,518 instances, covering 20 common categories with notable inter-class similarity and intra-class discrepancies. The previous version of DIOR-R, *i.e.*, DIOR (Li et al., 2020), was initially released in 2019 using HBB annotations. Later, in 2021, OBB annotations were added to form the DIOR-R dataset. There are 23,463 images chosen carefully from more than 80 countries thereby possessing richer variations in viewpoint, illumination, background, appearance, occlusion, etc. In particular, it contains some traffic infrastructures due to their significant value in transportation analysis, such as train stations, expressway service areas, and airports, as well as some common categories in the suburbs, such as dam and wind mill. In addition, the GSD ranges from 0.5m to 30m, causing a large range of size variations. Thus, the rich diversity among instances, images, and scales makes this dataset valuable for real-world tasks yet brings about challenges.

**Ship Datasets.** Recently, a series of ship datasets have drawn wide attention owing to the potential value of ship detection in fishing and maritime security. **HRSC2016** (Liu et al., 2016) is one of the most widely used datasets for evaluating algorithms of oriented object detection. It covers more than 25 categories of ships with large varieties of scales, orientations, appearances, shapes, and backgrounds (*e.g.*, sea, port). **FGSD** (Chen et al., 2020) is a new fine-grained ship detection dataset expanded based on HRSC2016. The instances are classified into 43 categories which are further divided into 4 high-level categories, including submarine, aircraft carrier, civil ship, and warship. Except for ships, a new category named dock is also annotated in this dataset for future research. **ShipRSImageNet** (Zhang et al., 2021) is the largest RS dataset for ship detection. It contains 3,435 images collected from xView (Lam et al., 2018), HRSC2016 (Liu et al., 2016), FGSD (Chen et al., 2020), Airbus Ship Detection Challenge, and Chinese satellites. A total number of 17,573 ships are divided into 50 categories. There are diverse spatial resolutions, scales, aspect ratios, backgrounds, and orientations in this dataset.

**DroneVehicle** (Sun et al., 2022) is a large-scale RGB-infrared cross-modal vehicle detection dataset captured by UAVs. This dataset is released to address vehicle detection challenges in smart city traffic management and disaster rescue, especially under conditions of insufficient lighting. The dataset includes two modalities: RGB images and infrared images, with an equal number of images in each modality, collectively forming image pairs. This dual-modal design can provide complementary information under different lighting conditions, *e.g.*, RGB images provide rich color information, while infrared images excel in low-light conditions, unaffected by darkness. Besides, it covers a wide range of scenarios from day to night, including urban roads, rural areas, residential areas, parking lots, etc., ensuring the diversity and practicality of the data.

**FAIR1M** (Sun et al., 2022) is currently the largest fine-grained object detection dataset for high-Resolution remote sensing images, containing more than one million instances and over 40,000 images. All instances in this dataset are carefully annotated with OBBs, covering 5 main categories and 37 fine-grained subcategories, such as different types of aircraft, ships, court, road, and vehicles. The images are sourced from different sensors and platforms, with target scenes covering hundreds of typical cities and towns as well as commonly used airports and ports globally, providing rich geographic information and practical application scenarios. The fine-grained annotations, intra-class variations and inter-class variations similarities, large ranges of sizes and orientations, and complex scenes make the dataset extremely challenging, while also promoting the development of object detection in the field of remote sensing.

**GLH-Bridge** (Li et al., 2024) is a large-scale bridge detection dataset comprising 6,000 very-high-resolution RS images sampled from diverse geographic locations around the globe. This dataset covers a wide range of scenarios and bridge types, enhancing its generalizability to real-world situations. Additionally, the various object scales and extreme aspect ratios poses a formidable challenge for oriented object detection methods.

### 7.3 Discussion

Early datasets often feature a limited number of instances and images, encompassing a narrow range of scenarios. Consequently, detection methods approach saturation in performance on these datasets, making them unable to provide reliable evaluations. Modern datasets generally encompass more challenging and general scenarios with relatively complex backgrounds. They not only cover an astonishing number of instances (up to millions) and fine-grained categories (*e.g.*, FGSD and FAIR1M), but also possess large-scale images (up to  $20,000 \times 20,000$  pixels), making them highly aligned with real-world application scenarios.

Both early and modern datasets play a pivotal role in propelling oriented object detection methods to new heights, making significant contributions to the field. HRSC2016 (Liu et al., 2016) is an early benchmark, but as detection methods reached their performance plateau on this dataset, it gradually fell out of favor. Although subsequent datasets, *e.g.*, FGSD (Chen et al., 2020) and ShipRSImageNet (Zhang et al., 2021), attempt to expand upon it, they failed to garner sufficient attention due to its relatively limited number of instances compared to those larger-scale datasets. DOTA-V1.0 (Xia et al., 2018), as the most representative datasets for oriented object

detection, serve as the most commonly used benchmark for evaluating the performance of detection methods. Subsequently, DOTA-V2.0 (Ding et al., 2022), characterized by its large scale and high level of challenge, and FAIR1M (Sun et al., 2022), which focuses on fine-grained oriented object detection, gradually become new benchmarks for evaluating the performance of cutting-edge methods.

Modern large-scale datasets provide a solid data foundation for the deployment and implementation of real-world applications. By utilizing large-scale datasets for pre-training and transfer learning, the development costs and time can be significantly reduced, while the recognition accuracy of oriented object detection models can be improved, facilitating their application in various fields.

**City management.** With the acceleration of urbanization and the continuous expansion of urban areas, traditional ground traffic monitoring systems gradually reveal their limitations in terms of delayed response. Leveraging their remarkable flexibility, UAVs are widely applied in traffic dispersion and traffic flow monitoring (Sun et al., 2022; Wang et al., 2022), emerging as a cutting-edge force in urban traffic management.

**Industrial inspection.** Industrial facilities such as bridges and wind turbines often require a significant amount of labor and time for inspections, posing challenges for manual inspections (Cheng et al., 2022; Li et al., 2024). Incorporating UAVs or satellites and intelligent detection technology can significantly improve inspection efficiency and ensure personnel safety.

**Port management.** Utilizing advanced image processing algorithms and object detection technology, various objects within the port area, such as ships and port facilities, can be automatically identified from satellite imagery, thereby optimizing port operational efficiency and enhancing safety (Liu et al., 2016; Zhang et al., 2021).

**Security surveillance.** The detection of critical objects in satellite imagery, such as airplane and airports, plays a vital role in security surveillance (Ding et al., 2022).

## 8 State-of-the-Art Methods

As a comprehensive survey on oriented object detection, this paper introduces recent advances and provides a structural taxonomy based on detection frameworks, OBB representations, and other strategies in Sections 3, 4, and 5, respectively. In this section, we select several publicly available detectors to compare them in a unified manner. Specifically, we take DOTA-V1.0 dataset since it contains almost all the typical challenges of this task, including arbitrary orientations, large-scale variations, and large aspect ratio. We report the performance of the state-of-the-art detectors in terms of mAP and show the crucial modules of each detector in Tab. 5. According to the performance comparison and previous discussion, we concentrate on the key elements that evolved in oriented object detection, including detection frameworks, OBB regression, feature representations, and common issues.

(1) **Detection Frameworks.** Two-stage detectors achieve the best performance in terms of mAP since they can extract accurate region-based features more suited for classification and regression tasks. The typical two-stage oriented object detection methods commonly designed a rotated proposal generation scheme to obtain more

accurate rotated proposals, such as RoI Transformer (Ding et al., 2019) and Oriented RCNN (Xie et al., 2021). Similarly, the majority of one-stage and anchor-free detectors introduce a refined stage to align features, including R<sup>3</sup>Det (Yang et al., 2021), S<sup>2</sup>ANet (Han et al., 2022), CFA (Guo et al., 2021, 2022), and Oriented Rep-Points (Li et al., 2022). Benefiting from the additional refined stage and the advanced loss functions, one-stage detectors can also reach approximate accuracy to two-stage detectors. Despite achieving State-of-the-Art performance in general object detection, DETR-based methods still lag behind other competitors in oriented object detection, even with more training epochs. This may be because the query paradigm could not cover rotated objects adequately. To this end, it is desirable to further investigate DETR-based methods to compete in this field.

(2) **OBB Regression.** Advanced loss functions are conducive to alleviating the problems caused by orientation parameters and achieving better regression, including Gaussian distance based loss (*e.g.*, GWD (Yang et al., 2021), KLD (Yang et al., 2021), KFIoU (Yang et al., 2022)). These methods draw upon the trigonometric encoder and joint optimization to achieve strong performance. On the other hand, there is a huge gap between different OBB representations, *e.g.*, the midpoint offset representation enable Oriented RCNN to outperform Rotated Faster RCNN by approximately 2 mAP in single-scale and multi-scale results. In addition, novel OBB representation methods elegantly avoid angular boundary discontinuity thus enhancing model performance, but they rely on complex post-processing and additional modules, including customized loss functions (*e.g.*, CIoU (Guo et al., 2021)) or assigner (*e.g.*, APAA (Li et al., 2022)). Therefore, advanced loss functions and OBB representations are crucial for improving regression accuracy.

(3) **Feature Representations.** As one of the most important components in oriented object detection, backbone networks play a critical role in learning high-level semantic feature representation. The most widely used backbone networks include ResNet (He et al., 2016; Xie et al., 2017) series and Transformer architectures (Dosovitskiy et al., 2021; Xu et al., 2021; Zhang et al., 2023; Liu et al., 2021). Although Transformer-based methods dominate the field of computer vision tasks, and significantly outperform CNN-based counterparts in oriented object detection, achieving state-of-the-art performance. Specifically, Oriented RCNN-RVSA (Wang et al., 2022) and Oriented RCNN-STD (Yu et al., 2024), as the top-performing detectors based on Transformer, surpass Oriented RCNN (Xie et al., 2021) by 1.22% and 2.22% in terms of mAP, respectively. Nevertheless, compared to CNNs, Transformers suffer from longer training convergence time and expensive computing costs.

(4) **Common Issues.** Attention mechanism and semantic mask modules are effective ways to reduce background noise and enhance object information, *e.g.*, SCRDet (Yang et al., 2019), TSH (Yu et al., 2023), HRDet (Yao et al., 2024). Regarding the issue of large aspect ratios, the re-weighted loss function and novel assignment strategies can effectively improve detection accuracy, *e.g.*, RPGAOD (Qiao et al., 2023), DFDet (Xie et al., 2024), CFL (Sun et al., 2024), CGCDet (Wang et al., 2024). These components will be removed during the inference process, thus they will not affect the inference

speed. On the other hand, as seen in Tab. 5, detectors with MS<sup>4</sup> achieve an average approximate 3% improvement in terms of mAP, proving that MS is a useful strategy to alleviate scale variations. However, MS suffers from extremely long times for training and inference, which are about 10 times that of SS. All in all, addressing common issues like background noise, large aspect ratios, and scale variations is crucial for improving oriented object detection.

## 9 Conclusions and Future Directions

Oriented object detection in RS images is an important and challenging task in the field of RS and has been actively investigated. As summarized in this survey, a variety of methods have been developed rapidly in recent years, showing remarkable progress. In this survey, we first review the evolution from horizontal to oriented object detection and summarize the typical challenges. Following that, we provide a structural taxonomy for detection frameworks and highlight milestone detectors. We also present a detailed elaboration of OBB regression and feature representations. Furthermore, we discuss the common issues in RS scenarios and corresponding methods. Finally, we summarize commonly used datasets and compare the excellent methods emerging in recent years.

Despite the rising prominence of artificial intelligence, deep learning has rapidly advanced the development of oriented object detection methods. However, due to the complex and ever-changing real-world scenarios, its performance still faces limitations, hindering robust and reliable practical applications. Over the years, a considerable amount of research effort has been dedicated to tackling the challenges of feature misalignment, spatial misalignment, OBB regression, as well as common issues (*e.g.*, complex background, scale variations, large aspect ratio, and lack of annotated samples). These efforts have led to marked improvements in detection performance. Nevertheless, it is imperative to acknowledge that a considerable gap persists between the current detection capabilities and the demands of practical applications. More critically, several issues remain insufficiently addressed, posing significant barriers to further advancements in oriented object detection technology.

**Low detection efficiency.** Detection efficiency stands as a pivotal factor in the real-world applications of detectors. Current state-of-the-art oriented object detection models are designed to be exceptional complexity to achieve superior detection accuracy. Nevertheless, their intricate network architectures markedly impede detection efficiency, rendering them unsuitable for real-time applications.

**Imbalance in datasets.** Modern datasets focus on general scenarios and contain images from a variety of different environments and contexts. While this diversity helps models learn a wider range of features, it may also lead to poor performance in specific scenarios (such as snow, fog, occlusion). Additionally, common scenes or objects may constitute the majority of the datasets, while rare or special scenes or objects may be scarce. This data imbalance issue may cause the model to develop biases towards certain scenes or objects during training, resulting in a degradation of performance.

---

<sup>4</sup>The multi-scale training and testing (MS) generally first resize the original images to three scales (*i.e.*, {0.5, 1.0, 1.5}), which are then cropped to patches of  $1,024 \times 1,024$  with a stride of 524. In contrast, the single-scale training and testing (SS) only crop the original images to patches of  $1,024 \times 1,024$  with a stride of 824.

**Table 5** Comparisons of state-of-the-art methods on DOTA-V1.0. (·)\* indicates the detection results provided by the MMRotate (Zhou et al., 2022). – indicates that the method follows the default modules of the corresponding baseline. RPN: Region proposal networks. Reg Loss: Regression loss.Cls loss: Classification loss. FE: Feature Enhancement Methods. mAP-SS: Single-scale test performance on DOTA-V1.0. mAP-MS: Multi-scale test performance on DOTA-V1.0. Res50: ResNet-50 (He et al., 2016). ReRes50: Rotation Equivariant ResNet-50. H104: Hourglass-104 (Newell et al., 2016). ViT: Vision Transformer (Dosovitskiy et al., 2021).

Method	Publication	Baseline	Backbone	RPN	Assigner	Head	Reg Loss	Cls Loss	OBB Representation	FE	mAP-SS	mAP-MS
<b>Two-stage</b>												
Rotated Faster RCNN (Ren et al., 2015)	NIPS 2015	Faster RCNN	Res50	–	–	–	–	–	–	–	73.40*	78.49*
RoI Transformer (Ding et al., 2019)	CVPR 2019	Faster RCNN	Res50	RRoI Learner	–	–	–	–	–	–	75.63*	80.43*
Oriented RCNN (Xie et al., 2021)	ICCV 2021	Faster RCNN	Res50	Oriented RPN	–	–	–	–	Midpoint Offset Gliding Vertex	–	75.69*	80.02*
Gliding Vertex (Xu et al., 2021)	TPAMI 2021	Faster RCNN	Res50	–	–	–	–	–	–	–	75.02	–
ReDet (Han et al., 2021)	CVPR 2021	RoI Transformer	ReRes50	–	–	Anchor-Free	–	GFL v2	Unordered Keypoints	–	76.25	80.10
OSKDet (Liu et al., 2022)	CVPR 2022	Faster RCNN	Res50	Rotated FCOS	–	–	–	–	–	–	76.37	80.91
AOPG (Cheng et al., 2022)	TGRS 2022	Faster RCNN	Res50	FCOS+RPN	–	–	–	–	–	–	75.22	80.66
DEA (Liang et al., 2022)	TGRS 2022	ReDet	ReRes50	–	–	–	–	–	–	–	80.37	–
RySA (Wang et al., 2022)	TGRS 2022	Oriented RCNN	ViT+RySA	–	–	–	–	–	–	–	78.61	80.80
RFGAOD (Qiao et al., 2023)	TGRS 2023	Oriented RCNN	Res50	GRG-RPN	–	AAO	–	–	Quadrant Point	–	70.47	81.20
QPDet (Yao et al., 2023)	TGRS 2023	Oriented RCNN	Res50	–	–	FRIoU	–	–	–	–	76.25	81.00
FRIoU Loss (Qian et al., 2023)	TGRS 2023	Oriented RCNN	Res50	–	–	OCG-Guided	–	–	–	–	76.45	80.78
CGCDet (Wang et al., 2024)	TNNLS 2024	RoI Transformer	Res50	–	–	CGC	–	–	–	–	77.34	80.70
STD (Yu et al., 2024)	AAAI 2024	Oriented RCNN	ViT	MAEB	–	–	–	–	–	–	82.24	–
<b>One-stage</b>												
Rotated RetinaNet (Lin et al., 2017)	ICCV 2017	RetinaNet	Res50	–	–	–	–	–	–	–	68.80*	–
SCRDet (Yang et al., 2019)	ICCV 2019	RetinaNet	SF-Net	–	–	IoU-Smooth LI	–	–	–	MDA	72.61	–
CSL (Yang and Yan, 2020)	ECCV 2020	RetinaNet	Res50	–	–	–	–	–	CSL	–	69.51*	–
R <sup>3</sup> Det (Yang et al., 2021)	AAAI 2021	RetinaNet	Res50	–	FRM	–	–	–	–	–	70.18*	–
DCL (Yang et al., 2021)	CVPR 2021	R <sup>3</sup> Det	Res50	DAS	–	–	–	–	DCL	–	71.21	–
DAL (Ming et al., 2021)	AAAI 2021	RetinaNet	Res50	–	–	–	–	–	–	–	71.44	–
ForDet (Zhang et al., 2022)	TGRS 2021	R <sup>3</sup> SSD	Res50	–	–	–	FARL	–	–	FRM	71.44	–
GWDD (Yang et al., 2021)	ICML 2021	R <sup>3</sup> Det	Res50	–	–	–	GWDD	–	–	–	71.56	–
KLD (Yang et al., 2021)	NeurIPS 2021	R <sup>3</sup> Det	Res50	–	–	–	KLD	–	Gaussian	–	71.73	–
BCD (Yang et al., 2022)	TPAMI 2022	R <sup>3</sup> Det	Res50	–	–	–	BCD	–	Gaussian	–	72.22	–
S <sup>2</sup> ANet (Han et al., 2022)	TGRS 2022	RetinaNet	Res50	–	FAM	–	–	–	–	–	74.12	79.42
CFC-Net (Ming et al., 2022)	TGRS 2022	RetinaNet	Res50	DAS	RARM	–	–	–	–	PAM	73.50	–
DCFL (Xu et al., 2023)	CVPR 2023	S <sup>2</sup> ANet	Res50	DCFL	–	–	–	–	–	–	74.26	–
KFLoU (Yang et al., 2022)	ICLR 2023	R <sup>3</sup> Det	Res50	–	–	–	–	–	Gaussian	–	71.60	–
TCD (Zhang et al., 2023)	TGRS 2023	RetinaNet	Res50	TCA	TCH	–	–	TCL	–	–	75.18	80.05
FADL-Net (Fu et al., 2024)	TII 2024	RetinaNet	Res50	GADL	–	–	–	JLRQ	–	–	74.80	73.97
TIR-Net (Li et al., 2024)	TGRS 2024	S <sup>2</sup> ANet	Res50	SIRK+RFR	–	–	–	–	–	–	75.23	80.63
CFL (Sun et al., 2024)	TII 2024	S <sup>2</sup> ANet	Res50	STS	CFS	–	–	–	–	–	75.35	–
<b>Anchor-Free</b>												
DRN (Pan et al., 2020)	CVPR 2020	CenterNet	H104	–	DRH	–	–	–	–	FSM	70.70	–
O2-DNet (Wei et al., 2020)	ISPRS 2021	FCOS	H104	–	–	–	–	–	Middle lines	–	72.80	–
CFA (Guo et al., 2021, 2022)	CVPR 2021	RepPoints	Res101	–	CFA	–	Clou	–	Convex-Hull	–	75.05	–
Oriented RepPoints (Li et al., 2022)	CVPR 2022	RepPoints	Res50	APAA	–	–	–	–	Adaptive Points	–	75.97	–
GFL (Wang et al., 2022)	TGRS 2022	CenterNet	Res50	–	–	–	GF-CSL	–	CSL	–	74.68	77.54
SASM (Hou et al., 2022)	AAAI 2022	RepPoints	Res50	SA-S	–	–	SA-M	–	–	–	74.92	77.19
DRRec (Nie and Huang, 2023)	TPAMI 2023	FCOS	Res50	–	–	–	–	–	DHRec	–	74.57	78.97
DRDet (Zhang et al., 2023)	TGRS 2023	FCOS	Res50	–	–	–	–	–	DRLs	–	74.85	79.34
TSH (Yu et al., 2023)	TGRS 2023	FCOS	Res50	–	–	–	JOE	–	PBL	–	77.18	–
HRDet (Yao et al., 2024)	TCSVT 2024	FCOS	Res50	–	–	–	EIoU	–	HMP	–	74.11	78.90
DFDet (Xie et al., 2024)	TGRS 2024	FCOS	Res50	–	–	–	PIAS	–	CDMN	–	74.71	80.37
<b>DETR-Based</b>												
AQ2-DETR (Dai et al., 2022)	TCSVT 2023	Deformable DETR	Res50	–	AOPR	–	–	–	–	–	70.91	–
ABS-DETR (Zeng et al., 2024)	TGRS 2024	DINO	Res50	ARM	RDA	–	ARA-CSL	–	–	–	73.79	–

**Detection in single-model image.** The current research community is dedicated to exploring and developing oriented object detection methods in single-model image. However, these methods are inherently constrained by their reliance on a solitary information source and the lack of contextual cues, exhibiting a heightened vulnerability to various interferences, including variations in lighting conditions, occlusions, and shadows.

Given that the aforementioned issues have not yet been explored and studied in oriented object detection, we further share some insights on future directions.

**Lightweight methods.** The demand for real-time object detectors on resource-limited mobile devices is on the rise, necessitating innovative solutions to overcome hardware constraints. Thus, light-weight oriented object detection architectures are required to fulfill the requirement of mobile and embedded applications. To promote the application of oriented object detection in real-world scenarios, a feasible approach is to adopt meticulously designed efficient network architectures or leverage Neural Architecture Search (Xiong et al., 2021) to discover optimal architectures. These light-weight network architectures enhance the efficiency and accuracy of feature extraction, while concurrently reducing model parameter count and computational burden. For example, several lightweight network structures, such as MobileNet (Howard et al., 2017) and ShuffleNet (Zhang et al., 2018), have gained widespread adoption in object detection tasks. Another feasible method is model compression to develop highly competitive, compact, and rapid detection models, including parameter pruning (Hanson and Pratt, 1988; Han et al., 2015; Gao et al., 2024; Zhang et al., 2024), quantization (Song et al., 2016; Xu et al., 2023; Ding et al., 2024), and knowledge distillation (Hinton et al., 2015; Zheng et al., 2023; Wang et al., 2024). These compression techniques have demonstrated remarkable effectiveness in bolstering generalization capabilities and mitigating underfitting during the training of efficient object detection models. These compression techniques have demonstrated remarkable effectiveness in improving generalization capabilities and mitigating underfitting during the training of object detection models.

**Mission-specific datasets.** In light of the prevailing imbalance in categories and scenarios within current datasets, coupled with the emerging trend of research on multi-modal large-scale models, we will delineate the future direction for datasets collection from three aspects: scenario-specific datasets, multi-modal datasets, and large-scale datasets.

Scenario-specific datasets can provide more refined and accurate data tailored to specific scenarios (*e.g.*, severe weather conditions, or rare scenarios), empowering models to achieve superior performance within those specific scenarios. Moreover, these datasets can effectively tackle the challenge of high-quality data scarcity in specialized scenarios, thereby enhancing models' generalization capabilities and promoting the practical application of oriented object detection in specialized fields.

Compared to single-model-based oriented object detection datasets, multi-modal ones integrate diverse data types that complement each other, providing a wealth of data resources essential for tackling intricate problems. By leveraging the connections and relationships among various data types, and fusing information from multiple modalities, the accuracy and performance of models can be substantially

enhanced, leading to more comprehensive and accurate analysis results. An interesting attempt is the DroneVehicle (Sun et al., 2022), in which the two modalities—RGB and infrared—offer complementary information across different lighting conditions. RGB images offer rich color information, while infrared images excel in low-light conditions and are not affected by darkness. In the future, with the continuous development of more efficient and accurate multi-modal technologies (Chen et al., 2020; Radford et al., 2021; Li et al., 2022, 2023), multi-modal datasets will play a pivotal role in a wide array of fields, driving continuous innovation in oriented object detection technology.

Owing to the exceptional representation and generalization capacities, large models have emerged as a focal point of current research (Vaswani et al., 2017; Ho et al., 2020; Liu et al., 2021; Kirillov et al., 2023). Relying on extensive data samples, large models can discern intricate features and underlying patterns within the data, thereby enhancing the both the accuracy and generalization prowess. As the technology pertaining to large models continues to advance, their ability to handle complex scenarios and multi-modal data will be further enhanced, which will bring more possibilities to oriented object detection. Consequently, there is a pressing need to develop high-quality, large-scale datasets tailored for oriented object detection. These datasets will not only provide a rich repository of samples but also serve as a robust validation platform to facilitate the training and evaluation of large models in this domain.

**Multi-modal large models.** Multi-modal large models, as a critical avenue for the progression of artificial intelligence towards Artificial General Intelligence (AGI), have emerged as a focal point of current research (Li et al., 2023; Kirillov et al., 2023). However, existing methods for oriented object detection predominantly concentrates on extracting valuable information from single-modal images, neglecting the guidance provided by multi-modal data. On the other hand, the scarcity of high-quality multi-modal data is a fundamental bottleneck that impedes the advancement of multi-modal large models within the domain of oriented object detection. Looking ahead, a prominent direction for future research entails the exploration and integration of multi-modal data. This encompasses the amalgamation of text and visual large models, the incorporation of GPS, IMU, and remote sensing imagery, as well as the fusion of diverse sensors. By harnessing the synergies among these various data modalities, we can unlock new potentials for enhancing the accuracy and robustness of oriented object detection methods. As technology continues to evolve, driven by the proliferation of data, and the expansion of application scenarios, multi-modal large models are expected to significantly elevate the performance of oriented object detection.

## Appendix A $\theta$ -based Representation

The  $\theta$ -based representation adopts a vector in the format of  $(x, y, w, h, \theta)$  to define an OBB. The present approaches can be classified into two types according to the definition of the angle  $\theta$ , including OpenCV definition (which follows the OpenCV protocol) and the long edge definition. As shown in Fig. A1a, the former defines  $\theta$  as the acute (or right) angle between the OBB and  $x$ -axis, leading to  $\theta \in (0, \frac{\pi}{2}]$ . Note that the width  $w$  is defined as the side of the acute angle and can be shorter than the height  $h$ , which is shown at the top of Fig. A1a. To tackle this issue, the long edge

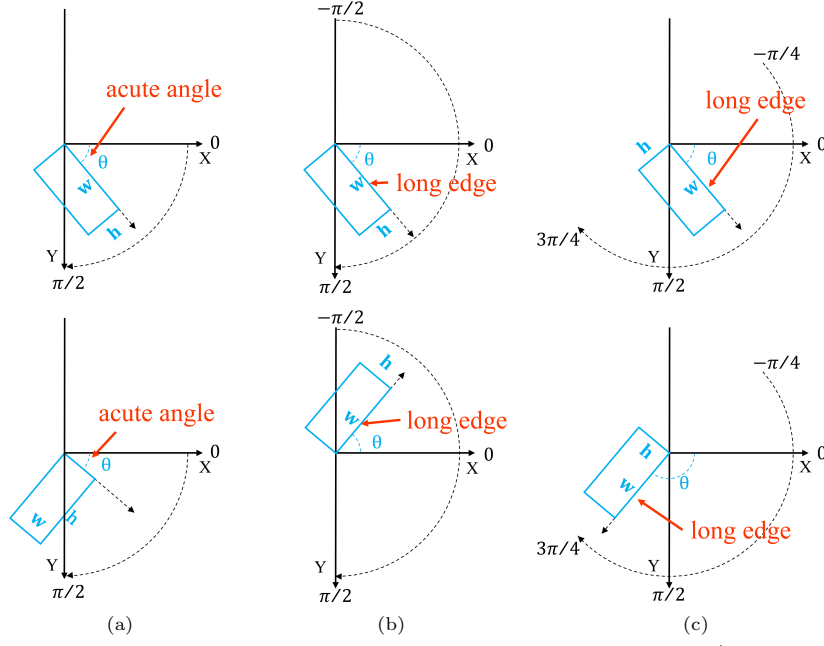


**Fig. A1** Definition of  $\theta$ -based representation. The OBBs depicted in the top/bottom row are the same. (a) OpenCV Definition ( $\theta \in (0, \frac{\pi}{2})$ ) (**Top**: height is longer than width. **Bottom**: width is longer than height). (b) Long edge definition with an angular range of  $[-\frac{\pi}{2}, \frac{\pi}{2})$ . (c) Long edge definition with an angular range of  $[-\frac{\pi}{4}, \frac{3\pi}{4})$ .

definition is proposed by setting  $\theta$  as the angle between the long edge of the OBB and  $x$ -axis. Therefore, the angular range is  $[-\frac{\pi}{2}, \frac{\pi}{2})$  (Ding et al., 2019; Han et al., 2021) or  $[-\frac{\pi}{4}, \frac{3\pi}{4})$  (Han et al., 2022), which are shown in Fig. A1b and Fig. A1c, respectively. As shown in the bottom of Fig. A1, the parameters of the same OBB have significant differences in different OBB representations.

Built upon well-designed horizontal detectors, most oriented object detectors predict OBBs in a regression fashion. In the  $\theta$ -based OBB representation, given an anchor box denoted by  $b_a = (x_a, y_a, w_a, h_a, \theta_a)$ , the neural network first predicts the offsets between the predicted OBB and the anchor box:

$$\begin{aligned}
 t_x^p &= \frac{x_p - x_a}{w_a}, t_y^p = \frac{y_p - y_a}{h_a}, \\
 t_w^p &= \log \frac{w_p}{w_a}, t_h^p = \log \frac{h_p}{h_a}, t_\theta^p = f\left(\frac{\theta_p - \theta_a}{\pi}\right)
 \end{aligned} \tag{A1}$$

where  $b_p = (x_p, y_p, w_p, h_p, \theta_p)$  denotes the predicted OBB.  $f(\cdot)$  is used to ensure that the angle difference stays within the preset range, thus avoiding the impact of PoA.

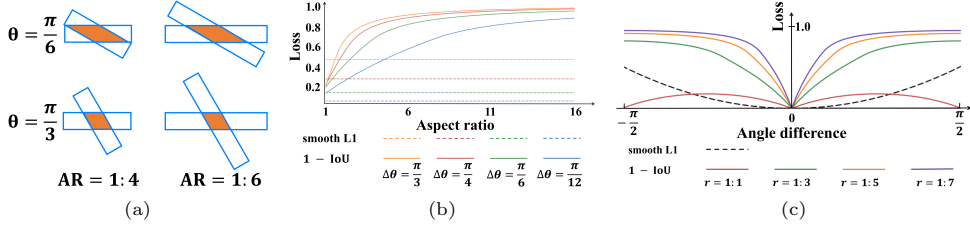


**Fig. A2** Comparison between metric and loss (Qian et al., 2021, 2022; Yang et al., 2021). (a) A sketch of RIoU change caused by angle and aspect ratio (AR) variation. (b) and (c) depict the changes of the regression loss and RIoU with aspect ratio and angle difference, respectively.

Similarly, the GT offsets are denoted by:

$$\begin{aligned}
 t_x^g &= \frac{x_g - x_a}{w_a}, t_y^g = \frac{y_g - y_a}{h_a}, \\
 t_w^g &= \log \frac{w_g}{w_a}, t_h^g = \log \frac{h_g}{h_a}, t_\theta^g = f\left(\frac{\theta_g - \theta_a}{\pi}\right)
 \end{aligned} \tag{A2}$$

where  $b_g = (x_g, y_g, w_g, h_g, \theta_g)$  denotes the GT OBB. Hence, the objective function for the regression task is:

$$L_{reg} = \sum_{i \in \{x, y, w, h, \theta\}} L_n(t_i^p - t_i^g) \tag{A3}$$

where  $L_n(\cdot)$  denotes the  $L_n$  norm and the smooth  $L_1$  loss (Girshick, 2015) is widely adopted. Due to the PoA (Qian et al., 2021, 2022; Yang et al., 2021, 2022), the OBB regression will encounter the following challenges.

(1) **Inconsistency between Metric and Loss.** Although the majority of detectors adopt the smooth  $L_1$  loss as the objective function of regression, the most commonly used metric for localization is RIoU. Therefore, there is an inconsistency between the loss function and the evaluation metric. This implies that an optimum choice for the regression task may not guarantee a high localization accuracy in terms of RIoU. What's more, a good regression loss function should take into account the central point distance, aspect ratio, and overlap area, which has been demonstrated to be effective in horizontal object detection (Rezatofighi et al., 2019; Zheng et al., 2020). However, the aspect ratio and the overlap area can be disregarded by the smooth  $L_1$  loss easily.

We illustrate the inconsistency between metric and loss in Fig. A2. As shown in Fig. A2a, the top and the bottom rows have different angle differences, while the aspect ratio of the OBBs on the left is different from those on the right. Meanwhile, the center points, width, and height of the four cases are the same. The orange area denotes the IoU between OBBs. Note that the regression loss is sensitive to angle variances but remains unchanged for different aspect ratios. Specifically, when the aspect ratio varies, the union of two OBBs will change but the intersection is constant, causing the change of RIoU. The same conclusion can be drawn from Fig. A2b, which shows the variation curves of the RIoU and smooth  $L_1$  loss w.r.t aspect ratio under different angle differences. Note that the RIoU changes drastically but the smooth  $L_1$

loss remains constant. Furthermore, Fig. A2c shows the variation curve of RIoU and smooth L1 loss w.r.t the angle under different aspect ratios. In the neighborhood of 0, both losses are consistent in monotonicity but not in convexity. The RIoU changes more intensely than the smooth L1 loss when the angle difference is close to zero.

(2) **Angular Boundary Discontinuity and Square-like Problem**

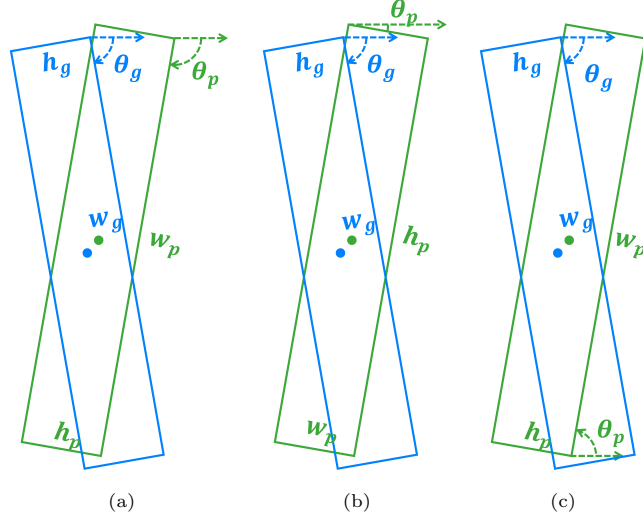


**Fig. A3** Illustration of angular boundary discontinuity (Yang et al., 2021). The predicted and GT OBB are represented by green and blue, respectively. (a) The ideal form of OBB representation. The two OBBs only differ slightly in terms of the angle and center point. (b) OBB representation with OpenCV definition, encountering PoA and exchangeability of edges (EoE). (c) OBB representation with long edge definition, encountering a significant angle difference.

Because of the PoA problem (Yang et al., 2021; Yang et al., 2022; Qian et al., 2021, 2022), the smooth L1 loss suffers from the problem of angular boundary discontinuity, which is illustrated in Fig. A3. Specifically, a small angle difference may cause a large loss change when the angular value approaches the angular boundary range. Fig. A3a illustrates an ideal OBB representation, where the predicted and GT OBB only differ slightly in terms of the angle and center point. For OBBs with OpenCV definition, the angular value must be an acute or right angle, *i.e.*,  $\theta \in (0, \frac{\pi}{2}]$ , as shown in Fig. A3b. As a result, the angle difference between the two OBBs increases sharply as the angular value is close to 0 or  $\frac{\pi}{2}$ . In addition, the width of the predicted OBB is the short edge, whereas the width of the GT OBB is the long edge, causing a significant regression loss of width and height. For OBBs under long edge definition with the angular range of  $[-\frac{\pi}{2}, \frac{\pi}{2})$ , the angular boundary discontinuity leads to a significant angle difference, *i.e.*,  $|\theta_g - \theta_p| \approx \pi$ , as shown in Fig. A3c. This problem will also occur in long edge definition with the angular range of  $[-\frac{\pi}{4}, \frac{3\pi}{4})$  when the angular value is close to  $-\frac{\pi}{4}$  or  $\frac{3\pi}{4}$ .

For square-like objects, including storage-tank and roundabouts, the long edge definition will encounter a so-called square-like problem due to the difference of angle

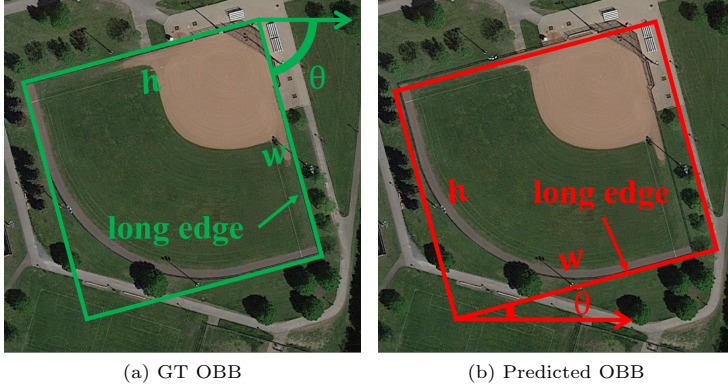


**Fig. A4** Illustration of the square-like problem (Yang et al., 2021).

parameters (Yang et al., 2021,?; Yang et al., 2022). As shown in Fig. A4, when the aspect ratio is close to 1 but the length and width of the predicted OBB are opposite to that of GT, the corresponding angle will differ by about  $\frac{\pi}{2}$ , leading to a large regression loss even if the RIoU is about 1.

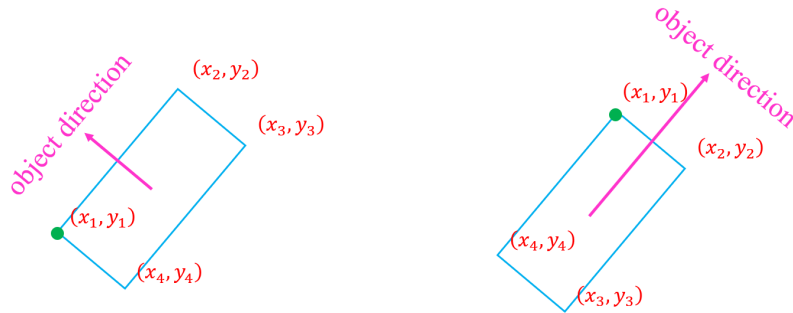
## Appendix B Quadrilateral Representation

The quadrilateral representation denotes an OBB as a vector  $(x_1, y_1, x_2, y_2, x_3, y_3, x_4, y_4)$ , where  $(x_i, y_i)$  indicates the image coordinates of the  $i$ -th vertex arranged in a clockwise order (Xu et al., 2021). This representation method can compactly enclose oriented objects with large deformation and has been widely adopted to annotate objects in large-scale RS datasets, including DOTA (Xia et al., 2018; Ding et al., 2022), and HRSC2016 (Liu et al., 2016). Significantly, the top-left vertex relative to the object orientation is chosen as the starting point  $(x_1, y_1)$ , as shown in Fig. B5a.

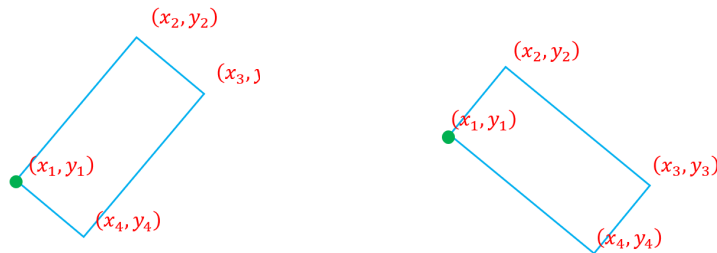
For the quadrilateral representation, the detector outputs a vector  $(\Delta x_1^p, \Delta y_1^p, \Delta x_2^p, \Delta y_2^p, \Delta x_3^p, \Delta y_3^p, \Delta x_4^p, \Delta y_4^p)$ , where  $(\Delta x_i^p, \Delta y_i^p)$  represent the relative offsets between the  $i$ -th vertex of the predicted OBB and the corresponding anchor box. Then, the predicted offsets are used to approximate the GT coordinate offsets  $(\Delta x_1^g, \Delta y_1^g, \Delta x_2^g, \Delta y_2^g, \Delta x_3^g, \Delta y_3^g, \Delta x_4^g, \Delta y_4^g)$  between the  $i$ -th vertex of the GT OBB and that of the anchor box. The regression loss of quadrilateral OBB representation can be expressed as:

$$L_{reg} = \sum_{i=1}^4 [L_n(\Delta x_i^p - \Delta x_i^g) + L_n(\Delta y_i^p - \Delta y_i^g)] \quad (\text{B4})$$

Generally, the anchor box selects the top-left vertex in the image as the starting point. To ensure consistency, the leftmost vertexes of the predicted OBB and the corresponding GT OBB are chosen as the starting point, as shown in Fig. B5b. However, the inappropriate vertex sorting may cause inconsistencies between the vertex



(a) Vertex sorting for annotated objects



(b) Vertex sorting in detection process

**Fig. B5** Definition of quadrilateral representation. **Top:** the top-left vertex relative to the object orientation is chosen as the start point. **Bottom:** the leftmost vertex is chosen as the starting point.

sequences of the anchor and the GT OBB, which is known as the vertexes sorting problem or the corners sorting problem (Qian et al., 2021, 2022; Xu et al., 2021). Fig. B6 shows a case of the problem. The anchor and the GT OBB are shown in blue and green respectively, and the dashed line and the solid line denote the actual and ideal vertexes matching during regression. In the ideal setting, the vertexes matching from the anchor to the GT is:  $(x_1, y_1) \rightarrow (x_2, y_2), (x_2, y_2) \rightarrow (x_3, y_3), (x_3, y_3) \rightarrow (x_4, y_4), (x_4, y_4) \rightarrow (x_1, y_1)$ . However, in the actual regression, the vertexes matching is:  $(x_1, y_1) \rightarrow (x_1, y_1), (x_2, y_2) \rightarrow (x_2, y_2), (x_3, y_3) \rightarrow (x_3, y_3), (x_4, y_4) \rightarrow (x_4, y_4)$ . Such inconsistency causes a large regression loss, confusing the network during the training process. Hence, it is critical to determine the sequence of vertexes in advance to stabilize the training process.

## Appendix C Datasets

In Tab. 3 of our main paper, we review a series of benchmarks regarding oriented object detection. However, space constraints prevent us from presenting all of them in detail. In this section, further details regarding the datasets mentioned in Sec. 7.2 are presented.

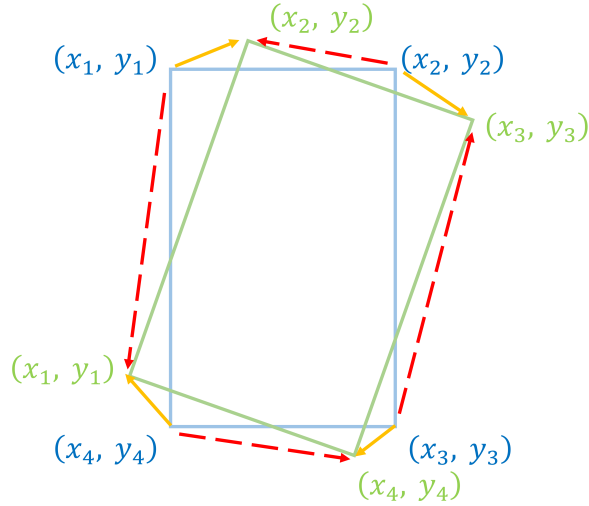


**Fig. B6** Illustration of vertices sorting problem. The dashed line and solid line represent the actual and ideal regression forms, respectively.

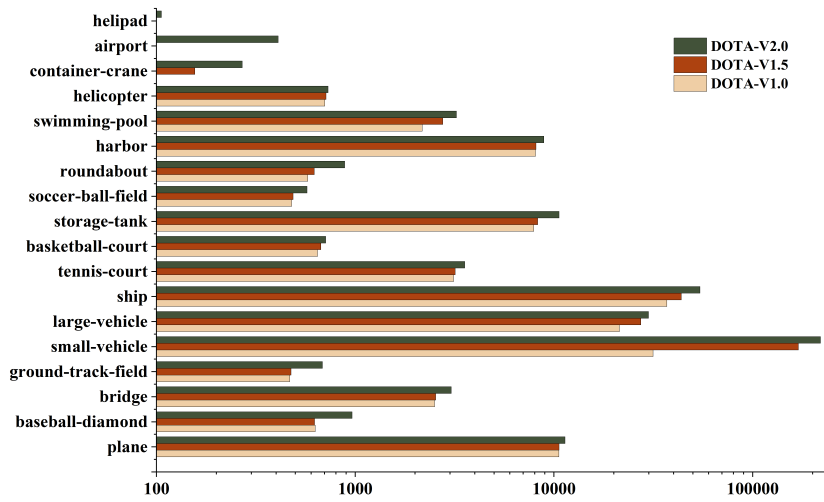


**Fig. B7** Number of instances for each category in training and validation subsets of DOTA-V1.0, V1.5, and V2.0 (Xia et al., 2018; Ding et al., 2022)

**SZTAKI-INRIA** (Benedek et al., 2012) contains 665 buildings in 9 multi-sensor aerial or satellite images taken from different cities. Due to the small capacity, this dataset is used to evaluate traditional object detection algorithms.

**3K vehicle** (Liu and Mattyus, 2015) is created for vehicle detection, comprising 20 images and 14,235 vehicles. The images have a resolution of  $5616 \times 3744$  and are

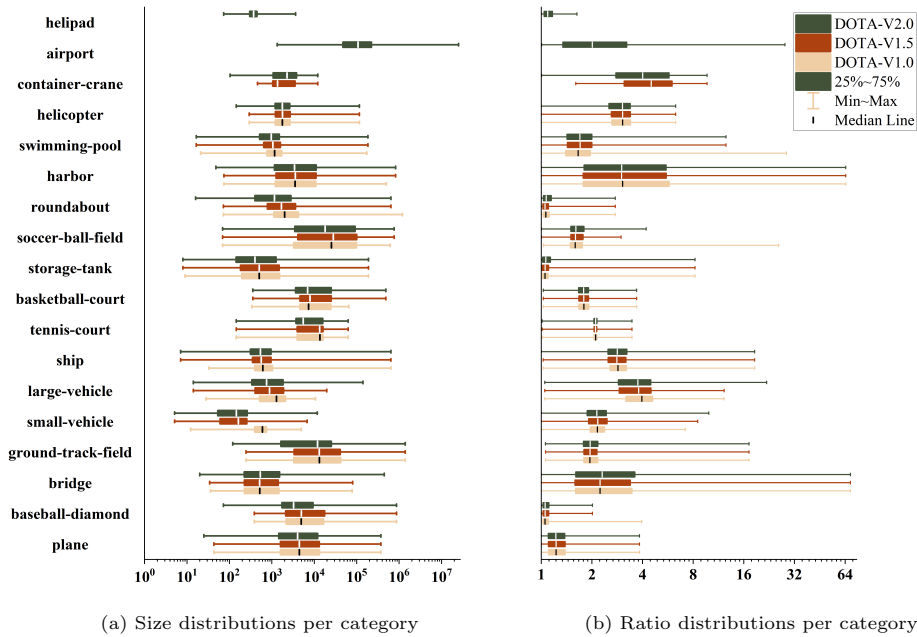


**Fig. B8** Size and ratio distributions for each category in training and validation subsets of DOTA-V1.0, V1.5, and V2.0 (Xia et al., 2018; Ding et al., 2022)

captured by a DLR camera system at a height of 1,000m above the ground. Therefore, the ground sample distance (GSD) is approximately 13 cm, leading to smaller scale variations. Besides, the images have a similar background. Hence, this dataset is excluded from the evaluation of algorithms on complicated scenes.

**VEDAI** (Razakarivony and Jurie, 2016) is also proposed for vehicle detection, containing more categories and a wider variety of backgrounds, *e.g.*, fields, grass, mountains, urban area, etc, making the detection more complicated. It comprises 1,210 images with a resolution of  $1,024 \times 1,024$ . The images are cropped from Very-High-Resolution (VHR) satellite images with a GSD of 12.5cm. However, the dataset only consists of 3,640 instances, because the images with too many dense vehicles are excluded. It is worth mentioning that each image has four color channels, including three visible channels and one 8-bit near-infrared channel.

**UCAS-AOD** (Zhu et al., 2015) contains 7,482 planes in 1,000 images, 7,114 cars in 510 images, and 910 negative images. All images in this dataset are cropped from Google Earth aerial images. Especially, the instances are carefully selected to ensure their orientations are distributed evenly.

**DOTA** (Xia et al., 2018; Ding et al., 2022). Fig. B7 shows the number of instances for each category in training and validation subsets of DOTA-V1.0, V1.5, and V2.0. Note that the distributions of different categories are severely imbalanced. The instances of small-vehicle and ship have a large quantity, while nearly half of

the other categories have quantities of less than 1,000, including plane, baseball diamond, ground track field, basketball court, soccer ball field, roundabout, helicopter, container crane, airport and helipad. The severe category imbalance makes the model seriously over-fitting to the many-shot categories but under-fitting to the low-shot categories (Gupta et al., 2019; Cui et al., 2019; Wang et al., 2021). Fig. B8 further summarizes the size and ratio distributions for each category in three versions of DOTA, respectively. As shown in Fig. B8a, the minimum size is 3 – 4 orders of magnitude lower than the maximum size in each category. Moreover, there is also a large range of size differences between categories. Fig. B8b indicates that the aspect ratios of different categories vary greatly. Furthermore, some categories have an extremely large aspect ratio, such as bridge, harbor, and airport. Up to now, DOTA has been the most challenging dataset for oriented object detection, due to its tremendous object instances, large aspect ratio, significant size variance, and complicated aerial scenes. All of these characteristics contribute to DOTA as the de facto benchmark for evaluating the efficacy of oriented object detectors in previous years.

## References

- Benedek, C., Descombes, X., Zerubia, J.: Building development monitoring in multi-temporal remotely sensed image pairs with stochastic birth-death dynamics. *IEEE Transactions on Pattern Analysis and Machine Intelligence* **34**(1), 33–50 (2012) <https://doi.org/10.1109/TPAMI.2011.94>
- Blaschke, T., Hay, G.J., Kelly, M., Lang, S., Hofmann, P., Addink, E., Queiroz Feitosa, R., van der Meer, F., van der Werff, H., van Coillie, F., Tiede, D.: Geographic object-based image analysis – towards a new paradigm. *ISPRS Journal of Photogrammetry and Remote Sensing* **87**, 180–191 (2014) <https://doi.org/10.1016/j.isprsjprs.2013.09.014>
- Blaschke, T.: Object based image analysis for remote sensing. *ISPRS Journal of Photogrammetry and Remote Sensing* **65**(1), 2–16 (2010) <https://doi.org/10.1016/j.isprsjprs.2009.06.004>
- Burochin, J.-P., Vallet, B., Brédif, M., Mallet, C., Brosset, T., Paparoditis, N.: Detecting blind building façades from highly overlapping wide angle aerial imagery. *ISPRS Journal of Photogrammetry and Remote Sensing* **96**, 193–209 (2014) <https://doi.org/10.1016/j.isprsjprs.2014.07.011>
- Chavali, N., Agrawal, H., Mahendru, A., Batra, D.: Object-proposal evaluation protocol is ‘gameable’. In: *IEEE/CVF Conference on Computer Vision and Pattern Recognition*, pp. 835–844 (2016). <https://doi.org/10.1109/CVPR.2016.97>
- Chen, Z., Chen, K., Lin, W., See, J., Yu, H., Ke, Y., Yang, C.: Piou loss: Towards accurate oriented object detection in complex environments. In: *European Conference on Computer Vision*, pp. 195–211 (2020). [https://doi.org/10.1007/978-3-030-58558-7\\_12](https://doi.org/10.1007/978-3-030-58558-7_12)

- Cheng, G., Han, J.: A survey on object detection in optical remote sensing images. *ISPRS Journal of Photogrammetry and Remote Sensing* **117**, 11–28 (2016) <https://doi.org/10.1016/j.isprsjprs.2016.03.014>
- Chollet, F.: Xception: Deep learning with depthwise separable convolutions. In: *IEEE/CVF Conference on Computer Vision and Pattern Recognition*, pp. 1800–1807 (2017). <https://doi.org/10.1109/CVPR.2017.195>
- Cheng, G., Han, J., Zhou, P., Guo, L.: Multi-class geospatial object detection and geographic image classification based on collection of part detectors. *ISPRS Journal of Photogrammetry and Remote Sensing* **98**, 119–132 (2014) <https://doi.org/10.1016/j.isprsjprs.2014.10.002>
- Cui, Y., Jia, M., Lin, T.-Y., Song, Y., Belongie, S.: Class-balanced loss based on effective number of samples. In: *IEEE/CVF Conference on Computer Vision and Pattern Recognition*, pp. 9260–9269 (2019). <https://doi.org/10.1109/CVPR.2019.00949>
- Cai, X., Lai, Q., Wang, Y., Wang, W., Sun, Z., Yao, Y.: Poly kernel inception network for remote sensing detection. In: *IEEE/CVF Conference on Computer Vision and Pattern Recognition*, pp. 27706–27716 (2024)
- Chen, Y.-C., Li, L., Yu, L., El Kholly, A., Ahmed, F., Gan, Z., Cheng, Y., Liu, J.: Uniter: Universal image-text representation learning. In: Vedaldi, A., Bischof, H., Brox, T., Frahm, J.-M. (eds.) *European Conference on Computer Vision*, pp. 104–120 (2020)
- Carion, N., Massa, F., Synnaeve, G., Usunier, N., Kirillov, A., Zagoruyko, S.: End-to-end object detection with transformers. In: *European Conference on Computer Vision*, pp. 213–229 (2020). [https://doi.org/10.1007/978-3-030-58452-8\\_13](https://doi.org/10.1007/978-3-030-58452-8_13)
- Chen, L.-C., Papandreou, G., Kokkinos, I., Murphy, K., Yuille, A.L.: Deeplab: Semantic image segmentation with deep convolutional nets, atrous convolution, and fully connected crfs. *IEEE Transactions on Pattern Analysis and Machine Intelligence* **40**(4), 834–848 (2018) <https://doi.org/10.1109/TPAMI.2017.2699184>
- Cao, J., Pang, Y., Xie, J., Khan, F.S., Shao, L.: From handcrafted to deep features for pedestrian detection: A survey. *IEEE Transactions on Pattern Analysis and Machine Intelligence* **44**(9), 4913–4934 (2022) <https://doi.org/10.1109/TPAMI.2021.3076733>
- Cortes, C., Vapnik, V.: Support-vector networks. *Machine Learning* **20**, 273–297 (1995) <https://doi.org/10.1023/A:1022627411411>
- Cai, Z., Vasconcelos, N.: Cascade r-cnn: Delving into high quality object detection. In: *IEEE/CVF Conference on Computer Vision and Pattern Recognition*, pp. 6154–6162 (2018). <https://doi.org/10.1109/CVPR.2018.00644>

- Cohen, T.S., Welling, M.: Group equivariant convolutional networks. In: International Conference on Machine Learning, pp. 2990–2999 (2016). <https://proceedings.mlr.press/v48/cohenc16.html>
- Cheng, G., Wang, J., Li, K., Xie, X., Lang, C., Yao, Y., Han, J.: Anchor-free oriented proposal generator for object detection. *IEEE Transactions on Geoscience and Remote Sensing* **60**, 1–11 (2022) <https://doi.org/10.1109/TGRS.2022.3183022>
- Chen, K., Wu, M., Liu, J., Zhang, C.: FGSD: A Dataset for Fine-Grained Ship Detection in High Resolution Satellite Images. arXiv e-prints, 2003–06832 (2020)
- Cheng, G., Yuan, X., Yao, X., Yan, K., Zeng, Q., Xie, X., Han, J.: Towards large-scale small object detection: Survey and benchmarks. *IEEE Transactions on Pattern Analysis and Machine Intelligence*, 1–20 (2023) <https://doi.org/10.1109/TPAMI.2023.3290594>
- Dosovitskiy, A., Beyer, L., Kolesnikov, A., Weissenborn, D., Zhai, X., Unterthiner, T., Dehghani, M., Minderer, M., Heigold, G., Gelly, S.: An image is worth 16x16 words: Transformers for image recognition at scale. In: International Conference on Learning Representations (2021)
- Duan, K., Bai, S., Xie, L., Qi, H., Huang, Q., Tian, Q.: Centernet: Keypoint triplets for object detection. In: IEEE/CVF International Conference on Computer Vision, pp. 6568–6577 (2019). <https://doi.org/10.1109/ICCV.2019.00667>
- Ding, Y., Feng, W., Chen, C., Guo, J., Liu, X.: Reg-ptq: Regression-specialized post-training quantization for fully quantized object detector. In: IEEE/CVF Conference on Computer Vision and Pattern Recognition, pp. 16174–16184 (2024). <https://doi.org/10.1109/CVPR52733.2024.01531>
- Dai, L., Liu, H., Tang, H., Wu, Z., Song, P.: Ao2-detr: Arbitrary-oriented object detection transformer. *IEEE Transactions on Circuits and Systems for Video Technology*, 1–1 (2022) <https://doi.org/10.1109/TCSVT.2022.3222906>
- Dai, J., Qi, H., Xiong, Y., Li, Y., Zhang, G., Hu, H., Wei, Y.: Deformable convolutional networks. In: IEEE International Conference on Computer Vision, pp. 764–773 (2017). <https://doi.org/10.1109/ICCV.2017.89>
- Dalal, N., Triggs, B.: Histograms of oriented gradients for human detection. In: IEEE Computer Society Conference on Computer Vision and Pattern Recognition, vol. 1, pp. 886–893 (2005). <https://doi.org/10.1109/CVPR.2005.177>
- Duan, C., Wei, Z., Zhang, C., Qu, S., Wang, H.: Coarse-grained density map guided object detection in aerial images. In: IEEE/CVF International Conference on Computer Vision Workshops, pp. 2789–2798 (2021). <https://doi.org/10.1109/ICCVW54120.2021.00313>

- Ding, J., Xue, N., Long, Y., Xia, G.-S., Lu, Q.: Learning roi transformer for oriented object detection in aerial images. In: IEEE/CVF Conference on Computer Vision and Pattern Recognition, pp. 2844–2853 (2019). <https://doi.org/10.1109/CVPR.2019.00296>
- Ding, J., Xue, N., Xia, G.-S., Bai, X., Yang, W., Yang, M.Y., Belongie, S., Luo, J., Datcu, M., Pelillo, M., Zhang, L.: Object detection in aerial images: A large-scale benchmark and challenges. *IEEE Transactions on Pattern Analysis and Machine Intelligence* **44**(11), 7778–7796 (2022) <https://doi.org/10.1109/TPAMI.2021.3117983>
- Fu, R., Chen, C., Yan, S., Zhang, R., Wang, X., Chen, H.: Fadl-net: Frequency-assisted dynamic learning network for oriented object detection in remote sensing images. *IEEE Transactions on Industrial Informatics* **20**(8), 9939–9951 (2024) <https://doi.org/10.1109/TII.2024.3378841>
- Fei-Fei, L., Perona, P.: A bayesian hierarchical model for learning natural scene categories. In: IEEE Computer Society Conference on Computer Vision and Pattern Recognition, vol. 2, pp. 524–531 (2005). <https://doi.org/10.1109/CVPR.2005.16>
- Felzenszwalb, P.F., Girshick, R.B., McAllester, D.: Cascade object detection with deformable part models. In: IEEE/CVF Conference on Computer Vision and Pattern Recognition, pp. 2241–2248 (2010). <https://doi.org/10.1109/CVPR.2010.5539906>
- Felzenszwalb, P., McAllester, D., Ramanan, D.: A discriminatively trained, multiscale, deformable part model. In: IEEE/CVF Conference on Computer Vision and Pattern Recognition, pp. 1–8 (2008). <https://doi.org/10.1109/CVPR.2008.4587597>
- Girshick, R., Donahue, J., Darrell, T., Malik, J.: Rich feature hierarchies for accurate object detection and semantic segmentation. In: IEEE/CVF Conference on Computer Vision and Pattern Recognition, pp. 580–587 (2014). <https://doi.org/10.1109/CVPR.2014.81>
- Gupta, A., Dollár, P., Girshick, R.: Lvis: A dataset for large vocabulary instance segmentation. In: IEEE/CVF Conference on Computer Vision and Pattern Recognition, pp. 5351–5359 (2019). <https://doi.org/10.1109/CVPR.2019.00550>
- Girshick, R.: Fast r-cnn. In: IEEE International Conference on Computer Vision, pp. 1440–1448 (2015). <https://doi.org/10.1109/ICCV.2015.169>
- Guo, Z., Liu, C., Zhang, X., Jiao, J., Ji, X., Ye, Q.: Beyond bounding-box: Convex-hull feature adaptation for oriented and densely packed object detection. In: IEEE/CVF Conference on Computer Vision and Pattern Recognition (CVPR), pp. 8788–8797 (2021). <https://doi.org/10.1109/CVPR46437.2021.00868>
- Gao, S., Zhang, Y., Huang, F., Huang, H.: Bilevelpruning: Unified dynamic and static

- channel pruning for convolutional neural networks. In: IEEE/CVF Conference on Computer Vision and Pattern Recognition, pp. 16090–16100 (2024). <https://doi.org/10.1109/CVPR52733.2024.01523>
- Guo, Z., Zhang, X., Liu, C., Ji, X., Jiao, J., Ye, Q.: Convex-hull feature adaptation for oriented and densely packed object detection. *IEEE Transactions on Circuits and Systems for Video Technology* **32**(8), 5252–5265 (2022) <https://doi.org/10.1109/TCSVT.2022.3140248>
- Gao, P., Zheng, M., Wang, X., Dai, J., Li, H.: Fast convergence of detr with spatially modulated co-attention. In: IEEE/CVF International Conference on Computer Vision, pp. 3601–3610 (2021). <https://doi.org/10.1109/ICCV48922.2021.00360>
- Gong, M., Zhao, H., Wu, Y., Tang, Z., Feng, K.-Y., Sheng, K.: Dual appearance-aware enhancement for oriented object detection. *IEEE Transactions on Geoscience and Remote Sensing* **62**, 1–14 (2024) <https://doi.org/10.1109/TGRS.2023.3344195>
- Haase, D., Amthor, M.: Rethinking depthwise separable convolutions: How intra-kernel correlations lead to improved mobilenets. In: IEEE/CVF Conference on Computer Vision and Pattern Recognition, pp. 14588–14597 (2020). <https://doi.org/10.1109/CVPR42600.2020.01461>
- Hosang, J., Benenson, R., Dollár, P., Schiele, B.: What makes for effective detection proposals? *IEEE Transactions on Pattern Analysis and Machine Intelligence* **38**(4), 814–830 (2016) <https://doi.org/10.1109/TPAMI.2015.2465908>
- Han, W., Chen, J., Wang, L., Feng, R., Li, F., Wu, L., Tian, T., Yan, J.: Methods for small, weak object detection in optical high-resolution remote sensing images: A survey of advances and challenges. *IEEE Geoscience and Remote Sensing Magazine* **9**(4), 8–34 (2021) <https://doi.org/10.1109/MGRS.2020.3041450>
- He, K., Chen, X., Xie, S., Li, Y., Dollár, P., Girshick, R.: Masked autoencoders are scalable vision learners. In: IEEE/CVF Conference on Computer Vision and Pattern Recognition, pp. 15979–15988 (2022). <https://doi.org/10.1109/CVPR52688.2022.01553>
- Han, J., Ding, J., Li, J., Xia, G.-S.: Align deep features for oriented object detection. *IEEE Transactions on Geoscience and Remote Sensing* **60**, 1–11 (2022) <https://doi.org/10.1109/TGRS.2021.3062048>
- Han, J., Ding, J., Xue, N., Xia, G.-S.: Redet: A rotation-equivariant detector for aerial object detection. In: IEEE/CVF Conference on Computer Vision and Pattern Recognition, pp. 2785–2794 (2021). <https://doi.org/10.1109/CVPR46437.2021.00281>
- He, K., Gkioxari, G., Dollár, P., Girshick, R.: Mask r-cnn. *IEEE Transactions on Pattern Analysis and Machine Intelligence* **42**(2), 386–397 (2020) <https://doi.org/>

[10.1109/TPAMI.2018.2844175](https://doi.org/10.1109/TPAMI.2018.2844175)

- Hei, L., Jia, D.: Cornernet: Detecting objects as paired keypoints. *International Journal of Computer Vision* **128**, 642–656 (2020) <https://doi.org/10.1007/s11263-019-01204-1>
- Ho, J., Jain, A., Abbeel, P.: Denoising diffusion probabilistic models. In: *Advances in Neural Information Processing Systems*, vol. 33, pp. 6840–6851 (2020)
- Hua, W., Liang, D., Li, J., Liu, X., Zou, Z., Ye, X., Bai, X.: Sood: Towards semi-supervised oriented object detection. In: *IEEE/CVF Conference on Computer Vision and Pattern Recognition*, pp. 15558–15567 (2023). <https://doi.org/10.1109/CVPR52729.2023.01493>
- Huang, G., Laradji, I., Vázquez, D., Lacoste-Julien, S., Rodríguez, P.: A survey of self-supervised and few-shot object detection. *IEEE Transactions on Pattern Analysis and Machine Intelligence* **45**(4), 4071–4089 (2023) <https://doi.org/10.1109/TPAMI.2022.3199617>
- Huang, Z., Li, W., Xia, X.-G., Wu, X., Cai, Z., Tao, R.: A novel nonlocal-aware pyramid and multiscale multitask refinement detector for object detection in remote sensing images. *IEEE Transactions on Geoscience and Remote Sensing* **60**, 1–20 (2022) <https://doi.org/10.1109/TGRS.2021.3059450>
- Huang, Z., Li, W., Xia, X.-G., Wang, H., Tao, R.: Task-wise sampling convolutions for arbitrary-oriented object detection in aerial images. *IEEE Transactions on Neural Networks and Learning Systems*, 1–15 (2024) <https://doi.org/10.1109/TNNLS.2024.3367331>
- Hou, L., Lu, K., Xue, J., Li, Y.: Shape-adaptive selection and measurement for oriented object detection. In: *AAAI Conference on Artificial Intelligence*, vol. 36, pp. 923–932 (2022). <https://doi.org/10.1609/aaai.v36i1.19975>
- Huang, Z., Li, W., Xia, X.-G., Tao, R.: A general gaussian heatmap label assignment for arbitrary-oriented object detection. *IEEE Transactions on Image Processing* **31**, 1895–1910 (2022) <https://doi.org/10.1109/TIP.2022.3148874>
- Hanson, S.J., Pratt, L.Y.: Comparing biases for minimal network construction with back-propagation. In: *International Conference on Neural Information Processing Systems*, pp. 177–185 (1988). <https://doi.org/10.5555/2969735.2969756>
- Han, S., Pool, J., Tran, J., Dally, W.J.: Learning both weights and connections for efficient neural networks. In: *International Conference on Neural Information Processing Systems - Volume 1*, pp. 1135–1143 (2015). <https://doi.org/10.5555/2969239.2969366>

- Hinton, G.E., Salakhutdinov, R.R.: Reducing the dimensionality of data with neural networks. *Science* **313**(5786), 504–507 (2006) <https://doi.org/10.1126/science.1127647>
- Hu, J., Shen, L., Albanie, S., Sun, G., Wu, E.: Squeeze-and-excitation networks. *IEEE Transactions on Pattern Analysis and Machine Intelligence* **42**(8), 2011–2023 (2020) <https://doi.org/10.1109/TPAMI.2019.2913372>
- Hinton, G., Vinyals, O., Dean, J.: Distilling the Knowledge in a Neural Network. arXiv e-prints, 1503–02531 (2015)
- Han, K., Wang, Y., Chen, H., Chen, X., Guo, J., Liu, Z., Tang, Y., Xiao, A., Xu, C., Xu, Y., Yang, Z., Zhang, Y., Tao, D.: A survey on vision transformer. *IEEE Transactions on Pattern Analysis and Machine Intelligence* **45**(1), 87–110 (2023) <https://doi.org/10.1109/TPAMI.2022.3152247>
- Howard, A.G., Zhu, M., Chen, B., Kalenichenko, D., Wang, W., Weyand, T., Andreetto, M., Adam, H.: MobileNets: Efficient Convolutional Neural Networks for Mobile Vision Applications. arXiv e-prints (2017) <https://doi.org/10.48550/arXiv.1704.04861>
- He, K., Zhang, X., Ren, S., Sun, J.: Deep residual learning for image recognition. In: *IEEE/CVF Conference on Computer Vision and Pattern Recognition*, pp. 770–778 (2016). <https://doi.org/10.1109/CVPR.2016.90>
- Khan, S.D., Alarabi, L., Basalamah, S.: A unified deep learning framework of multi-scale detectors for geo-spatial object detection in high-resolution satellite images. *Arabian Journal for Science and Engineering*, 9489–9504 (2022) <https://doi.org/10.1007/s13369-021-06288-x>
- Karatzas, D., Gomez-Bigorda, L., Nicolaou, A., Ghosh, S., Bagdanov, A., Iwamura, M., Matas, J., Neumann, L., Chandrasekhar, V.R., Lu, S., Shafait, F., Uchida, S., Valveny, E.: Icdar 2015 competition on robust reading. In: *International Conference on Document Analysis and Recognition*, pp. 1156–1160 (2015). <https://doi.org/10.1109/ICDAR.2015.7333942>
- Koyun, O.C., Keser, R.K., Batuhan Akkaya, Töreyn, B.U.: Focus-and-detect: A small object detection framework for aerial images. *Signal Processing: Image Communication* **104**, 116675 (2022) <https://doi.org/10.1016/j.image.2022.116675>
- Kirillov, A., Mintun, E., Ravi, N., Mao, H., Rolland, C., Gustafson, L., Xiao, T., Whitehead, S., Berg, A.C., Lo, W.-Y., Dollar, P., Girshick, R.: Segment anything. In: *Proceedings of the IEEE/CVF International Conference on Computer Vision (ICCV)*, pp. 4015–4026 (2023)
- Krizhevsky, A., Sutskever, I., Hinton, G.E.: Imagenet classification with deep convolutional neural networks. In: *International Conference on Neural Information*

- Processing Systems, Red Hook, NY, USA, pp. 1097–1105 (2012)
- Krizhevsky, A., Sutskever, I., Hinton, G.E.: Imagenet classification with deep convolutional neural networks. *Communications of the ACM* **60**(6), 84–90 (2017) <https://doi.org/10.1145/3065386>
- Liu, W., Anguelov, D., Erhan, D., Szegedy, C., Reed, S., Fu, C.-Y., Berg, A.C.: Ssd: Single shot multibox detector. In: *European Conference on Computer Vision*, pp. 21–37 (2016). [https://doi.org/10.1007/978-3-319-46448-0\\_2](https://doi.org/10.1007/978-3-319-46448-0_2)
- LeCun, Y., Bengio, Y., Hinton, G.: Deep learning. *Nature* **521**, 436–444 (2015) <https://doi.org/10.1038/nature14539>
- Li, W., Chen, Y., Hu, K., Zhu, J.: Oriented reppoints for aerial object detection. In: *IEEE/CVF Conference on Computer Vision and Pattern Recognition*, pp. 1819–1828 (2022). <https://doi.org/10.1109/CVPR52688.2022.00187>
- Li, Y., Chen, Y., Wang, N., Zhang, Z.-X.: Scale-aware trident networks for object detection. In: *IEEE/CVF International Conference on Computer Vision*, pp. 6053–6062 (2019). <https://doi.org/10.1109/ICCV.2019.00615>
- Liu, F., Chen, R., Zhang, J., Ding, S., Liu, H., Ma, S., Xing, K.: Esrtmdet: An end-to-end super-resolution enhanced real-time rotated object detector for degraded aerial images. *IEEE Journal of Selected Topics in Applied Earth Observations and Remote Sensing* **16**, 4983–4998 (2023) <https://doi.org/10.1109/JSTARS.2023.3278295>
- Lin, T.-Y., Dollár, P., Girshick, R., He, K., Hariharan, B., Belongie, S.: Feature pyramid networks for object detection. In: *IEEE/CVF Conference on Computer Vision and Pattern Recognition (CVPR)*, pp. 936–944 (2017). <https://doi.org/10.1109/CVPR.2017.106>
- Lin, T.-Y., Goyal, P., Girshick, R., He, K., Dollár, P.: Focal loss for dense object detection. In: *2017 IEEE International Conference on Computer Vision (ICCV)*, pp. 2999–3007 (2017). <https://doi.org/10.1109/ICCV.2017.324>
- Lin, T.-Y., Goyal, P., Girshick, R., He, K., Dollár, P.: Focal loss for dense object detection. *IEEE Transactions on Pattern Analysis and Machine Intelligence* **42**(2), 318–327 (2020) <https://doi.org/10.1109/TPAMI.2018.2858826>
- Liang, D., Geng, Q., Wei, Z., Vorontsov, D.A., Kim, E.L., Wei, M., Zhou, H.: Anchor retouching via model interaction for robust object detection in aerial images. *IEEE Transactions on Geoscience and Remote Sensing* **60**, 1–13 (2022) <https://doi.org/10.1109/TGRS.2021.3136350>
- Long, Y., Gong, Y., Xiao, Z., Liu, Q.: Accurate object localization in remote sensing images based on convolutional neural networks. *IEEE Transactions on Geoscience and Remote Sensing* **55**(5), 2486–2498 (2017) <https://doi.org/10.1109/TGRS.2016>

- Leitloff, J., Hinz, S., Stilla, U.: Vehicle detection in very high resolution satellite images of city areas. *IEEE Transactions on Geoscience and Remote Sensing* **48**(7), 2795–2806 (2010) <https://doi.org/10.1109/TGRS.2010.2043109>
- Lu, X., Ji, J., Xing, Z., Miao, Q.: Attention and feature fusion ssd for remote sensing object detection. *IEEE Transactions on Instrumentation and Measurement* **70**, 1–9 (2021) <https://doi.org/10.1109/TIM.2021.3052575>
- Lam, D., Kuzma, R., McGee, K., Dooley, S., Laielli, M., Klaric, M., Bulatov, Y., McCord, B.: xView: Objects in Context in Overhead Imagery. *arXiv e-prints*, 1802–07856 (2018)
- Liu, Z., Lin, Y., Cao, Y., Hu, H., Wei, Y., Zhang, Z., Lin, S., Guo, B.: Swin transformer: Hierarchical vision transformer using shifted windows. In: *IEEE/CVF International Conference on Computer Vision*, pp. 9992–10002 (2021). <https://doi.org/10.1109/ICCV48922.2021.00986>
- Lu, D., Li, D., Li, Y., Wang, S.: Oskdet: Orientation-sensitive keypoint localization for rotated object detection. In: *IEEE/CVF Conference on Computer Vision and Pattern Recognition*, pp. 1172–1182 (2022). <https://doi.org/10.1109/CVPR52688.2022.00125>
- Lei, S., Lu, D., Qiu, X., Ding, C.: Srsdd-v1.0: A high-resolution sar rotation ship detection dataset. *Remote Sensing* **13**(24) (2021) <https://doi.org/10.3390/rs13245104>
- Li, J., Li, D., Savarese, S., Hoi, S.: BLIP-2: Bootstrapping language-image pre-training with frozen image encoders and large language models. In: Krause, A., Brunskill, E., Cho, K., Engelhardt, B., Sabato, S., Scarlett, J. (eds.) *International Conference on Machine Learning*, vol. 202, pp. 19730–19742 (2023)
- Li, J., Li, D., Xiong, C., Hoi, S.: BLIP: Bootstrapping language-image pre-training for unified vision-language understanding and generation. In: *International Conference on Machine Learning*, vol. 162, pp. 12888–12900 (2022)
- Liu, Y., Li, Q., Yuan, Y., Du, Q., Wang, Q.: Abnet: Adaptive balanced network for multiscale object detection in remote sensing imagery. *IEEE Transactions on Geoscience and Remote Sensing* **60**, 1–14 (2022) <https://doi.org/10.1109/TGRS.2021.3133956>
- Liu, S., Li, F., Zhang, H., Yang, X., Qi, X., Su, H., Zhu, J., Zhang, L.: Dab-detr: Dynamic anchor boxes are better queries for detr. In: *International Conference on Learning Representations* (2022)
- Li, Y., Luo, J., Zhang, Y., Tan, Y., Yu, J.-G., Bai, S.: Learning to holistically detect bridges from large-size vhr remote sensing imagery. *IEEE Transactions on Pattern*

- Analysis and Machine Intelligence **46**(12), 11507–11523 (2024) <https://doi.org/10.1109/TPAMI.2024.3393024>
- Liu, K., Mattyus, G.: Fast multiclass vehicle detection on aerial images. *IEEE Geoscience and Remote Sensing Letters* **12**(9), 1938–1942 (2015) <https://doi.org/10.1109/LGRS.2015.2439517>
- Liu, Z., Mao, H., Wu, C.-Y., Feichtenhofer, C., Darrell, T., Xie, S.: A convnet for the 2020s. In: *IEEE/CVF Conference on Computer Vision and Pattern Recognition*, pp. 11966–11976 (2022). <https://doi.org/10.1109/CVPR52688.2022.01167>
- Lowe, D.G.: Distinctive image features from scale-invariant keypoints. *International Journal of Computer Vision* **60**, 91–110 (2004) <https://doi.org/10.1023/B:VISI.0000029664.99615.94>
- Liu, L., Ouyang, W., Wang, X., Fieguth, P., Chen, J., Liu, X., Pietikäinen, M.: Deep learning for generic object detection: A survey. *International Journal of Computer Vision* **128**(2), 261–318 (2020) <https://doi.org/10.1007/s11263-019-01247-4>
- Li, H., Pan, R., Liu, G., Dang, M., Xu, Q., Wang, X., Wan, B.: Tir-net: Task integration based on rotated convolution kernel for oriented object detection in aerial images. *IEEE Transactions on Geoscience and Remote Sensing* **62**, 1–13 (2024) <https://doi.org/10.1109/TGRS.2024.3412167>
- Lenc, K., Vedaldi, A.: Understanding image representations by measuring their equivariance and equivalence. In: *IEEE/CVF Conference on Computer Vision and Pattern Recognition*, pp. 991–999 (2015). <https://doi.org/10.1109/CVPR.2015.7298701>
- Li, K., Wan, G., Cheng, G., Meng, L., Han, J.: Object detection in optical remote sensing images: A survey and a new benchmark. *ISPRS Journal of Photogrammetry and Remote Sensing* **159**, 296–307 (2020) <https://doi.org/10.1016/j.isprsjprs.2019.11.023>
- Liu, Z., Wang, H., Weng, L., Yang, Y.: Ship rotated bounding box space for ship extraction from high-resolution optical satellite images with complex backgrounds. *IEEE Geoscience and Remote Sensing Letters* **13**(8), 1074–1078 (2016) <https://doi.org/10.1109/LGRS.2016.2565705>
- Li, B., Xie, X., Wei, X., Tang, W.: Ship detection and classification from optical remote sensing images: A survey. *Chinese Journal of Aeronautics* **34**(3), 145–163 (2021) <https://doi.org/10.1016/j.cja.2020.09.022>
- Luo, J., Yang, X., Yu, Y., Li, Q., Yan, J., Li, Y.: Pointobb: Learning oriented object detection via single point supervision. In: *IEEE/CVF Conference on Computer Vision and Pattern Recognition*, pp. 16730–16740 (2024)

- Liu, W., Zhang, T., Huang, S., Li, K.: A hybrid optimization framework for uav reconnaissance mission planning. *Computers & Industrial Engineering* **173**, 108653 (2022) <https://doi.org/10.1016/j.cie.2022.108653>
- Li, F., Zhang, H., Liu, S., Guo, J., Ni, L.M., Zhang, L.: Dn-detr: Accelerate detr training by introducing query denoising. In: *IEEE/CVF Conference on Computer Vision and Pattern Recognition*, pp. 13609–13617 (2022). <https://doi.org/10.1109/CVPR52688.2022.01325>
- Liu, S., Zhang, L., Lu, H., He, Y.: Center-boundary dual attention for oriented object detection in remote sensing images. *IEEE Transactions on Geoscience and Remote Sensing* **60**, 1–14 (2022) <https://doi.org/10.1109/TGRS.2021.3069056>
- Liao, M., Zhu, Z., Shi, B., Xia, G.-s., Bai, X.: Rotation-sensitive regression for oriented scene text detection. In: *IEEE/CVF Conference on Computer Vision and Pattern Recognition*, pp. 5909–5918 (2018). <https://doi.org/10.1109/CVPR.2018.00619>
- Li, W., Zhao, D., Yuan, B., Gao, Y., Shi, Z.: Petdet: Proposal enhancement for two-stage fine-grained object detection. *IEEE Transactions on Geoscience and Remote Sensing* **62**, 1–14 (2024) <https://doi.org/10.1109/TGRS.2023.3343453>
- Liang, X., Zhang, J., Zhuo, L., Li, Y., Tian, Q.: Small object detection in unmanned aerial vehicle images using feature fusion and scaling-based single shot detector with spatial context analysis. *IEEE Transactions on Circuits and Systems for Video Technology* **30**(6), 1758–1770 (2020) <https://doi.org/10.1109/TCSVT.2019.2905881>
- Ma, W., Li, N., Zhu, H., Jiao, L., Tang, X., Guo, Y., Hou, B.: Feature split–merge–enhancement network for remote sensing object detection. *IEEE Transactions on Geoscience and Remote Sensing* **60**, 1–17 (2022) <https://doi.org/10.1109/TGRS.2022.3140856>
- Ma, T., Mao, M., Zheng, H., Gao, P., Wang, X., Han, S., Ding, E., Zhang, B., Doermann, D.: Oriented Object Detection with Transformer. *arXiv e-prints*, 2106–03146 (2021)
- Ming, Q., Miao, L., Zhou, Z., Song, J., Pizurica, A.: Gradient calibration loss for fast and accurate oriented bounding box regression. *IEEE Transactions on Geoscience and Remote Sensing* **62**, 1–15 (2024) <https://doi.org/10.1109/TGRS.2024.3367294>
- Ming, Q., Miao, L., Zhou, Z., Dong, Y.: Cfc-net: A critical feature capturing network for arbitrary-oriented object detection in remote-sensing images. *IEEE Transactions on Geoscience and Remote Sensing* **60**, 1–14 (2022) <https://doi.org/10.1109/TGRS.2021.3095186>
- Ma, J., Shao, W., Ye, H., Wang, L., Wang, H., Zheng, Y., Xue, X.: Arbitrary-oriented scene text detection via rotation proposals. *IEEE Transactions on Multimedia*

- 20(11), 3111–3122 (2018) <https://doi.org/10.1109/TMM.2018.2818020>
- Marcos, D., Volpi, M., Komodakis, N., Tuia, D.: Rotation equivariant vector field networks. In: IEEE International Conference on Computer Vision, pp. 5058–5067 (2017). <https://doi.org/10.1109/ICCV.2017.540>
- Ming, Q., Zhou, Z., Miao, L., Zhang, H., Li, L.: Dynamic anchor learning for arbitrary-oriented object detection. In: AAAI Conference on Artificial Intelligence, vol. 35, pp. 2355–2363 (2021). <https://doi.org/10.1609/aaai.v35i3.16336>
- Nie, G., Huang, H.: Multi-oriented object detection in aerial images with double horizontal rectangles. IEEE Transactions on Pattern Analysis and Machine Intelligence **45**(4), 4932–4944 (2023) <https://doi.org/10.1109/TPAMI.2022.3191753>
- Newell, A., Yang, K., Deng, J.: Stacked hourglass networks for human pose estimation. In: Leibe, B., Matas, J., Sebe, N., Welling, M. (eds.) European Conference on Computer Vision, pp. 483–499 (2016). [https://doi.org/10.1007/978-3-319-46484-8\\_29](https://doi.org/10.1007/978-3-319-46484-8_29)
- Oscó, L.P., dos Santos de Arruda, M., Gonçalves, D.N., Dias, A., Batistoti, J., de Souza, M., Gomes, F.D.G., Ramos, A.P.M., de Castro Jorge, L.A., Liesenberg, V., Li, J., Ma, L., Marcato, J., Gonçalves, W.N.: A cnn approach to simultaneously count plants and detect plantation-rows from uav imagery. ISPRS Journal of Photogrammetry and Remote Sensing **174**, 1–17 (2021) <https://doi.org/10.1016/j.isprsjprs.2021.01.024>
- Pannone, S.A.A.C.C.L.F.G.R.M.M.: Few-shot object detection: A survey. ACM Computing Surveys, 1–37 (2022)
- Pan, X., Ren, Y., Sheng, K., Dong, W., Yuan, H., Guo, X., Ma, C., Xu, C.: Dynamic refinement network for oriented and densely packed object detection. In: IEEE/CVF Conference on Computer Vision and Pattern Recognition, pp. 11204–11213 (2020). <https://doi.org/10.1109/CVPR42600.2020.01122>
- Pu, Y., Wang, Y., Xia, Z., Han, Y., Wang, Y., Gan, W., Wang, Z., Song, S., Huang, G.: Adaptive rotated convolution for rotated object detection. In: IEEE/CVF International Conference on Computer Vision, pp. 6566–6577 (2023). <https://doi.org/10.1109/ICCV51070.2023.00606>
- Qiao, S., Chen, L.-C., Yuille, A.: Detectors: Detecting objects with recursive feature pyramid and switchable atrous convolution. In: IEEE/CVF Conference on Computer Vision and Pattern Recognition, pp. 10208–10219 (2021). <https://doi.org/10.1109/CVPR46437.2021.01008>
- Qiao, Y., Miao, L., Zhou, Z., Ming, Q.: A novel object detector based on high-quality rotation proposal generation and adaptive angle optimization. IEEE Transactions on Geoscience and Remote Sensing **61**, 1–15 (2023) <https://doi.org/10.1109/TGRS.2023.3301610>

- Qian, X., Wu, B., Cheng, G., Yao, X., Wang, W., Han, J.: Building a bridge of bounding box regression between oriented and horizontal object detection in remote sensing images. *IEEE Transactions on Geoscience and Remote Sensing* **61**, 1–9 (2023) <https://doi.org/10.1109/TGRS.2023.3256373>
- Qian, W., Yang, X., Peng, S., Yan, J., Guo, Y.: Learning modulated loss for rotated object detection. In: *AAAI Conference on Artificial Intelligence*, vol. 35, pp. 2458–2466 (2021). <https://doi.org/10.1609/aaai.v35i3.16347>
- Qian, W., Yang, X., Peng, S., Zhang, X., Yan, J.: Rsdet++: Point-based modulated loss for more accurate rotated object detection. *IEEE Transactions on Circuits and Systems for Video Technology* **32**(11), 7869–7879 (2022) <https://doi.org/10.1109/TCSVT.2022.3186070>
- Redmon, J., Divvala, S., Girshick, R., Farhadi, A.: You only look once: Unified, real-time object detection. In: *IEEE/CVF Conference on Computer Vision and Pattern Recognition*, pp. 779–788 (2016). <https://doi.org/10.1109/CVPR.2016.91>
- Russakovsky, O., Deng, J., Su, H., Krause, J., Satheesh, S., Ma, S., Huang, Z., Karpathy, A., Khosla, A., Bernstein, M., Berg, A.C., Fei-Fei, L.: Imagenet large scale visual recognition challenge. *International Journal of Computer Vision* **115**, 211–252 (2015) <https://doi.org/10.1007/s11263-015-0816-y>
- Redmon, J., Farhadi, A.: Yolo9000: Better, faster, stronger. In: *IEEE/CVF Conference on Computer Vision and Pattern Recognition*, pp. 6517–6525 (2017). <https://doi.org/10.1109/CVPR.2017.690>
- Ren, S., He, K., Girshick, R., Sun, J.: Faster r-cnn: Towards real-time object detection with region proposal networks. In: *Advances in Neural Information Processing Systems*, vol. 28 (2015)
- Ren, S., He, K., Girshick, R., Sun, J.: Faster r-cnn: Towards real-time object detection with region proposal networks. *IEEE Transactions on Pattern Analysis and Machine Intelligence* **39**(6), 1137–1149 (2017) <https://doi.org/10.1109/TPAMI.2016.2577031>
- Razakarivony, S., Jurie, F.: Vehicle detection in aerial imagery : A small target detection benchmark. *Journal of Visual Communication and Image Representation* **34**, 187–203 (2016) <https://doi.org/10.1016/j.jvcir.2015.11.002>
- Radford, A., Kim, J.W., Hallacy, C., Ramesh, A., Goh, G., Agarwal, S., Sastry, G., Askell, A., Mishkin, P., Clark, J., Krueger, G., Sutskever, I.: Learning transferable visual models from natural language supervision. In: *International Conference on Machine Learning*, vol. 139, pp. 8748–8763 (2021)
- Rezatofghi, H., Tsoi, N., Gwak, J., Sadeghian, A., Reid, I., Savarese, S.: Generalized intersection over union: A metric and a loss for bounding box regression. In:

- IEEE/CVF Conference on Computer Vision and Pattern Recognition, pp. 658–666 (2019). <https://doi.org/10.1109/CVPR.2019.00075>
- Sun, Z., Cao, S., Yang, Y., Kitani, K.: Rethinking transformer-based set prediction for object detection. In: IEEE/CVF International Conference on Computer Vision, pp. 3591–3600 (2021). <https://doi.org/10.1109/ICCV48922.2021.00359>
- Sun, Y., Cao, B., Zhu, P., Hu, Q.: Drone-based rgb-infrared cross-modality vehicle detection via uncertainty-aware learning. *IEEE Transactions on Circuits and Systems for Video Technology* **32**(10), 6700–6713 (2022) <https://doi.org/10.1109/TCSVT.2022.3168279>
- Singh, B., Davis, L.S.: An analysis of scale invariance in object detection - snip. In: IEEE/CVF Conference on Computer Vision and Pattern Recognition, pp. 3578–3587 (2018). <https://doi.org/10.1109/CVPR.2018.00377>
- Song, G., Liu, Y., Wang, X.: Revisiting the sibling head in object detector. In: IEEE/CVF Conference on Computer Vision and Pattern Recognition, pp. 11560–11569 (2020). <https://doi.org/10.1109/CVPR42600.2020.01158>
- Sifre, L., Mallat, S.: Rotation, scaling and deformation invariant scattering for texture discrimination. In: IEEE/CVF Conference on Computer Vision and Pattern Recognition, pp. 1233–1240 (2013). <https://doi.org/10.1109/CVPR.2013.163>
- Song, H., Mao, H., Dally, W.J.: Deep compression: Compressing deep neural networks with pruning, trained quantization and huffman coding. In: International Conference on Learning Representations (2016)
- Singh, B., Najibi, M., Davis, L.S.: Sniper: Efficient multi-scale training. In: Advances in Neural Information Processing Systems, vol. 31 (2018). <https://proceedings.neurips.cc/paper/2018/file/166cee72e93a992007a89b39eb29628b-Paper.pdf>
- Shermeyer, J., Van Etten, A.: The effects of super-resolution on object detection performance in satellite imagery. In: IEEE/CVF Conference on Computer Vision and Pattern Recognition Workshops, pp. 1432–1441 (2019). <https://doi.org/10.1109/CVPRW.2019.00184>
- Sun, X., Wang, P., Yan, Z., Xu, F., Wang, R., Diao, W., Chen, J., Li, J., Feng, Y., Xu, T., Weinmann, M., Hinz, S., Wang, C., Fu, K.: Fair1m: A benchmark dataset for fine-grained object recognition in high-resolution remote sensing imagery. *ISPRS Journal of Photogrammetry and Remote Sensing* **184**, 116–130 (2022) <https://doi.org/10.1016/j.isprsjprs.2021.12.004>
- Sun, P., Zheng, Y., Wu, W., Xu, W., Bai, S., Lu, X.: Learning critical features for arbitrary-oriented object detection in remote-sensing optical images. *IEEE Transactions on Instrumentation and Measurement* **73**, 1–12 (2024) <https://doi.org/10.1109/TIM.2024.3378265>

- Tian, S., Kang, L., Xing, X., Tian, J., Fan, C., Zhang, Y.: A relation-augmented embedded graph attention network for remote sensing object detection. *IEEE Transactions on Geoscience and Remote Sensing* **60**, 1–18 (2022) <https://doi.org/10.1109/TGRS.2021.3073269>
- Tian, Z., Shen, C., Chen, H., He, T.: Fcos: Fully convolutional one-stage object detection. In: 2019 IEEE/CVF International Conference on Computer Vision (ICCV), pp. 9626–9635 (2019). <https://doi.org/10.1109/ICCV.2019.00972>
- Tarvainen, A., Valpola, H.: Mean teachers are better role models: Weight-averaged consistency targets improve semi-supervised deep learning results. In: International Conference on Neural Information Processing Systems, pp. 1195–1204 (2017). <https://doi.org/10.5555/3294771.3294885>
- Tian, Y., Zhang, M., Li, J., Li, Y., Yang, H., Li, W.: Fpnformer: Rethink the method of processing the rotation-invariance and rotation-equivariance on arbitrary-oriented object detection. *IEEE Transactions on Geoscience and Remote Sensing* **62**, 1–10 (2024) <https://doi.org/10.1109/TGRS.2024.3351156>
- Viola, P., Jones, M.: Rapid object detection using a boosted cascade of simple features. In: *IEEE/CVF Conference on Computer Vision and Pattern Recognition*, vol. 1, p. (2001). <https://doi.org/10.1109/CVPR.2001.990517>
- Viola, P., Jones, M.J.: Robust real-time face detection. *International Journal of Computer Vision* **57**, 137–154 (2004) <https://doi.org/10.1023/B:VISI.0000013087.49260.fb>
- Vaswani, A., Shazeer, N., Parmar, N., Uszkoreit, J., Jones, L., Gomez, A.N., Kaiser, L., Polosukhin, I.: Attention is all you need. In: International Conference on Neural Information Processing Systems, pp. 6000–6010 (2017)
- Weiler, M., Cesa, G.: General  $e(2)$ -equivariant steerable cnns. In: *Advances in Neural Information Processing Systems*, vol. 32 (2019). <https://proceedings.neurips.cc/paper/2019/file/45d6637b718d0f24a237069fe41b0db4-Paper.pdf>
- Wen, L., Cheng, Y., Fang, Y., Li, X.: A comprehensive survey of oriented object detection in remote sensing images. *Expert Systems with Applications* **224**, 119960 (2023) <https://doi.org/10.1016/j.eswa.2023.119960>
- Wang, J., Chen, Y., Zheng, Z., Li, X., Cheng, M.-M., Hou, Q.: Crosskd: Cross-head knowledge distillation for object detection. In: *IEEE/CVF Conference on Computer Vision and Pattern Recognition*, pp. 16520–16530 (2024). <https://doi.org/10.1109/CVPR52733.2024.01563>
- Wang, C., Guo, G., Liu, C., Shao, D., Gao, S.: Effective rotate: Learning rotation-robust prototype for aerial object detection. *IEEE Transactions on Geoscience and Remote Sensing* **62**, 1–14 (2024) <https://doi.org/10.1109/TGRS.2024.3374880>

- Worrall, D.E., Garbin, S.J., Turmukhambetov, D., Brostow, G.J.: Harmonic networks: Deep translation and rotation equivariance. In: IEEE/CVF Conference on Computer Vision and Pattern Recognition, pp. 7168–7177 (2017). <https://doi.org/10.1109/CVPR.2017.758>
- Weiler, M., Hamprecht, F.A., Storath, M.: Learning steerable filters for rotation equivariant cnns. In: IEEE/CVF Conference on Computer Vision and Pattern Recognition, pp. 849–858 (2018). <https://doi.org/10.1109/CVPR.2018.00095>
- Wang, J., Li, F., Bi, H.: Gaussian focal loss: Learning distribution polarized angle prediction for rotated object detection in aerial images. *IEEE Transactions on Geoscience and Remote Sensing* **60**, 1–13 (2022) <https://doi.org/10.1109/TGRS.2022.3175520>
- Wu, X., Li, W., Hong, D., Tao, R., Du, Q.: Deep learning for unmanned aerial vehicle-based object detection and tracking: A survey. *IEEE Geoscience and Remote Sensing Magazine* **10**(1), 91–124 (2022) <https://doi.org/10.1109/MGRS.2021.3115137>
- Wu, X., Sahoo, D., Hoi, S.C.H.: Recent advances in deep learning for object detection. *Neurocomputing* **396**, 39–64 (2020) <https://doi.org/10.1016/j.neucom.2020.01.085>
- Wang, J., Teng, X., Li, Z., Yu, Q., Bian, Y., Wei, J.: Vsai: A multi-view dataset for vehicle detection in complex scenarios using aerial images. *Drones* **6**(7) (2022) <https://doi.org/10.3390/drones6070161>
- Wu, W., Wong, H.-S., Wu, S.: Pseudo-siamese teacher for semi-supervised oriented object detection. *IEEE Transactions on Geoscience and Remote Sensing* **62**, 1–14 (2024) <https://doi.org/10.1109/TGRS.2024.3380645>
- Wu, W., Wong, H.-S., Wu, S., Zhang, T.: Relational matching for weakly semi-supervised oriented object detection. In: Proceedings of the IEEE/CVF Conference on Computer Vision and Pattern Recognition (CVPR), pp. 27800–27810 (2024)
- Wang, K., Xiao, Z., Wan, Q., Xia, F., Chen, P., Li, D.: Global focal learning for semi-supervised oriented object detection. *IEEE Transactions on Geoscience and Remote Sensing* **62**, 1–13 (2024) <https://doi.org/10.1109/TGRS.2024.3438844>
- Wright, J., Yang, A.Y., Ganesh, A., Sastry, S.S., Ma, Y.: Robust face recognition via sparse representation. *IEEE Transactions on Pattern Analysis and Machine Intelligence* **31**(2), 210–227 (2009) <https://doi.org/10.1109/TPAMI.2008.79>
- Wei, H., Zhang, Y., Chang, Z., Li, H., Wang, H., Sun, X.: Oriented objects as pairs of middle lines. *ISPRS Journal of Photogrammetry and Remote Sensing* **169**, 268–279 (2020) <https://doi.org/10.1016/j.isprsjprs.2020.09.022>
- Wei, S., Zeng, X., Qu, Q., Wang, M., Su, H., Shi, J.: Hrsid: A high-resolution sar images dataset for ship detection and instance segmentation. *IEEE Access* **8**,

120234–120254 (2020) <https://doi.org/10.1109/ACCESS.2020.3005861>

- Wu, Y., Zhang, K., Wang, J., Wang, Y., Wang, Q., Li, X.: Gcwnet: A global context-weaving network for object detection in remote sensing images. *IEEE Transactions on Geoscience and Remote Sensing* **60**, 1–12 (2022) <https://doi.org/10.1109/TGRS.2022.3155899>
- Wang, D., Zhang, Q., Xu, Y., Zhang, J., Du, B., Tao, D., Zhang, L.: Advancing plain vision transformer towards remote sensing foundation model. *IEEE Transactions on Geoscience and Remote Sensing*, 1–1 (2022) <https://doi.org/10.1109/TGRS.2022.3222818>
- Wang, Y., Zhang, Z., Xu, W., Chen, L., Wang, G., Yan, L., Zhong, S., Zou, X.: Learning oriented object detection via naive geometric computing. *IEEE Transactions on Neural Networks and Learning Systems* **35**(8), 10513–10525 (2024) <https://doi.org/10.1109/TNNLS.2023.3242323>
- Wang, T., Zhu, Y., Zhao, C., Zeng, W., Wang, J., Tang, M.: Adaptive class suppression loss for long-tail object detection. In: *IEEE/CVF Conference on Computer Vision and Pattern Recognition*, pp. 3102–3111 (2021). <https://doi.org/10.1109/CVPR46437.2021.00312>
- Xia, G.-S., Bai, X., Ding, J., Zhu, Z., Belongie, S., Luo, J., Datcu, M., Pelillo, M., Zhang, L.: Dota: A large-scale dataset for object detection in aerial images. In: *IEEE/CVF Conference on Computer Vision and Pattern Recognition*, pp. 3974–3983 (2018). <https://doi.org/10.1109/CVPR.2018.00418>
- Xie, X., Cheng, G., Rao, C., Lang, C., Han, J.: Oriented object detection via contextual dependence mining and penalty-incentive allocation. *IEEE Transactions on Geoscience and Remote Sensing* **62**, 1–10 (2024) <https://doi.org/10.1109/TGRS.2024.3385985>
- Xie, X., Cheng, G., Wang, J., Yao, X., Han, J.: Oriented r-cnn for object detection. In: *IEEE/CVF International Conference on Computer Vision*, pp. 3500–3509 (2021). <https://doi.org/10.1109/ICCV48922.2021.00350>
- Xu, C., Ding, J., Wang, J., Yang, W., Yu, H., Yu, L., Xia, G.-S.: Dynamic coarse-to-fine learning for oriented tiny object detection. In: *IEEE/CVF Conference on Computer Vision and Pattern Recognition*, pp. 7318–7328 (2023). <https://doi.org/10.1109/CVPR52729.2023.00707>
- Xu, Y., Fu, M., Wang, Q., Wang, Y., Chen, K., Xia, G.-S., Bai, X.: Gliding vertex on the horizontal bounding box for multi-oriented object detection. *IEEE Transactions on Pattern Analysis and Machine Intelligence* **43**(4), 1452–1459 (2021) <https://doi.org/10.1109/TPAMI.2020.2974745>
- Xie, S., Girshick, R., Dollár, P., Tu, Z., He, K.: Aggregated residual transformations for

- deep neural networks. In: IEEE/CVF Conference on Computer Vision and Pattern Recognition, pp. 5987–5995 (2017). <https://doi.org/10.1109/CVPR.2017.634>
- Xiong, Y., Liu, H., Gupta, S., Akin, B., Bender, G., Wang, Y., Kindermans, P.-J., Tan, M., Singh, V., Chen, B.: Mobiledets: Searching for object detection architectures for mobile accelerators. In: IEEE/CVF Conference on Computer Vision and Pattern Recognition, pp. 3824–3833 (2021). <https://doi.org/10.1109/CVPR46437.2021.00382>
- Xu, S., Li, Y., Lin, M., Gao, P., Guo, G., Lü, J., Zhang, B.: Q-detr: An efficient low-bit quantized detection transformer. In: IEEE/CVF Conference on Computer Vision and Pattern Recognition, pp. 3842–3851 (2023). <https://doi.org/10.1109/CVPR52729.2023.00374>
- Xiao, Z., Liu, Q., Tang, G., Zhai, X.: Elliptic fourier transformation-based histograms of oriented gradients for rotationally invariant object detection in remote-sensing images. *International Journal of Remote Sensing* **36**(2), 618–644 (2015) <https://doi.org/10.1080/01431161.2014.999881>
- Xu, Y., Zhang, Q., Zhang, J., Tao, D.: Vitae: Vision transformer advanced by exploring intrinsic inductive bias. In: *Advances in Neural Information Processing Systems*, vol. 34 (2021). [https://openreview.net/pdf?id=\\_RnHyIeu5Y5](https://openreview.net/pdf?id=_RnHyIeu5Y5)
- Yao, Y., Cheng, G., Lang, C., Yuan, X., Xie, X., Han, J.: Hierarchical mask prompting and robust integrated regression for oriented object detection. *IEEE Transactions on Circuits and Systems for Video Technology*, 1–1 (2024) <https://doi.org/10.1109/TCSVT.2024.3444795>
- Yao, Y., Cheng, G., Wang, G., Li, S., Zhou, P., Xie, X., Han, J.: On improving bounding box representations for oriented object detection. *IEEE Transactions on Geoscience and Remote Sensing* **61**, 1–11 (2023) <https://doi.org/10.1109/TGRS.2022.3231340>
- Ye, Q., Doermann, D.: Text detection and recognition in imagery: A survey. *IEEE Transactions on Pattern Analysis and Machine Intelligence* **37**(7), 1480–1500 (2015) <https://doi.org/10.1109/TPAMI.2014.2366765>
- Yu, Y., Da, F.: Phase-shifting coder: Predicting accurate orientation in oriented object detection. In: IEEE/CVF Conference on Computer Vision and Pattern Recognition, pp. 13354–13363 (2023). <https://doi.org/10.1109/CVPR52729.2023.01283>
- Yu, Y., Da, F.: On boundary discontinuity in angle regression based arbitrary oriented object detection. *IEEE Transactions on Pattern Analysis and Machine Intelligence* **46**(10), 6494–6508 (2024) <https://doi.org/10.1109/TPAMI.2024.3378777>
- Yang, X., Hou, L., Zhou, Y., Wang, W., Yan, J.: Dense label encoding for boundary discontinuity free rotation detection. In: IEEE/CVF Conference on Computer

- Vision and Pattern Recognition, pp. 15814–15824 (2021). <https://doi.org/10.1109/CVPR46437.2021.01556>
- Yang, Z., Liu, S., Hu, H., Wang, L., Lin, S.: Reppoints: Point set representation for object detection. In: IEEE/CVF International Conference on Computer Vision, pp. 9656–9665 (2019). <https://doi.org/10.1109/ICCV.2019.00975>
- Ye, T., Qin, W., Li, Y., Wang, S., Zhang, J., Zhao, Z.: Dense and small object detection in uav-vision based on a global-local feature enhanced network. *IEEE Transactions on Instrumentation and Measurement* **71**, 1–13 (2022) <https://doi.org/10.1109/TIM.2022.3196319>
- Yang, X., Sun, H., Fu, K., Yang, J., Sun, X., Yan, M., Guo, Z.: Automatic ship detection in remote sensing images from google earth of complex scenes based on multiscale rotation dense feature pyramid networks. *Remote Sensing* **10**(1) (2018) <https://doi.org/10.3390/rs10010132>
- Yu, H., Tian, Y., Ye, Q., Liu, Y.: Spatial transform decoupling for oriented object detection. In: *AAAI Conference on Artificial Intelligence*, vol. 38, pp. 6782–6790 (2024). <https://doi.org/10.1609/aaai.v38i7.28502>
- Yang, X., Yan, J.: Arbitrary-oriented object detection with circular smooth label. In: *European Conference on Computer Vision*, pp. 677–694 (2020). [https://doi.org/10.1007/978-3-030-58598-3\\_40](https://doi.org/10.1007/978-3-030-58598-3_40)
- Yang, X., Yan, J., Feng, T. Z. and He: R3det: Refined single-stage detector with feature refinement for rotating object. In: *AAAI Conference on Artificial Intelligence*, vol. 35, pp. 3163–3171 (2021). <https://doi.org/10.1609/aaai.v35i4.16426>
- Yang, X., Yan, J., Liao, W., Yang, X., Tang, J., He, T.: Scrdet++: Detecting small, cluttered and rotated objects via instance-level feature denoising and rotation loss smoothing. *IEEE Transactions on Pattern Analysis and Machine Intelligence*, 1–1 (2022) <https://doi.org/10.1109/TPAMI.2022.3166956>
- Yu, Y., Yang, X., Li, Q., Zhou, Y., Da, F., Yan, J.: H2rbox-v2: Incorporating symmetry for boosting horizontal box supervised oriented object detection. In: *Advances in Neural Information Processing Systems*, vol. 36, pp. 59137–59150 (2023). [https://proceedings.neurips.cc/paper\\_files/paper/2023/file/b9603de9e49d0838e53b6c9cf9d06556-Paper-Conference.pdf](https://proceedings.neurips.cc/paper_files/paper/2023/file/b9603de9e49d0838e53b6c9cf9d06556-Paper-Conference.pdf)
- Yu, Y., Yang, X., Li, Q., Da, F., Dai, J., Qiao, Y., Yan, J.: Point2rbox: Combine knowledge from synthetic visual patterns for end-to-end oriented object detection with single point supervision. In: *IEEE/CVF Conference on Computer Vision and Pattern Recognition*, pp. 16783–16793 (2024)
- Yu, Y., Yang, X., Li, J., Gao, X.: Task-specific heterogeneous network for object detection in aerial images. *IEEE Transactions on Geoscience and Remote Sensing*

61, 1–15 (2023) <https://doi.org/10.1109/TGRS.2023.3311966>

- Yang, X., Yan, J., Ming, Q., Wang, W., Zhang, X., Tian, Q.: Rethinking rotated object detection with gaussian wasserstein distance loss. In: International Conference on Machine Learning, vol. 139, pp. 11830–11841 (2021). <https://proceedings.mlr.press/v139/yang211.html>
- Yang, X., Yang, J., Yan, J., Zhang, Y., Zhang, T., Guo, Z., Sun, X., Fu, K.: Srdet: Towards more robust detection for small, cluttered and rotated objects. In: IEEE/CVF International Conference on Computer Vision, pp. 8231–8240 (2019). <https://doi.org/10.1109/ICCV.2019.00832>
- Yang, X., Yang, X., Yang, J., Ming, Q., Wang, W., Tian, Q., Yan, J.: Learning high-precision bounding box for rotated object detection via kullback-leibler divergence. In: Advances in Neural Information Processing Systems, vol. 34, pp. 18381–18394 (2021). <https://proceedings.neurips.cc/paper/2021/file/98f13708210194c475687be6106a3b84-Paper.pdf>
- Yang, X., Zhang, G., Li, W., Wang, X., Zhou, Y., Yan, J.: H2RBox: Horizontal Box Annotation is All You Need for Oriented Object Detection. In: International Conference on Learning Representations (2023)
- Yang, X., Zhang, G., Yang, X., Zhou, Y., Wang, W., Tang, J., He, T., Yan, J.: Detecting rotated objects as gaussian distributions and its 3-d generalization. IEEE Transactions on Pattern Analysis and Machine Intelligence, 1–18 (2022) <https://doi.org/10.1109/TPAMI.2022.3197152>
- Yang, X., Zhou, Y., Zhang, G., Yang, J., Wang, W., Yan, J., Zhang, X., Tian, Q.: The KFIoU Loss for Rotated Object Detection. arXiv e-prints, 2201–12558 (2022)
- Zhu, H., Chen, X., Dai, W., Fu, K., Ye, Q., Jiao, J.: Orientation robust object detection in aerial images using deep convolutional neural network. In: 2015 IEEE International Conference on Image Processing, pp. 3735–3739 (2015). <https://doi.org/10.1109/ICIP.2015.7351502>
- Zou, Z., Chen, K., Shi, Z., Guo, Y., Ye, J.: Object detection in 20 years: A survey. Proceedings of the IEEE 111(3), 257–276 (2023) <https://doi.org/10.1109/JPROC.2023.3238524>
- Zhang, S., Chi, C., Yao, Y., Lei, Z., Li, S.Z.: Bridging the gap between anchor-based and anchor-free detection via adaptive training sample selection. In: IEEE/CVF Conference on Computer Vision and Pattern Recognition, pp. 9756–9765 (2020). <https://doi.org/10.1109/CVPR42600.2020.00978>
- Zeng, Y., Chen, Y., Yang, X., Li, Q., Yan, J.: Ars-detr: Aspect ratio-sensitive detection transformer for aerial oriented object detection. IEEE Transactions on Geoscience and Remote Sensing 62, 1–15 (2024) <https://doi.org/10.1109/TGRS.2024.3364713>

- Zhu, Y., Du, J., Wu, X.: Adaptive period embedding for representing oriented objects in aerial images. *IEEE Transactions on Geoscience and Remote Sensing* **58**(10), 7247–7257 (2020) <https://doi.org/10.1109/TGRS.2020.2981203>
- Zhou, H., Ge, Z., Liu, S., Mao, W., Li, Z., Yu, H., Sun, J.: Dense teacher: Dense pseudo-labels for semi-supervised object detection. In: Avidan, S., Brostow, G., Cissé, M., Farinella, G.M., Hassner, T. (eds.) *European Conference on Computer Vision*, pp. 35–50 (2022)
- Zhang, Z., Guo, W., Zhu, S., Yu, W.: Toward arbitrary-oriented ship detection with rotated region proposal and discrimination networks. *IEEE Geoscience and Remote Sensing Letters* **15**(11), 1745–1749 (2018) <https://doi.org/10.1109/LGRS.2018.2856921>
- Zhang, D., Han, J., Cheng, G., Yang, M.-H.: Weakly supervised object localization and detection: A survey. *IEEE Transactions on Pattern Analysis and Machine Intelligence* **44**(9), 5866–5885 (2022) <https://doi.org/10.1109/TPAMI.2021.3074313>
- Zhang, H., Liu, L., Huang, Y., Yang, Z., Lei, X., Wen, B.: Cakdp: Category-aware knowledge distillation and pruning framework for lightweight 3d object detection. In: *IEEE/CVF Conference on Computer Vision and Pattern Recognition*, pp. 15331–15341 (2024). <https://doi.org/10.1109/CVPR52733.2024.01452>
- Zhang, H., Li, F., Liu, S., Zhang, L., Su, H., Zhu, J., Ni, L.M., Shum, H.-Y.: DINO: DETR with Improved DeNoising Anchor Boxes for End-to-End Object Detection. *arXiv e-prints* (2022) <https://doi.org/10.48550/arXiv.2203.03605>
- Zhang, J., Lei, J., Xie, W., Fang, Z., Li, Y., Du, Q.: Superyolo: Super resolution assisted object detection in multimodal remote sensing imagery. *IEEE Transactions on Geoscience and Remote Sensing* **61**, 1–15 (2023) <https://doi.org/10.1109/TGRS.2023.3258666>
- Zhang, S., Long, J., Xu, Y., Mei, S.: Pmho: Point-supervised oriented object detection based on segmentation-driven proposal generation. *IEEE Transactions on Geoscience and Remote Sensing* **62**, 1–18 (2024) <https://doi.org/10.1109/TGRS.2024.3450732>
- Zhang, M., Qiu, H., Mei, H., Wang, L., Meng, F., Xu, L., Li, H.: Drdet: Dual-angle rotated line representation for oriented object detection. *IEEE Transactions on Geoscience and Remote Sensing* **61**, 1–13 (2023) <https://doi.org/10.1109/TGRS.2023.3311870>
- Zou, Z., Shi, Z.: Random access memories: A new paradigm for target detection in high resolution aerial remote sensing images. *IEEE Transactions on Image Processing* **27**(3), 1100–1111 (2018) <https://doi.org/10.1109/TIP.2017.2773199>

- Zhu, X., Su, W., Lu, L., Li, B., Wang, X., Dai, J.: Deformable detr: Deformable transformers for end-to-end object detection. In: International Conference on Learning Representations (2021)
- Zheng, S., Wu, Z., Du, Q., Xu, Y., Wei, Z.: Oriented object detection for remote sensing images via object-wise rotation-invariant semantic representation. *IEEE Transactions on Geoscience and Remote Sensing* **62**, 1–15 (2024) <https://doi.org/10.1109/TGRS.2024.3402825>
- Zheng, Z., Wang, P., Liu, W., Li, J., Ye, R., Ren, D.: Distance-iou loss: Faster and better learning for bounding box regression. In: *AAAI Conference on Artificial Intelligence*, vol. 34, pp. 12993–13000 (2020). <https://doi.org/10.1609/aaai.v34i07.6999>
- Zhang, F., Wang, X., Zhou, S., Wang, Y., Hou, Y.: Arbitrary-oriented ship detection through center-head point extraction. *IEEE Transactions on Geoscience and Remote Sensing* **60**, 1–14 (2022) <https://doi.org/10.1109/TGRS.2021.3120411>
- Zhao, F., Xia, L., Kylling, A., Li, R.Q., Shang, H., Xu, M.: Detection flying aircraft from landsat 8 oli data. *ISPRS Journal of Photogrammetry and Remote Sensing* **141**, 176–184 (2018) <https://doi.org/10.1016/j.isprsjprs.2018.05.001>
- Zhang, C., Xiong, B., Li, X., Kuang, G.: Tcd: Task-collaborated detector for oriented objects in remote sensing images. *IEEE Transactions on Geoscience and Remote Sensing* **61**, 1–14 (2023) <https://doi.org/10.1109/TGRS.2023.3244953>
- Zhang, Q., Xu, Y., Zhang, J., Tao, D.: Vitaev2: Vision transformer advanced by exploring inductive bias for image recognition and beyond. *International Journal of Computer Vision*, 1573–1405 (2023) <https://doi.org/10.1007/s11263-022-01739-w>
- Zhang, Y., Yuan, Y., Feng, Y., Lu, X.: Hierarchical and robust convolutional neural network for very high-resolution remote sensing object detection. *IEEE Transactions on Geoscience and Remote Sensing*. **57**(8), 5535–5548 (2019) <https://doi.org/10.1109/TGRS.2019.2900302>
- Zheng, Z., Ye, R., Hou, Q., Ren, D., Wang, P., Zuo, W., Cheng, M.-M.: Localization distillation for object detection. *IEEE Transactions on Pattern Analysis and Machine Intelligence* **45**(8), 10070–10083 (2023) <https://doi.org/10.1109/TPAMI.2023.3248583>
- Zhou, Y., Ye, Q., Qiu, Q., Jiao, J.: Oriented response networks. In: *IEEE/CVF Conference on Computer Vision and Pattern Recognition*, pp. 4961–4970 (2017). <https://doi.org/10.1109/CVPR.2017.527>
- Zhou, Y., Yang, X., Zhang, G., Wang, J., Liu, Y., Hou, L., Jiang, X., Liu, X., Yan, J., Lyu, C., Zhang, W., Chen, K.: Mmrotate: A rotated object detection benchmark using pytorch. In: *ACM International Conference on Multimedia*, pp. 7331–7334

(2022). <https://doi.org/10.1145/3503161.3548541>

Zhang, T., Zhuang, Y., Chen, H., Wang, G., Ge, L., Chen, L., Dong, H., Li, L.: Posterior instance injection detector for arbitrary-oriented object detection from optical remote-sensing imagery. *IEEE Transactions on Geoscience and Remote Sensing* **61**, 1–18 (2023) <https://doi.org/10.1109/TGRS.2023.3327123>

Zhou, X., Zhuo, J., Krähenbühl, P.: Bottom-up object detection by grouping extreme and center points. In: *IEEE/CVF Conference on Computer Vision and Pattern Recognition*, pp. 850–859 (2019). <https://doi.org/10.1109/CVPR.2019.00094>

Zhang, T., Zhang, X., Liu, C., Shi, J., Wei, S., Ahmad, I., Zhan, X., Zhou, Y., Pan, D., Li, J., Su, H.: Balance learning for ship detection from synthetic aperture radar remote sensing imagery. *ISPRS Journal of Photogrammetry and Remote Sensing* **182**, 190–207 (2021) <https://doi.org/10.1016/j.isprsjprs.2021.10.010>

Zhang, X., Zhou, X., Lin, M., Sun, J.: Shufflenet: An extremely efficient convolutional neural network for mobile devices. In: *IEEE/CVF Conference on Computer Vision and Pattern Recognition*, pp. 6848–6856 (2018). <https://doi.org/10.1109/CVPR.2018.00716>

Zhang, Z., Zhang, L., Wang, Y., Feng, P., He, R.: Shippersimagnet: A large-scale fine-grained dataset for ship detection in high-resolution optical remote sensing images. *IEEE Journal of Selected Topics in Applied Earth Observations and Remote Sensing* **14**, 8458–8472 (2021) <https://doi.org/10.1109/JSTARS.2021.3104230>

Zhang, X., Zhang, T., Wang, G., Zhu, P., Tang, X., Jia, X., Jiao, L.: Remote sensing object detection meets deep learning: A metareview of challenges and advances. *IEEE Geoscience and Remote Sensing Magazine* **11**(4), 8–44 (2023) <https://doi.org/10.1109/MGRS.2023.3312347>

Zhao, Z.-Q., Zheng, P., Xu, S.-T., Wu, X.: Object detection with deep learning: A review. *IEEE Transactions on Neural Networks and Learning Systems* **30**(11), 3212–3232 (2019) <https://doi.org/10.1109/TNNLS.2018.2876865>

Zhang, T., Zhang, X., Zhu, P., Chen, P., Tang, X., Li, C., Jiao, L.: Foreground refinement network for rotated object detection in remote sensing images. *IEEE Transactions on Geoscience and Remote Sensing* **60**, 1–13 (2022) <https://doi.org/10.1109/TGRS.2021.3109145>